MONASH University

Intense Tropical Thunderstorms in a Future Warmer Climate

Emmanuel Sarbeng

BSc. Kwame Nkrumah University of Science and Technology (2011)

Gradcert. Institute of Meteorological Training and Research (2014)

MSc. Nanjing University of Information, Science and Technology (2018)

A Thesis Submitted for the Degree of Doctor of Philosophy at

Monash University in 2023

Falculty of Science, School of Earth, Atmosphere and Environment

Copyright notice

Abstract

In this thesis, the connections between some characteristic features of the land surface and the intensity of continental thunderstorms are investigated using idealized simulations of radiative-convective equilibrium (RCE). These land surface features have been hypothesized to control the intensity of thunderstorms that form over land surfaces.

Firstly, the relationship between the high surface Bowen ratio (SBR) over a homogeneous and heterogeneous land surfaces and the intensities of continental thunderstorms was examined. It is argued that the intensity of thunderstorms over land surfaces is largely insensitive to the depth of the boundary layer over both homogeneous and heterogeneous land surfaces, and the idea that larger patch sizes of a heterogeneous land surface would lead to stronger updraughts is not supported by the set of idealized simulations in this study.

The influence of the large diurnal cycle of land surface temperature on the intensity of continental storms was investigated in idealized simulations with an imposed diurnal cycle of temperature at the lower boundary. It is found that the diurnal cycle of surface temperature exerts some control on the intensity of thunderstorms in idealized model simulations. It is argued that the large diurnal cycle of surface temperature can be physically linked to the most buoyant convective clouds.

Finally, the response of moist convection to warming over wet and dry land surfaces was assessed using idealized RCE simulations. It is found that the intensity of thunderstorms over wet land surfaces increased significantly with warming. However over dry land surfaces, the intensity of the storms remained largely unchanged. This suggests that future thunderstorms over islands and other wet land surfaces could be much intense, and the dangers associated with thunderstorms amplified.

Declaration

This thesis is an original work of my research and contains no material which has been accepted for the award of any other degree or diploma at any university or equivalent institution and that, to the best of my knowledge and belief, this thesis contains no material previously published or written by another person, except where due reference is made in the text of the thesis.

Student name: Emmanuel Sarbeng **Date:**

Student signature:

Main Supervisor name: Martin Singh **Date:**

Main Supervisor signature:

Acknowledgements

This thesis was supported by an Australian Government Research Training Program (RTP) scholarship with additional support from the ARC Centre of Excellence for Climate Extremes (DE190100866 and DP200102954). Computational resources and services of this thesis was provided by the Australian Government's National Computing Infrastructure (NCI).

There are many who have gone out of their way to support me throughout this journey. This research and my journey to this point would not have been possible if not for your genuine kindness and dedication to help me in my dark moments. I am sincerely grateful to you all.

I particularly want to thank my supervisors, especially Dr. Martin S. Singh who kept faith in me and guided me in every step of my PhD journey, particularly at the point when I was overwhelmed and had given up on myself. His patience and dedication is unparalleled, and I have leant a lot of moral and academic lessons from him.

I wish to thank my thesis panelists, Michael Reeder, Steven Siems and Bethan White, for their time and good feedbacks throughout my time as a PhD candidate at Monash University.

I also would like to thank the following individuals for their immense role played in my life up to this point. Nana Boakye Ansah Debrah, thank you for all the financial support throughout my academic journey, To my uncle, Dr. Berchie and wife, I say thank you for taking me in and being good role models for my life. I appreciate the continual support form my uncle Kwaku Fosu, my aunt Yaa Dufie and my grandmother Nana Serwaah who thought me most of the things I know about life. I am grateful for the emotional support from my siblings; Yaw, Afia, Adwoa, Akua, Kwasi and Abaawa, You guys made this journey a lot easier.

To all friends and colleagues in Martin's research group, my office mates especially Sonny and Uchi, thank you guys for the times we shared discussing science, religion, politics and all other topics that kept us together even through the difficult times of COVID and all the lockdowns. To my Wednesday soccer mates, I say thank you for all the good memories and and medals. To my two best friends Richard and Mustapha, I am grateful for all the good memories and the brotherly support that kept us going.

Finally, and most importantly, I dedicate this thesis to the memories of my sister Ceclia Pokuah who died few months to the start of my PhD and my mum Agnes Awuah who died seven months into my PhD journey; your lost unsettled me in all spheres, but I hope you can look down on me and smile now with a proud heart.

Contents

List of Figures

List of Tables

Chapter 1

Introduction

1.1 Motivation

At the heart of the concerns of climate change is how local weather phenomena might change in response to warming across the different climatic zones. Over the tropics, thunderstorms are one of the most dominant weather phenomena with far reaching socioeconomic and climatic importance. In their intense form, thunderstorms may be associated with extreme precipitation, gusty winds and lightning that can sometimes be detrimental to human life and property. It is therefore important to understand how the intensities and distribution of these storms might change in the future when climate change is in full swing.

Predicting the intensities of these future storms is however not trivial, primarily because the convective processes that lead to the formation of these thunderstorms are poorly represented in current global climate models (GCMs). Convective processes usually occur on relatively finer scales, and are therefore not explicitly resolved in current GCMs which are conventionally run at coarser resolutions (Grabowski and Smolarkiewicz, 1999; Randall *et al.*, 2003). Convective processes have therefore been a major source of uncertainty in current climate models and climate projections (Bony *et al.*, 2015).

Another fundamental reason for the difficulty in projecting these future storms arise from the fact that there are still unanswered questions on the behaviour and distribution of thunderstorms especially over the tropics. For example, as observed by a number of studies (e.g., Lucas *et al.*, 1994; Zipser *et al.*, 2006; Liu *et al.*,

2010; Liu and Zipser, 2015), the most intense storms tend to form over tropical land surfaces as opposed to ocean surfaces, but there is not yet a comprehensive explanation to this widely observed contrast in intensity of thunderstorms over these surfaces. This area of research has seen substantial scientific interest over the years. Particularly, the question of how the underlying characteristic features of the land and ocean surfaces influence the intensity of convective storms has been vigorously studied.

A key goal of this thesis is therefore to investigate how some of these surface features are connected to the intensities of thunderstorms that form over land surfaces, and to explore how these connections might change in response to global warming.

Notwithstanding the aforementioned challenges, there have been some advances made towards understanding and predicting these future thunderstorms. Particularly, some studies (e.g., Romps, 2011; Muller, 2013; Van de Walle *et al.*, 2021) have shown increases in thunderstorms associated precipitation in response warming. However, many of these mechanistic studies have focused on convection over tropical ocean surfaces as opposed to convection over land surfaces. The land surface presents its own complexities and has a significant number of features that can influence convection, hence simulating convection over land is far more difficult than simulating convection over the ocean (Rochetin *et al.*, 2014). Human habitats are however largely over land. Given that the most intense storms form over land, it becomes even more important to investigate how intense or otherwise thunderstorms over land would be in the future, to assist policy makers make informed decisions on how the dangers posed by these intense thunderstorms can be reduced in the future.

The rest of this chapter is dedicated to reviewing some importance and dangers of thunderstorms over the tropics (Section 1.1.1), we discuss the largely observed land-ocean contrast in thunderstorm intensity, and the some hypotheses put forward by some researchers as the basis for this observed contrast in intensity of storms over the two surfaces (Section 1.1.2). We then discuss some of the techniques and advances made in the projection of these future storms over ocean surfaces (Section 1.1.3). Finally we highlight the main research questions of this study (Section 1.2), and present an overall outline of this thesis in Section 1.3.

1.1.1 Thunderstorms in the tropical climate

Thunderstorms are formed when water vapour within a rising air parcel condenses leading to explosive release of energy into the atmosphere. The convective processes that lead to the formation of these thunderstorms are the main mechanism by which energy is transported from the surface to the upper troposphere (Page, 1982; Keenan *et al.*, 1994). Hence, thunderstorms play a significant role in the general circulation of the atmosphere, and to a larger extent the global climate.

In their intense form, electrical charges within thunderstorms produce varying degrees of lightning which poses a number of public safety concerns. Lightning from thunderstorms is a major cause of wildfires (Dowdy and Mills, 2012). Lightning is known to influence the composition of the atmosphere through the production of species of reactive nitrogen. Some of these reactive species of nitrogen act as precursors for the formation of tropospheric ozone that contributes to global warming and can sometimes be harmful to human life (Koike *et al.*, 2007). About 78 percent (78%) of the earth's total lightning occurs in the tropics and subtropics (Christian *et al.*, 2003). In the tropics, lightning from thunderstorms are responsible for the destruction of about 832 million forest trees annually (Gora *et al.*, 2020).

Thunderstorms produce the bulk of precipitation over the tropics. These large amounts of precipitation support livelihood in diverse ways and are central to socioeconomic development across the tropics. In the equatorial tropics for example where agriculture and electricity generation depend largely on rainfall (Nieuwolt, 1982; Lin *et al.*, 2006), the societal importance of thunderstorms cannot be overemphasized. However, severe thunderstorms mostly produce extreme precipitation that may be injurious to agriculture and to a larger extent human life over the tropics . Such extreme precipitation results in excessive erosions, landslides, and flash flooding, resulting in the destruction of farms, colossal damages to property and loss of human life (Nieuwolt, 1982).

Across the tropical climate, and indeed all other places where thunderstorms are prevalent, there is a good measure of their importance as well as their dangers. A conclusive understanding of their formation, distribution and potential changes remains significant to the debate of climate change. There is an overall understanding that thunderstorms are prevalent over the tropics especially during the pre-monsoon seasons when temperatures and humidity are high (Zipser *et al.*,

2006; Das, 2017). What is not certain is how the individual conditions required for the development of storms in the tropics might change in the future.

1.1.2 Land - Ocean contrast in thunderstorm intensity

Across the tropical climate, the most intense storms form predominantly over land surfaces (Lucas *et al.*, 1994; Williams and Stanfill, 2002; Zipser *et al.*, 2006; Matsui *et al.*, 2016). This has been shown in different observation studies using different intensity metrics. Liu and Zipser (2005) for example assessed the vertical growth and overshooting of clouds into the tropopause and concluded that a greater number of cumulonimbus clouds that overshot into the tropopause formed over land. Toracinta and Zipser (2001) in a study of global tropical lightning over a 3 month period showed that only 15% - 21% of total lightning clusters were from oceanic sources as compared about 66% from continental storms. Christian *et al.* (2003) also showed a ∼10:1 ratio of annual lightning flash rate between land and ocean storms.

From the different metrics used in observation and model studies, it is apparent that storms over land are more intense than those over the ocean. The all important question yet to be answered is the underlying mechanisms that control the intensity of thunderstorms over land, and how these mechanisms differ from processes over ocean surfaces.

The intensity of convective storms are also known to be influenced by environmental parameters such as the convective available potential energy (CAPE), convective inhibition (CIN) and wind shear (Trapp *et al.*, 2007; Brooks, 2013). CAPE describes the maximum obtainable kinetic energy by an idealized rising parcel of air, and therefore gives an indication of the instability of the atmosphere. An opposing parameter to CAPE is CIN, a measure of the energy required by rising air parcel to overcome the stable layers of the atmosphere. In the tropics, wind shear which is defined as change in wind speed and direction with height, tends to be weaker and are mainly related to organization of storms. While CIN is related to the triggering of convections, the intensity of local storms are found to be more related to CAPE (Singh *et al.*, 2017). However, large differences in these large scale environmental parameters between land and ocean surfaces have not been clearly found in observation studies.

It is a particularly interesting conundrum because few studies (e.g., Williams and Renno, 1993) done on assessing the climatology of CAPE do not show large differences in mean CAPE between land and ocean surfaces to support the huge differences in updraught intensities found on these surfaces. Riemann-Campe *et al.* (2009) in their assessment of ERA-40 reanalysis data showed that high CAPE values are predominantly found over tropical land surfaces but they exhibit very high seasonal variability. It is not immediately clear how this seasonal variability in CAPE explain the huge difference in intensity of local thunderstorm in a day. As noted by Agard and Emanuel (2017), continental CAPEs are by themselves highly transient. It is possible that the peak values of such transient CAPEs rather than their climatological averages are significant for convection over land surfaces.

Differences in entrainment rates over land and ocean surfaces can significantly influence the intensity of their respective convective storms. Entrainment of subsaturated air into a convective cloud core has been shown to have a dilution effect on their available energy (Zhang, 2009; Hannah, 2017). Entrainment is however a very complex environmental parameter to study and as such, its influence also depends on the environment and the convective core itself. Differences in entrainment rates between land and ocean surfaces has not been explicitly shown in current literature.

In view of the complex nature of convection especially over land, quite a number of reasons have emerged as possible explanations to the large land-ocean contrast in storm intensity. A strong hypothesis that has seen considerable scientific interest over the years is the argument that some characteristic features peculiar to the land surface control the intensity of storms that form over land (Williams and Stanfill, 2002). Naturally, the land surface have many distinguishing features from the ocean; from low heat capacity, to differences in concentration of aerosols. In the context of the hypothesis by Williams and Stanfill (2002), all these features could potentially control the development of storms over land. It is therefore not surprising that there is a growing scientific interest geared towards identifying the main surface feature that enhances convection over land.

1.1.2.1 Characteristic features of the land surface

Among the numerous features of the land surface, scientific interest has been drawn to a handful, and there has been vigorous investigation on their linkages to convection and its intensity over land. Particularly, the high boundary layer depth set by high surface Bowen ratio (SBR), the heterogeneous nature of the land surface, the large diurnal cycle of surface temperature, and high aerosol concentration over the land surface have all been mentioned and explored in different observation and modeling studies.

Scientific studies dedicated to this land surface and storm intensity hypothesis, in practice seek to establish a physical linkage between the surface feature being studied and a measure of intensity of the convective storm. A common style of choice is to be able to show that the surface feature being studied results in an increase in CAPE, and this CAPE is enough to invigorate the convective storms. Notwithstanding the growing scientific interest in identifying the specific features of the land surface that are connected to the intensity of continental storms, there has not been good agreement amongst the different studies that investigate these land surface mechanisms. Indeed, it is common to find contrasting results between two studies that investigates the same surface feature.

We present a brief review of the physics behind some of the popular land surface features in literature and some examples of studies done on such features. Here, we discuss the deep boundary layer depth (high surface Bowen ratio), the high concentration of aerosols, the large diurnal cycle of surface temperature, and the heterogeneity of surface fluxes.

Deep boundary layer depth:

In comparison to a saturated water surface, the land has a lower water availability. This is reflected by the enhanced turbulent fluxes of sensible heat and subsequent higher Bowen ratio over the land surface as compared to the ocean. The high surface Bowen ratio (SBR) of the land surface is what sets the depth of the boundary layer. According to Williams and Stanfill (2002), the large boundary layer forces an increase of the cloud base height (CBH) which results in relatively large clouds that experience less dilution from the environment. They argued that, buoyant parcels arising from these large clouds effectively transform CAPE to kinetic energy and therefore invigorate the storms. This can be understood loosely as; the

deeper the boundary layer, the bigger the cloud size and the less dilution from the environment to erode the conversion of CAPE to kinetic energy required to intensify the storms. The caveat however is, there should be readily available surface moisture. In very dry land surfaces, the enhanced boundary layer depth prevents clouds from forming as the relative humidity in such situations is extremely low. Williams and Stanfill (2002) gave a relative humidity range of 50-60% and a cloud base height (CBH) below 3 km as a favorable condition within which the boundary layer depth contribution to the invigoration of continental storms is most attainable.

Williams *et al.* (2005a) using analysis of satellite data and ground observations found that mean lightning flash rate increases with increasing cloud base height (CBH). However, Hansen and Back (2015) showed in RCE model simulations with different SBR values that, increasing the CBH does not in itself lead to an increase in the intensity of thunderstorms as measured by the high percentiles of updraught velocity from their simulations. They argue that entrainment is independent of the boundary layer depth even though their high SBR cases had reasonably larger cloud sizes at birth, it did not result in invigoration of the clouds that formed. Unequivocal evidence of the high boundary depth of the land surface resulting in stronger storms over land is yet to be seen.

High concentration of aerosols:

Two main mechanisms have been used to explain the hypothesis that the high concentration of aerosols over land surfaces contributes to the intensity of convective storms that form over land. The first mechanism is premised on the role of aerosols as cloud condensation nuclei in the atmosphere. As suggested by Rosenfeld *et al.* (2008), higher concentrations of aerosols delay the formation of precipitation by the creation of smaller cloud droplets allowing for enhanced released of latent heat into the atmosphere as these drops freeze when they cross the zero degree isotherm. This is expected to result in enhanced buoyancy. A relatively new mechanism that focuses on increases in environmental humidity through detrainment moistening has emerged Abbott and Cronin (2021). They argue that higher concentrations of aerosols increase the detrainment from clouds into the environment, this in turn reduces the dilution effect of entrainment and allows for large-scale accent and enhanced buoyancy.

As noted by Li *et al.* (2017), higher aerosol concentration can have both positive and negative effect on clouds formation and their intensity. For example, Anber *et al.* (2019) in an idealized study argued that higher concentration of aerosols reduces surface enthalpy fluxes and suppresses evaporative cooling leading to reduction of mean precipitation. This study appear to contradict the different mechanisms that have been used to support the hypothesis that high concentrations of aerosols over land surfaces control the intensity of continental storms.

Large diurnal cycle of surface temperature:

The large diurnal cycle of surface temperature hypothesis is centred around the thermal difference between land and ocean surfaces and their interaction with the a relatively cold troposphere Williams and Stanfill (2002). The hypothesis holds that convection over ocean surfaces induces gravity waves (Sobel *et al.*, 2001) that modifies free-tropospheric temperature over land surface, and therefore maintain a similar free-tropospheric temperature profiles over land and ocean surfaces (Charney, 1963). During day time, the land surface by virtue of its low heat capacity warms faster than the ocean and thus interacts with the relatively colder free-troposphere. This interaction sets up heating of the boundary layer which in turn lead to the build up of CAPE to sustain buoyant cloud parcels during the day. Hansen *et al.* (2020) however, found no evidence of high CAPE over their island region when they tested this mechanism in an idealized cloud-resolving simulation with a simplified island geometry. Rather, they found that CAPE peaked in the early morning over the island and decreased during the day, contrary to the hypothesis.

Heterogeneity of the land surface: The different vegetations, orography, soil moisture and other geographical features make the land surface naturally heterogeneous in comparison to the ocean surface. The heterogeneity of the land surface produces differential heating in different locations which results in cold and warm patches over the land surface. Essentially, a horizontal variation in boundary layer properties is set on the land surface, and this is hypothesized to result in deeper clouds over the land surface. The heterogeneous land surface set horizontal variation in surface fluxes and temperature is expected to induce mesoscale secondary circulation that could potentially result in enhanced buoyancy over the warm patches of the heterogeneous domain (Cheng and Cotton, 2004).

Some studies (e.g., Taylor *et al.*, 1997; Rieck *et al.*, 2014; Wu *et al.*, 2015a; Kang and Ryu, 2016; Lee *et al.*, 2018) have focused on the combined effect of two or more of these surface features and have shown significant enhancement in convective storms over land. Lee *et al.* (2018) for example studied the transitioning of shallow to deep convection over a heterogeneous surface with prescribed surface fluxes and diurnal cycle of insolation, and found that clouds transition faster into deep clouds over the dry patches of their heterogeneous domain. It is possible that the combined effect of heterogeneity and diurnal cycle is what accelerates the transitioning and intensity in these studies. However to totally understand the role of the individual land surface feature on convection, it is imperative to study the relative influence of these surface features individually, to establish their connection with the intensity of continental storms.

Notwithstanding the scientific interest and the numerous studies in this area, the question of which specific land surface feature controls the intensity of convective storms over land is far from being answered, especially when studies of the same land surface feature appear to have contrasting results. Differences in experimental designs, model setup, and how the land surface is defined in modeling studies may all be potential reasons for the differences in these results. The intensity metric used in assessing the intensity of the convective storm, and the underlying objective of the individual scientific studies of these land surface features can also influence the conclusions made on these surface mechanisms. For example, some studies (e.g., Rieck *et al.*, 2014) mainly focuses on the transitioning of shallow clouds to deeper clouds over a defined land surface but are not necessarily interested in the intensity of the deep clouds once they are formed.

The idea that land surface features contribute to the invigoration of convective storms over land surface remains a viable hypothesis for understanding the controls of thunderstorm intensity over land, and a potential explanation to the land-ocean contrast in storm intensity. However, a complete understanding of which land surface feature exerts the dominant control on the updraught strength of continental storms, and the scales at which these controls are still relevant is an open question yet to be answered.

1.1.3 Prediction of intensity of future storms

The difficulty in representing convective processes in current GCMs is a major bottleneck to prediction of future thunderstorms. The coarse resolution and parameterization of cloud processes in global atmospheric models has been a major source of uncertainty in our understanding of current climate and projection into the future (Randall *et al.*, 2003).

In view of the persisting limitations of GCMs in predicting future storms, an alternate approach employed by some studies (e.g., Trapp *et al.*, 2007; Diffenbaugh *et al.*, 2013; Singh *et al.*, 2017) is to use GCM simulations to assess large-scale environments known to favour thunderstorm development. Since GCMs explicitly resolve these large-scale processes, future projections of them can easily be made in climate simulations. CAPE is one of such large-scale environmental parameters, and has been shown to increase significantly with warming.

Trapp *et al.* (2007) showed significance increases in CAPE over continental United State in their global warming simulation with a GCM. As shown in Figure 1.1, Singh *et al.* (2017) analysed an ensemble of climate models and found robust increases in high percentiles of CAPE with warming over the tropics and subtropics. Their analysis showed robust increases in CAPE mainly over land across the different models used. Such robust increases in CAPE in the tropics could potentially indicate a high distribution of intense storms especially over land. However, in the context of storm intensity, CAPE is not the only driver of convection in the tropics. The effects of parameters such as wind shear and entrainment may also change with warming (Trapp and Hoogewind, 2016), and could have substantial input as to how much of the extreme CAPE increases would realistically result in intensification of convection over the tropics.

The are also fundamental questions on the use of GCMs in simulating CAPE over the tropics. Generally, vertical profiles of temperature are crucial in the estimation of CAPE. However, in the tropics the free tropospheric temperature are known to be influenced by convective processes (Charney and Eliassen, 1964). These convective processes are not explicitly resolved in GCMs. Hence, the accuracy of the CAPE simulated by these GCMs are to a larger extent questionable. How convective processes are parameterized in a particular GCM may also play a major role in the biases in the estimation of CAPE over the tropics, and may be the reason

for the substantial differences in both climatological and predicted CAPE values across different GCMs (Singh *et al.*, 2017).

The robust increases in CAPE from GCM global warming simulations seen in the various studies can only motivate scientific research into understanding the underlying mechanisms that drives such increases in CAPE. Thus far, there is an incomplete understanding of what mechanisms account for CAPE increase over different surfaces and how these mechanisms might change with warming. Different theories have emerged in this respect mainly in highly idealized settings but unambiguous evidence of such theories have not been seen in the real world.

Two of such CAPE theories are the saturation deficit theory (Singh and O'Gorman, 2013) and the transient CAPE theory by Agard and Emanuel (2017). Using idealized RCE simulations, Singh *et al.* (2017) developed a theory of CAPE based on humidity difference between a cloud parcel and its environment. The so-called saturation deficit theory highlights the effect of entrainment on convection. They assumed that the atmosphere remained close to neutral buoyancy with respect to clouds that experience a fixed entrainment profile. The saturation deficit would then increase with temperature if relative humidity remain constant setting up an increased influence of entrainment on the lapse rate, and ultimately increased CAPE with warming. However, important factors such as the nature of the underlying surface and large-scale circulations were not taking into account in the development of this theory. It is possible this theories found in RCE do not apply in the real world. It is therefore important to understand the applicability of this theory over different surfaces (land or ocean) and to find evidence of it in the real world.

The use of high resolution cloud scale models remain the most viable option in understanding convective processes and their sensitivity to underlying surfaces (Guichard and Couvreux, 2017). There is a drive towards the development and usage of global cloud-resolving models (Sato *et al.*, 2019). However, they are yet to be used extensively in climate simulations. CRMs have however been used in a number of idealized simulations with simple numerical frameworks to study the intensity of convective storms in response to increasing temperatures over an albeit small domains.

For example, CRMs in idealized RCE simulations have been used to show significant increases in extreme precipitation with warming over the tropical ocean

surfaces (Muller *et al.*, 2011; Romps, 2011). They have also been used to show increases in CAPE with increasing sea surface temperature (SST) (Singh and O'Gorman, 2013; Seeley and Romps, 2015). Again, CRMs have been used to show increases in intensity of thunderstorms with warming over the tropics. Singh and O'Gorman (2015) using idealized RCE simulations showed that the updraught velocities of storms that form over tropical oceans increase with warming, with the fractional increases most noticeable at the upper troposphere. Romps (2019a) also showed increases in the product of CAPE and precipitation (CAPE $\times$ P) with warming in RCE simulations over tropical ocean surfaces. CAPE $\times$ P is a proxy for lightning from thunderstorms. By any measure of intensity, CRMs have been used to study the intensity of convective storms in different temperature regimes. Since convective processes are better represented in these CRMs, findings from such studies presents a better pathway to understanding tropical convective processes than results from conventional GCMs. The point should however be made that for convection to be fully resolved, model grid spacing should be less than 100 m.

In terms of the use of CRMs in simplified numerical frameworks like RCE in predicting future storms, current studies mostly focus on tropical ocean surfaces (e.g., Singh and O'Gorman, 2015). The distribution and intensities of future storms over tropical land surfaces remains an open area of scientific research.

1.2 Research questions

In this thesis, we are guided by three very broad questions that are investigated in tandem with sets of model simulations. The idea here is to identify those land surface features that control the intensity of thunderstorms over land, and assess how the intensities of storms over our conceptual land defined by these surface features changes under different temperature regimes.

This study is guided by the following questions:

Question one:
Which of the land surface features considered in this study is connected to the intensity of storms that form over land?
The hypotheses that characteristic features of the land surface control the intensity of storms over land remains a viable basis for understanding moist convection over

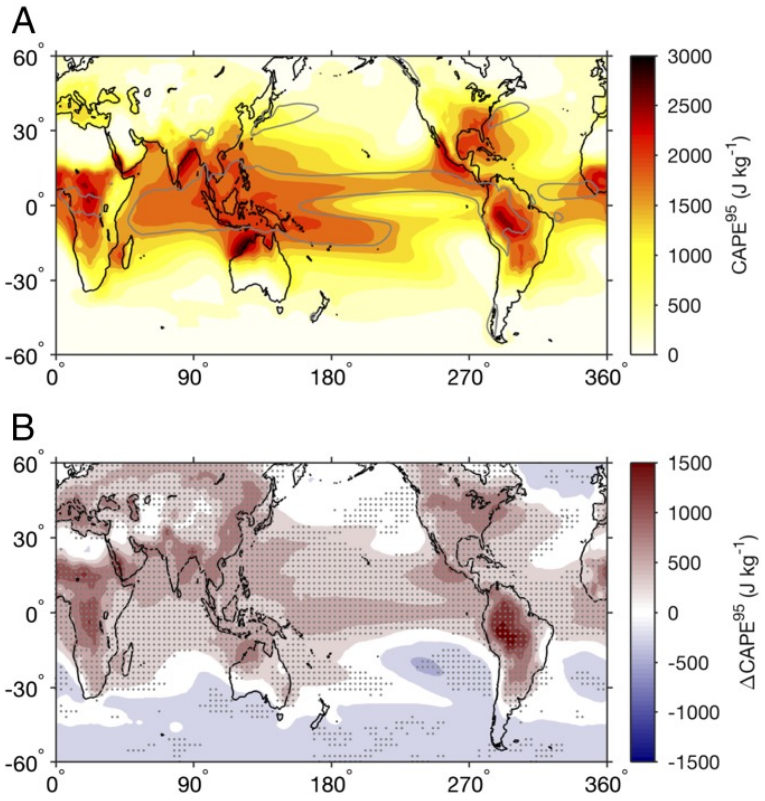

FIGURE 1.1: Projected increases in CAPE over the tropics and subtopics under business-as-usual scenario. Plot A is the ensemble mean of the 95th percentile of CAPE. Plot B is the difference in 95th percentile of CAPE between the current and future climate as projected. Taking with permission from (Singh *et al.*, 2017).

land, and plausibly explaining the huge differences in storm intensity over land and ocean surfaces. The conundrum perhaps is identifying the land surface feature singularly responsible or exerting the greatest influence on convection over land. The land surface by its nature have several distinguishing features from the ocean surface, hence identifying a single or group of features controlling convection over land is not trivial, especially so when studies on particular surface feature seem to give contrasting results. We contribute to this area of research by assessing how three of these land surface features are connected to the intensity of convective clouds that form over land. We investigate these land surface features in RCE simulations in Chapter 3 and Chapter 4 of this thesis.

Question two:

Are there physical linkages between these surface features and large-scale environmental parameters like CAPE known to favour thunderstorm development?

Another broad but significant question explored in this thesis is understanding

the environment within which convection thrives. The basis of a particular land surface feature exerting any form of control on the intensity of storms is centred around the features ability to provide a conducive environment that supports the enhancement of convection. Therefore a condition set in this thesis in assessing these surface features tested is that; the feature being studied should be able to shown increases in updraught velocity, and should also be able to show increases in CAPE. Since all the surface features tested in this thesis are founded on thermal difference between land and ocean surfaces, physical connection of the surface being tested to CAPE is an achievable condition if the feature indeed has any connection with the intensity of the convective storms over land. In line with this, part of the work in Chapter 3 and Chapter 4 is dedicated to investigating whether or not the surface features considered here have a physical relationship with CAPE. In both instances of a physical relationship or not, we attempt to understand the fundamental reasons for our results.

Question three:
How does the intensity of convective storms over a conceptual land surface respond to different temperature regimes? The last question generally seek to understand how moist convection response to warming over land surfaces. In this context, we are interested in all key aspects of convection. We are interested in the intensity of precipitation, there is a keen interest in how the intensity of convective storms over land response to warming as well understanding how environments conducive for storm enhancement may change in response to warming. We address these questions in Chapter 5 of this thesis.

Questions 1 and 2 set the basis for question 3, The land surface features found to be significantly linked to our defined metric of storm intensity is used to define our conceptual land surface. In this thesis we investigate three (3) characteristic features of the land surface; the deep boundary layer depth (high surface Bowen ratio), the heterogeneity of boundary layer depth, and the large diurnal cycle of surface temperature.

1.3 Outline of the thesis

So far we have discussed the significance and dangers of tropical thunderstorms and highlighted the need to study the distribution and intensities of these storms in response to global warming. The challenges and advances made in studying these future storms have also been discussed. The foundation of this thesis is therefore in two folds:
1. The thesis is founded on the observed land-ocean contrast in thunderstorm intensity over the tropics, and the hypothetical explanation given in literature.
2. The thesis is also founded on the general interest to understand moist convection over land and their potential changes with warming.

Guided by the three research questions (Section 1.2), this thesis uses a relatively high resolution CRM in idealized RCE simulations to first identify land surface features significant to the intensity of convective storms, and also investigate the response of the intensities of thunderstorms to warming of an idealized land surface.

The rest of the thesis is structured as follows:
In Chapter 2 we discus the general approach employed in this thesis. We describe the cloud-resolving model (CRM) and numerical framework used in this study. We also describe the general setup and simulation design that runs through the various experiments.

In Chapter 3 we address parts of the first and second research questions by examining two land surface features and their connection to thunderstorm intensity over the idealized land surface. We show that updraught intensity is insensitive to boundary layer depth over both homogeneous and heterogeneous land surfaces.

We further address the first and second research questions in Chapter 4 by investigating the connection between the large diurnal cycle of land surface temperature and intensity of thunderstorms over land. We show that the large diurnal cycle of surface temperature exerts some control on the intensity of convective storms in our idealized land-like simulations, and also has physical connections with CAPE over the land surface. The final research question is addressed in Chapter 5. Here we study how two surfaces forced to assume wet and dry land characteristics respond to warming. We show that updraught intensity, CAPE and precipitation

increases significantly to warming over the wet land surface in comparison to the dry land surface.

In Chapter 6 we discuses the key findings and synthesis of this thesis and make some conclusions. We highlight on the potential and failures of the different land surface features we studied. We recap on how the research questions in this thesis are addressed in the various experiments, and the key conclusions drawn from those experiments. We discuss the significance and shortcomings of this study and make some concluding remarks.

In Chapter 7 we present a general outlook and pathways to further understand findings in this thesis. We present our view on how future research with similar objectives as this study could be formulated to reduce some of the challenges of this research.

Chapter 2

General model description and setup

In this chapter we discuss briefly the general approach used in this thesis (Section 2.1), we describe the cloud resolving model (CRM) used in this work (Section 2.2), and present some background of the radiative-convective equilibrium (RCE) framework adopted for our simulations (Section 2.3). We finally describe the general setup that runs through the individual experiments of this thesis in Section 2.4.

2.1 General approach of the thesis

The overall approach of this thesis involves running relatively high resolution simulations of deep convection over a highly idealized land and ocean surfaces. Here, we used a cloud resolving model called System for Atmosphere Model (SAM) and adopt the radiative-convective equilibrium (RCE) approximation in all simulations. The first sets of simulations are designed to study specific land surface features hypothesized to control the intensity of storms that form over land. To isolate the individual effect of the surface feature being investigated, what we term land or land-like in our simulations only differ from a generic ocean surface by the imposed land surface feature being studied.

Results of the simulations of these land surface features are compared with simulations of deep convection over ocean (ocean-like) surfaces. For each land surface

feature investigated, we are first interested in identifying differences in updraught intensity between the simulated clouds of the particular land surface feature and that of the ocean's simulated convective clouds. Here, updraught intensity is measured by the 99.99th percentile of updraught velocity across all vertical levels of the atmosphere. For all land surface features identified to be linked to the intensity of convective storms and those that are not, we attempt to explain our results by appealing to conceptual models and theories that physically links updraught strength to parameters like CAPE, and entrainment. In all instances, we compare results from analysis of simulations of our land-like surface features to analysis of simulations over the ocean surface. These sets of simulations and analysis are designed to answer research questions one and two.

The final set of simulations are designed to address research question three. Here we run idealized high resolution simulations over a conceptual land surface with surface features found to exert some control on the intensity of convective storms from our earlier tests.

Our approach therefore does not involve the use land surface model. Essentially the ocean surface is made to behave like a land surface by imposing land surface features on the albeit ocean surface. The approach and results presented in this thesis are therefore not intended to replicate real world convection scenarios but to improve our understanding of convective processes and their underlying surfaces, and give an insight to how convection over land might likely change in the future.

2.2 System of Atmosphere Model (SAM)

As noted by Guichard and Couvreux (2017), cloud phenomenology, sensitivity and response to specific forcing are best studied with cloud resolving models (CRMs). In contrast to GCMs, CRMs have finer horizontal grid spacing to explicitly simulate individual clouds and cloud systems and they can be run long enough to study the entire cycle of clouds Randall *et al.* (2003). CRMs by virtue of their finer resolutions are useable in the study of all aspects of convection, and have been used as substitutes of conventional cloud parameterization schemes in GCM in the so-called superparameterization (Grabowski and Smolarkiewicz, 1999; Khairoutdinov and Randall, 2001). Earlier CRMs were mainly used in studies over relatively small domain sizes. However, modern CRMs are built to be able to resolve convection

on global scale with their model formulation set on longitudinal and latitudinal grids. The overwhelming advancement in technology and improvement in computation power have birth the so-called global cloud-resolving models (GCRMs) which appears to be the way forward in numerical study of the atmosphere Satoh *et al.* (2019).

The System of Atmosphere Model (SAM) is one such CRM/GCRM that has been used extensively to study various aspects of convection and other cloud processes. SAM is a non-hydrostatic model (Khairoutdinov and Randall, 2003) that can either be configured as a large-eddy simulation (LES) model to study shallow clouds and boundary layer processes, or a CRM to study deep convection. Ocean or land surface can be specified as the lower boundary in SAM simulations. In simulations with a typical land as the boundary surface, one can use a fully coupled simple land surface model (Jungmin M. Lee, 2016).

In SAM, the equations of motions are solved using the analestic approximation, finite difference of equations in the model uses the staggered Arakwa C - type staggering (Khairoutdinov and Randall, 2006).The model uses three prognostic variables (liquid/ice water static energy, non-precipitating cloud water/ice, and precipitating water) to describe thermodynamics.

There are three microphysics scheme options in SAM including the Thompsons single moment microphysics scheme, and the Morrison double moment microphysics scheme (Morrison *et al.*, 2005). Radiation in SAM can be simulated using either the Rapid Radiative Transfer Model (RRTM: Clough *et al.*, 2005), or version 3 of the Community Atmosphere Model (CAM3: Collins *et al.*, 2006) from the National Centre for Atmospheric Research (NCAR). The Monin-Obukhov similarity approach is used in the computation of surface fluxes in SAM, and subgrid-scale (SGS) fluxes can be computed using the 1.5-order SGS closure or the Smagorinsky SGS closure.

Simulations in SAM can be run using periodic lateral boundaries over the domain, there is also an option to use rigid horizontal walls. The model applies Newtonian damping at the top of the domain to reduce the buildup and reflection of gravity waves. SAM can be run on parallel computers using the Message Passing Interface (MPI) protocol. Simulations can be run in two (2D) or three-dimensions (3D). The newest version of SAM which is not yet available to the public can be run

on longitudinal and latitudinal grids and can be used as a global cloud resolving model (GCRM: Khairoutdinov *et al.*, 2022).

In the context of the objectives of this thesis, SAM have been used effectively in other parallel studies of convective processes of land and ocean surfaces (e.g., Lee *et al.*, 2018). SAM have also been used to study precipitation extremes and response of convection to warming (e.g., Muller *et al.*, 2011; Abbott *et al.*, 2020).

2.3 The Radiative-Convective Equilibrium Framework

In this thesis, the main numerical framework used in our model simulations is the radiative-convective equilibrium (RCE). RCE is an idealized energetic constraint of the global atmosphere (Jakob *et al.*, 2019), where there is a statistical balance between radiative cooling and convective heating in the atmosphere (Rochetin *et al.*, 2014). In this simplified approximation of the atmosphere, the assumption is that radiation acting on the atmosphere stirs up instability, convection lofts water upwards from the surface that eventually develops into clouds that affects radiative transfer. By this process the atmosphere continues to cool and convective clouds continue to form until such a time where the net loss in energy of the atmosphere by the radiative processes are in statistical balance with turbulent fluxes of latent and sensible energy represented as convection in the atmosphere. Generally, relaxation times of radiations are in days ($\sim$40 days) while convection occurs in a rather short time period (few hours) (Cronin and Emanuel, 2013). Therefore it is almost impossible to achieve total equilibrium due to chaotic variability in the atmosphere. However at longer time-scales, there is a statistical near-balance between time-averages of radiative and convective profiles. Although RCE approximation presents its own challenges, it remains a simple but yet power tool for the study of deep convection and convective processes in the tropics.

First introduced by Manabe and Strickler (1964) following earlier works (e.g., Goody, 1949), RCE simulations have evolved from the initial one-dimensional studies aimed at understanding the fundamentals of the atmosphere and climate and their sensitivities, through to two-dimensional studies on convection and its relationship with the environment (e.g., Held *et al.*, 1993; Randall *et al.*, 1994), to its current usability in three-dimensional studies of almost all aspects of the

climate system. Using a one-dimensional column model, Manabe and Strickler (1964) made adjustment to the radiative-equilibrium state of the atmosphere by prescribing a lapse-rate of 6.5 °C/km in the convective regions of the atmosphere. This approach set the basis of the radiative-convective equilibrium, as they found reasonable agreement of their calculate equilibrium in profiles of observed temperature in cloudy regions. Held *et al.* (1993) found a similar temperature profile between their two-dimensional model run to RCE, and observed temperature profile in the tropics. Their model explicitly predicted moist convection from an interactive radiation transfer within the atmosphere.

In recent years, improvement in computation power has broadened the use of RCE as the numerical framework of choice in different atmospheric models. The RCE approximation has been used in GCMs (e.g., Bony *et al.*, 2016; Reed *et al.*, 2021), they have been used extensively in cloud resolving models (CRMs) (e.g., Held *et al.*, 1993; Tompkins and Craig, 1998), and large-eddy simulations (LES) (e.g., Wing *et al.*, 2020) which are run in very high resolutions and therefore precludes the need for use of sub-grid scale parameterization scheme. Perhaps, the most interesting discovery in the use of RCE approximation across different spatial and temporal scales is the aggregation of convection or self-aggrefation as they have come to be known (Silvers *et al.*, 2016; Wing *et al.*, 2017) in CRM simulations.

Studies of RCE are mostly done over a horizontally uniform domain with constant sea surface temperature (SST) or SST prescribed using the slab ocean model (Wing *et al.*, 2018). Mostly the surface boundary has been an ocean. Few studies (e.g., Rochetin *et al.*, 2014) have explored RCE over land. Parallel to the set objectives of this thesis, idealized RCE simulations have been used to investigate deep convection response to different land-like surface features. Hansen and Back (2015) and Hansen *et al.* (2020) used RCE approximation to study deep convection response to the deep boundary layer and large diurnal cycle of temperature over land respectively. They have also been extensively used to simulate the response extreme precipitation and updraught intensity to warming (Muller *et al.*, 2011; Singh and O'Gorman, 2015; Seeley and Romps, 2016; Romps, 2019b).

The extensive use of the RCE framework in studies of idealized surface processes, and in simulations of future convective processes underpins its adoption for the simulations in this thesis. In this thesis, all simulations are run to RCE using the cloud resolving model described in Section 2.2.

2.4 General model setup

All simulations in this study are run to radiative-convective equilibrium (RCE) using version 6.11.2 of the System of Atmosphere Model (SAM: Khairoutdinov and Randall, 2003) over an ocean or land-like domain with a relatively fine resolution of 500 m. For all simulations, the domain dimension are 128 km $\times$ 128 km with 64 vertical levels ($\sim$ 27 km) as shown in Figure 2.1. The vertical grid has a 50 m spacing at the lower levels and 500 m grid space at the middle and upper levels, and the lateral boundaries are doubly periodic. The sea surface temperature (SST) in the various simulations is made to vary across the domain using the slab ocean model option available in SAM, with slight modification of the slab-ocean model made to achieve specific purposes in some simulations as detailed in the subsequent chapters. The depth of the slab ocean layer is pegged at 0.05 m to allow for shorter equilibration times of our simulations (Cronin and Emanuel, 2013). All simulations are run with a fixed solar constant of 551.58 W m^{-2} and at a zenith angle of 42.05° which translates to a total insolation of $\sim$409.6 W m^{-2}. This value is equal to the annual mean insolation over the tropics (Wing *et al.*, 2018). There is therefore no diurnal and seasonal cycle of insolation in our simulations, and the simulations are non-rotational as the effect of Coriolis is neglected.

In all simulations done in this thesis, the computation of shortwave and longwave radiations are done using the Rapid Radiative transfer model (RRTM) radiation scheme in SAM. Subgrid-scale turbulence are simulated using the first-order Smagorinsky SGS closure. We have used both single moment and double moment microphysics scheme in different simulations; details of the specific microphysics scheme used for a specific experiment is given in the subsequent chapters. Surface fluxes are calculated by SAM using the bulk aerodynamic formula with transfer coefficients evaluated using the Monin-Obuhkov similarity theory. For some experiments, these formulas are altered to achieve specific surface features being simulated; we present details of such alteration in Section 3.3.1. Newtonian damping is applied near the top of the domain to reduce reflection of gravity waves in our simulations.

The surface boundary of our simulations are either an ocean surface or an ocean surface forced to assume land surface features (land-like or land simulations). The land surface model option in SAM is not used in our set of land-like simulations and there is no background wind imposed in our simulations. Again, the domain in our

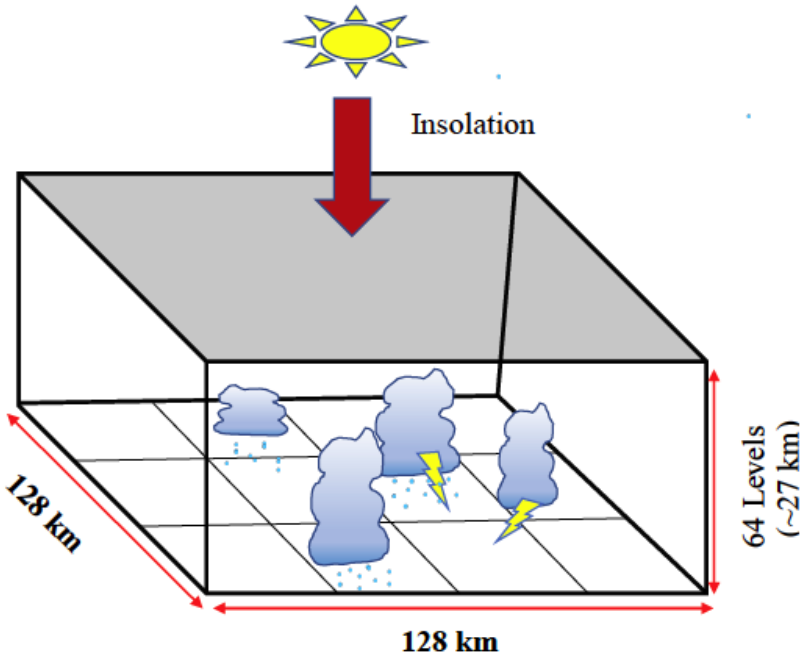

FIGURE 2.1: Schematic representation of SAM setup for idealized RCE simulations. The domain has a horizontal grid spacing of 500 m, vertical levels have 50 m spacing at the lower levels and 500 m spacing at the middle and upper levels.

simulation can either be homogeneous or heterogeneous depending on the specific experimental design and the surface feature being investigated. In simulations where the surface boundary is assumed to be heterogeneous, we elaborate on how the heterogeneity is achieved in the description of such experiments. Details of the duration of simulation and collection of simulation output for analysis are given in the subsequent chapters describing the different experiments.

Chapter 3

The insensitivity of convective intensity to different Surface Bowen Ratio and surface heterogeneity in radiative-convective equilibrium

This chapter is a full reproduction of a paper submitted to the Quarterly Journal of the Royal Meteorological Society (QJRMS) for publication. Section and figure numbers are modified to align with the thesis structure but the text and figures are unchanged.

3.1 Abstract

Previous modelling studies have come to mixed conclusions as to how changes in different surface properties may affect cloud updraft velocities in seeking to explain observed land-ocean contrasts in convective intensity. Here we show that varying surface Bowen ratio in idealised radiative-convective equilibrium (RCE) simulations over both homogeneous and heterogeneous surfaces does not result in significant changes to the intensity of convective storms as measured by high

percentiles of the updraught velocity distribution. While both a deeper boundary layer and heterogeneity of the surface can lead to a change in the cloud size distribution and consequent changes in cloud entrainment, we find that this only marginally affects the intensity of the strongest updraughts. These results are explained by appealing to a model of convection as a spectrum of entraining plumes. According to this model, updraft strength is primarily sensitive to the width of the distribution of entrainment among the spectrum of plumes. This is because entrainment sets both the profile within cloud updrafts and the mean lapse rate of the troposphere. If cloud sizes are increased, entrainment is reduced, and this both protects clouds from their unsaturated environment but increases the stability of the troposphere; each of these effects have countervailing influences on cloud updrafts.

3.2 Introduction

Multiple observation studies (e.g.; Lucas *et al.*, 1994; Christian *et al.*, 2003; Zipser *et al.*, 2006; Liu and Zipser, 2015) using different intensity metrics have argued that convective storms that form over land are substantially deeper and stronger than those that form over the ocean. Common metrics that have been used in assessing the intensity of storms include lightning flash rate (e.g; Zipser *et al.*, 2006), overshooting distances of convective clouds into the stratosphere (e.g; Liu and Zipser, 2005; Hong *et al.*, 2008), and the updraft velocity in convective clouds (e.g. Lucas *et al.*, 1994). For all these measures, continental storms have been shown to be substantially more vigorous than their oceanic counterparts.

To help explain the strong land-ocean contrast in storm intensity, Williams and Stanfill (2002) hypothesized a link between the intensity of storms over land and some physical characteristics peculiar to the land surface. Specifically, they highlighted the high boundary layer depth, high aerosol concentration, heterogeneous nature of the land surface, and strong diurnal cycle of temperature as characteristics that plausibly enhance the intensity of storms that form over land. However, a full theoretical understanding of the relative importance of these different surface features remains lacking. In this study, we focus on two of these characteristic features of the land surface, high boundary layer depth and spatial heterogeneity of surface fluxes, to assess their linkage to storm intensity in an idealized radiative-convective equilibrium (RCE) setting using a cloud resolving model.

As a result of the different partitioning between sensible and latent heat fluxes, the boundary layer tends to be substantially deeper over land surfaces compared to over the ocean (Avissar and Schmidt, 1998). A key measure of this partitioning is the surface Bowen ratio (SBR), given by the ratio of the sensible heat flux to the latent heat flux, which has been shown to be closely related to the boundary layer depth over much of the tropics (Kang and Bryan, 2011). Lucas *et al.* (1994) argued that the width of convective clouds scale with the size of boundary layer thermals; therefore, clouds that form over surfaces with higher Bowen ratio are rather wider at birth because the boundary layer is deeper. Such clouds therefore experience less dilution through mixing with the environment, potentially allowing them to achieve higher velocities.

Williams *et al.* (2004), using observations over islands of different sizes, affirmed that variations in boundary layer depth provide a plausible candidate in explaining the land-ocean contrast in storm intensity. A modelling study by Kang (2016) on the diurnal cycle of convective clouds with prescribed surface fluxes showed that afternoon convective storms were wider and more vigorous in cases with high SBR compared to those with low SBR. However, a contrasting study by Hansen and Back (2015) with no imposed diurnal cycle explored the sensitivity of different convective intensity metrics to changes in SBR in both RCE and initial-condition simulations, concluding that varying the boundary layer depth has little to no effect on the strength of convective storms as measured by high-percentile updraft velocity. Hansen and Back (2015) found the argument of deeper boundary layer depth leading to wider clouds and less entrainment made by some studies (e.g.; Williams and Stanfill, 2002; Williams *et al.*, 2005b) to be partially true; whereas the deeper boundary layer depth resulted in wider clouds, it did not lead to stronger convection, and the convective entrainment was found to be independent of the boundary layer depth.

The contrasting findings in the different studies may be attributed to a number of reasons including the experimental design, the numerical model used, and the metrics used in assessing the strength of the convective storms. It is also important to note that most studies that show intense storms over surfaces with a deeper boundary layer have an imposed diurnal cycle in their experimental design, the coupled effect of these two surface features (high SBR and strong diurnal cycle of temperature) may be the reason for the enhanced convection over land in these

studies, and possibly the reason for the difference in their results from studies that only consider the boundary layer depth of the land surface.

Heterogeneity of the land surface has also been suggested as a surface feature with potential control on the intensity of storms that form over land (e.g.: Hansen and Back, 2015; Romps *et al.*, 2018). For example, a number of studies have investigated the acceleration of the transition from shallow clouds to deep convective clouds over a heterogeneous land surface compared to a homogenous one. However, these studies do not focus on the intensity of deep convective clouds once they reach full maturity. A key goal in this study is therefore to understand how the intensity of deep convective clouds respond to a defined heterogeneous land surface within a radiative-convective equilibrium framework.

The land surface is made of different orographic features and vegetative cover, producing spatial differences in soil wetness and surface roughness and introducing heterogeneity at a variety of scales (Avissar and Schmidt, 1998). The nonuniform heating of the heterogeneous land surface results in spatial differences in surface fluxes which affect the state of the atmospheric boundary layer (Rieck *et al.*, 2014; Wu *et al.*, 2015b). For example, spatially varying soil moisture may produce patches of low (dry patch) and high (wet patch) evaporative fractions, which ultimately lead to different partitioning between the sensible heat flux (SHF) and latent heat flux (LHF) over the patches.

High resolution modelling studies on the effect of land surface heterogeneity on convection (e.g.: Giorgi *et al.*, 1997; Avissar and Schmidt, 1998; Kang and Bryan, 2011; Rochetin *et al.*, 2017; Lee *et al.*, 2018; Knist *et al.*, 2019) have found that surface heterogeneity induces mesoscale circulations that result in enhanced updraft velocity and faster transitioning of shallow to deep clouds mainly over regions with high SHF (dry patch). Lee *et al.* (2018) performed large-eddy simulations (LES) in which heterogeneity was introduced through a prescribed spatially varying SHF and found that shallow clouds that were able to transition into deep clouds formed mainly over the dry patches. They attributed this to the secondary circulation induced by the heterogeneity of the domain. They found that only simulations with heterogeneity patch size greater than 5 km could induced such circulations, highlighting the importance of the spatial scale of heterogeneity. A similar study by Rieck *et al.* (2014) also showed that shallow clouds transition faster into deep clouds over heterogeneous surfaces with large patch size compared to those over homogeneous surfaces. However, similar cloud size distributions were

found regardless of the heterogeneity patch size simulated. While the above studies demonstrate the effect of heterogeneity of surface fluxes on the initiation and transitioning of clouds, there are still outstanding questions as to whether and how a heterogeneous surface affects the peak intensity of storms.

Here we perform series of relatively high resolution simulations aimed at assessing the effects of varying SBR over both a homogeneous and heterogeneous domain on the intensity of storms as measured by high percentile updraught velocity. We vary the SBR by altering the moisture availability of the surface, guided by the available literature and hypotheses on land surface features and storm intensity. For each idealized RCE simulation, we are interested in finding the relationship between the SBR, the cloud size distribution, the convective available potential energy (CAPE), the dilution of the cloud core by environmental air (entrainment) and the resulting convective strength. We also run simulations for different heterogeneity patch sizes to assess whether the intensity of storms is affected by the size of the heterogeneous surface.

Although simulations of RCE present their own limitations, RCE has been shown to be an ideal tool for estimating convective processes and the sensitivity of deep clouds to specific surface features (Rochetin *et al.*, 2014). The idea here is to test the response of the intensity of convective storms to different surface features. Our approach therefore does not seek to replicate real-world convection scenarios.

The rest of the paper is structured as follows; we first describe the model setup and simulations (section 2). We then present results for the intensity of updrafts and its relationship to the cloud size distribution (section 3). We analyze the linkages between the surface moisture availability and its heterogeneity and large scale parameters like CAPE by applying a simple entraining plume representation of convection (Section 4). We finally recap the main findings and present conclusions (section 5).

3.3 Model description and setup

We run simulations to radiative-convective equilibrium (RCE) using version 6.11.2 of the System For Atmospheric Modeling (SAM; Khairoutdinov and Randall, 2003). All simulations are conducted with a horizontal grid spacing of 500 m over

a doubly periodic domain of 128 km × 128 km and 64 vertical levels. The simulations are non-rotational and have no imposed background flow. Subgrid-scale turbulence and microphysics are parameterised using a Smagorinsky SGS closure and Morrison two-moment microphysics scheme, respectively. Surface fluxes are evaluated using bulk aerodynamic formulas with transfer coefficients calculated using Monin-Obukov similarity theory. These formulas are altered to introduce variations in the moisture availability as described below.
Our simulations utilise the fully interactive Rapid Radiative Transfer Model scheme (RRTM; Clough *et al.*, 2005). There is no diurnal cycle in our simulations, we assume a constant solar flux of 551.58 W m^{-2} and a zenith angle of 42.05°. All simulations are run in 3D for a total of 50 days with statistics sampled at 30 minute intervals. Data from the last 20 days of the simulations are used in all analysis.

3.3.1 Altering the available surface moisture

The first set of simulations follow the approach of Hansen and Back (2015) to assess the effect of boundary layer depth on the intensity of convective storms over a homogeneous surface. An important control of the tropical boundary layer depth is the Bowen ratio, with the land surface generally having a higher Bowen ratio and consequently a deeper boundary layer than the ocean surface.

Here we alter the Bowen ratio in our RCE simulations by the introduction of an evaporative conductance parameter (α) into the bulk equation for the latent heat flux. The latent heat flux (LHF) is given by:

$$LHF = \alpha C_e |v| (q_s - q), \tag{3.1}$$

where C_e is the bulk transfer coefficient, $|v|$ is the magnitude of wind speed, q_s is the surface saturated specific humidity, and q is the near-surface specific humidity. The α value so introduced increases or decreases the latent heat flux; a higher α value results in higher latent heat flux and vice versa.

3.3.2 Simulations

For our control simulation, we use an α value of 1 which represents a simulation with higher latent heat flux (low SBR) typical of a tropical ocean-like surface (hereafter, HOM). For our homogeneous land-like simulation (hereafter, HOML), we use an α value of 0.25.

Extending the work of Hansen and Back (2015), we also run simulations over heterogeneous land-like domains to assess the impact of horizontal gradients of moisture availability and SBR on the intensity of convective storms. Heterogeneity is imposed over our domain in a checkerboard pattern with alternating α values of 1 and 0.25 to represent low SBR (cool and wet patch) and high SBR (warm and dry patch) regions respectively. We run four different simulations HET8, HET16, HET32 and HET64 to represent simulations over a heterogeneous land-like surface with patch sizes of side length 8 km, 16 km, 32 km and 64 km, respectively. For all land-like simulations, we devise an iterative approach to maintain a similar free-tropospheric temperature profile in each simulation, as described below.

3.3.3 Maintaining a similar free-tropospheric temperature profile

As noted by Hansen and Back (2015), lowering the α value to differentiate simulations over ocean and land surfaces result in cooling of the lower free troposphere and therefore requires a corresponding increment of the SST to ensure a relatively similar free-tropospheric temperature profile in the simulations. This is important because the free-tropospheric temperature is known to influence the intensity of storms (Singh and O'Gorman, 2015), and the tropics is known to have a relatively weak horizontal gradient in free-tropospheric temperature. A similar free-tropospheric temperature in all simulations is therefore achieved through an iterative process that works to nudge the mean SST at every time step until the lower-tropospheric temperature in the simulation is close to that of a reference temperature profile.

Firstly, for our control simulation HOM, the SST is made to be interactive across the model domain using a coupled slab ocean but a mean SST of 300 K is retained at each time step. The time and domain-mean temperature profile of this

simulation is then used as the reference profile for HOML and the heterogeneous simulations. Next, we run the land-like simulations with a modified slab-ocean lower boundary condition where there is marginal increment in mean SST at every time step until a mid-tropospheric temperature profile similar to the referenced profile from HOM is achieved. Specifically, the SST at each grid point is governed by a local energy balance equation given by:

$$c_{pl}h\frac{dSST}{dt} = F'_{\text{net}} - LHF' - SHF' + c_{pl}h\delta T \tag{3.2}$$

Here F_{net} is the net radiative flux into the surface, c_{pl} is the specific heat capacity of liquid water, and h is the depth of the slab. The primes refer to anomalies from the domain mean such that the energy imbalance over the entire domain does not cause any change in the domain-mean SST. Rather, the evolution of the domain-mean SST is governed by the final term, which is defined by a temperature increment δT. The temperature increment is given by

$$\delta T = \frac{(\int_{2km}^{6km} \overline{T} - \int_{2km}^{6km} T_t)}{H\tau} \tag{3.3}$$

where $\overline{T}$ is the mean reference temperature profile from our control simulation, T_t is the temperature profile for the current simulation at every time step, $H = 4$ km and $\tau = 6$ hours. The above procedure allows the surface to locally respond to energy imbalances to produce gradients in surface temperature, but it decouples the mean SST from the surface energy balance. Instead, the domain-mean SST evolves in such a way that the land-like simulations develop a similar temperature profile in the lower free troposphere (between 2 and 6 km) as HOM. In this way the free-tropospheric temperature remains almost equal between our low and high Bowen ratio cases. After implementing the free troposphere warming approach discussed above, the mean surface temperature for the homogeneous land-like simulation (HOML) was found to be 304.5K and a mean SST value of 301.7K was obtained for all the heterogeneous simulations. This results in a free-tropospheric temperature similar to that of HOM for all cases as shown in Figure 3.1

3.4 Results

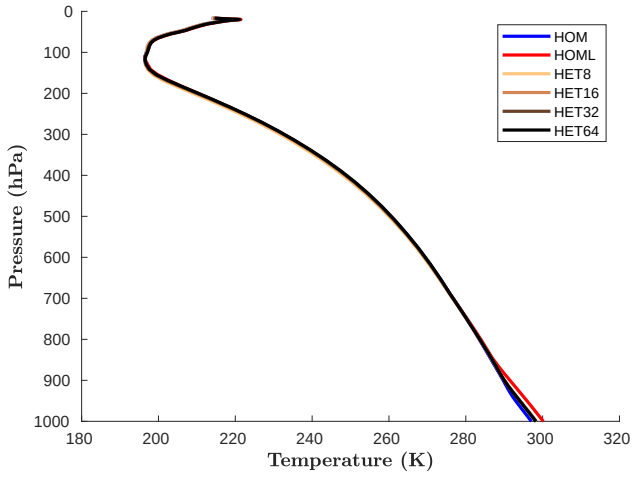

FIGURE 3.1: Time-and domain-mean temperature profile for homogeneous ocean-like case (HOM; blue), homogeneous land-like case (HOML; red), and heterogeneous cases with patch sizes ranging from 8 km (HET8; orange) to 64 km (HET64; black).

TABLE 3.1: Surface and boundary-layer properties averaged over the domain and for the last 20 days of each simulation. Boundary layer height h_{BL}, surface Bowen ratio (SBR), and relative humidity at the first model level (RH_{surf}). Boundary layer height defined as the lowest level with a non-zero cloud fraction, where cloudy grid points are taken as those with cloud water content greater than 0.01 g kg^{-1}.

Case	h_{BL} (m)	SBR	RH_{surf} (%)
HOM	598	0.09	76
HOML	1304	0.32	52
HET8	836	0.18	66
HET16	836	0.18	65
HET32	836	0.18	65
HET64	836	0.18	64

3.4.1 Boundary layer depth and cloud organization

As shown in Table 3.1, altering the moisture availability results in different boundary layer depths (as measured by the height of the cloud base) for the different simulations. Considering the two homogeneous cases, the land-like (HOML) simulation with an α value of 0.25 results in a relatively deeper boundary layer of approximately 1300 m, more than twice the boundary layer depth of the control case (HOM). The SBR for the HOML and HOM cases are 0.32 and 0.09 respectively. The influence of the surface fluxes on the near surface moisture is clearly

shown in the values of relative humidity at the first model level. The HOM case has a relatively wet surface with a relative humidity of 76% compared to the relatively dry HOML case with a mean near-surface relative humidity of 52%. For the heterogeneous simulations, the boundary layer depth, SBR and surface relative humidity are all approximately independent of patch size, and their values fall in-between those of HOM and HOML. The similar domain-and-time average structure of variables within the boundary layer in the heterogeneous cases agree with earlier findings of Liu *et al.* (2017) who concluded that domain-and-time averages of state variables and fluxes in the boundary layer are insensitive to the heterogeneity of the land surface. With the same evaporative conductance parameter (α) and mean surface temperature in the heterogeneous cases, similar surface fluxes are set amongst the different simulations resulting in similar surface relative humidity and ultimately similar cloud base heights.

Figure 3.2 shows the time-mean distribution and organisation of cloud water path (CWP) in each simulation. This provides a sense of the arrangement of clouds over both the homogeneous and heterogeneous surfaces. Clouds appear to form relatively randomly in simulations with a homogeneous surface (HOM and HOML), with little evidence of organization or aggregation behavior that is seen in some previous RCE simulation studies (e.g: Bretherton *et al.*, 2005). For the heterogeneous cases (HET8, HET16, HET32, HET64), clouds predominantly form over regions with low evaporative fraction (dry patches), consistent with earlier findings (e.g.: Kang and Bryan, 2011; Rieck *et al.*, 2014; Wu *et al.*, 2015a; Lee *et al.*, 2018).

This may be explained by appealing to the mesoscale secondary circulation mechanism reported in various studies; the horizontal gradients in SHF over the heterogeneous domains result in horizontal pressure gradients which lead to the advection of moisture from the cool and wet patches to the warm and dry patches (Giorgi *et al.*, 1997). The so-induced circulation results in vertical transport of moisture and subsequent cloud formation over the dry patches.

3.4.2 Updraught Velocities

Figure 3.3 shows the updraught strength of the simulations as measured by the 99.99th percentile vertical velocity (Figure 3.3a) and the mean in-cloud vertical velocity (Figure 3.3b) at each vertical level. Variations in the surface conditions have a very weak effect on the intensity of storms. For both intensity metrics

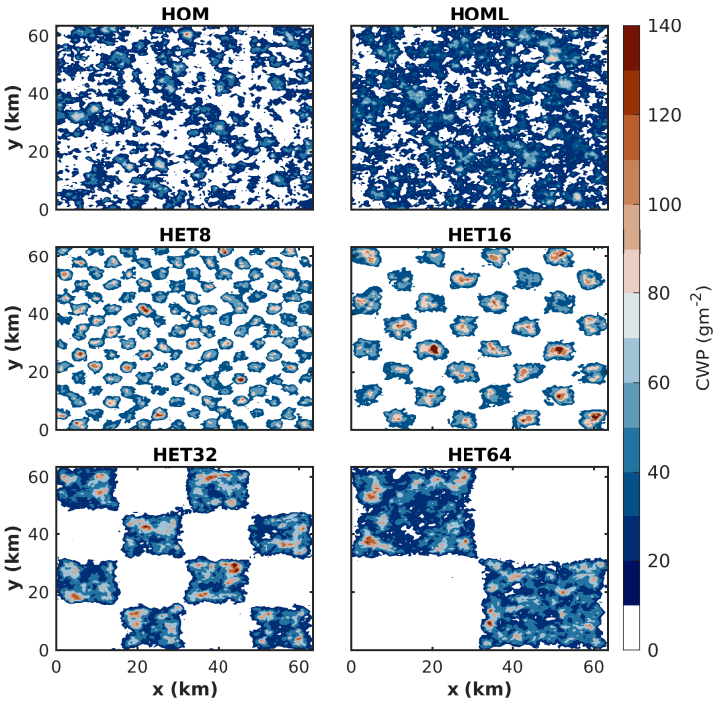

FIGURE 3.2: Time-mean cloud water path in each simulation. Upper row gives homogeneous ocean-like (HOM) and land-like (HOML) cases, middle and bottom row gives heterogeneous simulations with increasing patch size ranging from 8 km (HET8) to 64 km (HET64) in side length.

considered, there appears to be no invigoration of the storms with boundary layer depth. This agrees with similar findings by Rieck *et al.* (2014) and Hansen and Back (2015). Indeed, our simulations show an in-cloud vertical velocity of about 1 ms^{-1} higher over the ocean-like (HOM) simulation at the 500 hPa level compared to the land-like simulation (HOML).

There is no definite pattern in our heterogenous simulations to support the hypothesis that updraught velocity over a heterogenous surface increases with increasing heterogeneity patch size. Again, there is no significant difference in the updraught velocities between the homogeneous simulations and the heterogeneous simulations. Hence, the hypothesis that a heterogeneous surface could invigorate storms is not supported in our idealised simulations when the entire domain is considered.

3.4.3 Cloud Sizes

We explore our results further by assessing the sizes of clouds from the simulations. Differences in cloud sizes, driven by variations in boundary layer depth, provides

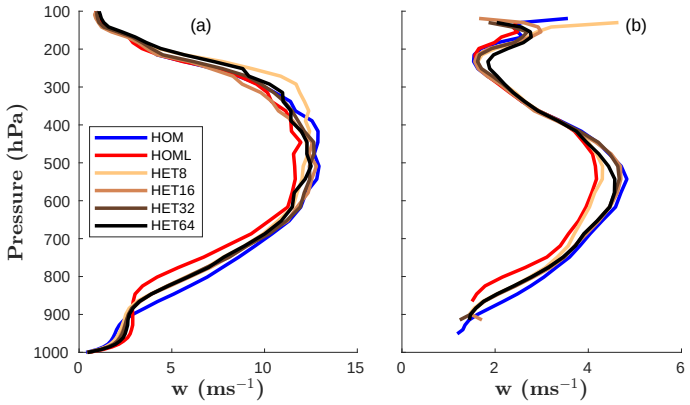

FIGURE 3.3: Profile of updraft velocities for homogeneous and heterogeneous simulations as given in the legend. (a) 99.99th percentile vertical velocity at each vertical level, and (b) cloud core vertical velocity at each vertical level, where cloud cores are defined as any cloudy point with vertical velocity w greater than 1 ms^{-1}.

one possible mechanism by which the SBR may influence the intensity of storms (Williams *et al.*, 2005a). It is argued that the deeper boundary layer over land leads to larger cloud sizes which are less affected by entrainment therefore achieving higher buoyancies. To estimate cloud size, we define cloudy grid points as those with a non-precipitating condensate value of 0.01 g kg^{-1} or greater. We then form clusters of cloudy points by taking 8-connected regions of clouds that occupy 8 grid-points or more. The size of the cloud is then given by the horizontal area of a given cluster.

Figure 3.4 shows the distribution of cloud area between 2 and 5 km from each simulation. For the homogeneous simulations, the land-like case (HOML) exhibits a shift in the distribution from small clouds (< 5 km^2) to larger clouds when compared to the ocean-like case (HOM).

Considering the heterogeneous simulations, cloud area tends to increase with the heterogeneity patch size; the largest clouds are twice as large in the simulation with largest patch size (HET64) compared to the simulation with the smallest patch size (HET8). Although the cloud areas calculated in the heterogeneous simulations increase with patch size, the difference in cloud area does not necessarily scale with the difference in patch sizes. Furthermore, from our simulations, there is no evidence to support the notion that clouds that form over heterogeneous surfaces are larger than those that form over homogeneous surfaces. Indeed at the 99.99th percentile (not shown), the largest clouds are over the homogeneous land-like case

(HOML) albeit marginally wider than the heterogeneous case with large patch size (HET64).

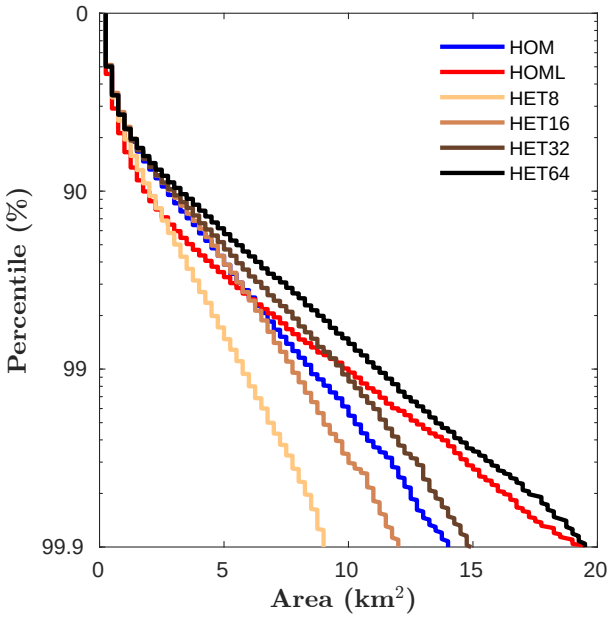

FIGURE 3.4: Cumulative distribution function of cloud area for levels between 2 and 5 km in height. Cloud area is calculated based on 8-connected clusters of cloudy grid points with non-precipitating condensate 0.01g kg^{-1} or greater. Cloud sizes at each model level between 2 and 5 km are considered separately and then combined to form a single distribution.

3.5 Physical mechanisms

We have seen that neither boundary layer depth variations nor heterogeneity of surface moisture availability result in substantial invigoration of convective storms in RCE despite having some effect on the size distribution of clouds. We now attempt to understand the physical basis for this lack of sensitivity. Specifically, we examine the effect of convective entrainment on our simulations. Williams and Stanfill (2002) hypothesized that wider clouds would experience less dilution from entrainment, thereby achieving higher updraft speeds. However, Singh and O'Gorman (2013) found that, in RCE, convective entrainment also plays a role in setting the tropospheric lapse rate. They introduced a theoretical model for the lapse rate based on a neutrally buoyant entraining plume that implies that CAPE increases with the entrainment rate. Extending this work, Singh and O'Gorman (2015) developed a two-plume model, in which the second plume represents the most intense updrafts, to account for changes in updraft speeds with warming in

RCE. According to this two-plume model, cloud updraft velocities are determined by a measure of the width of the distribution of entrainment rates experienced by different updrafts. Here, we examine to what extent these ideas are able to explain the results of our simulations with varying boundary-layer depth and varying surface heterogeneity.

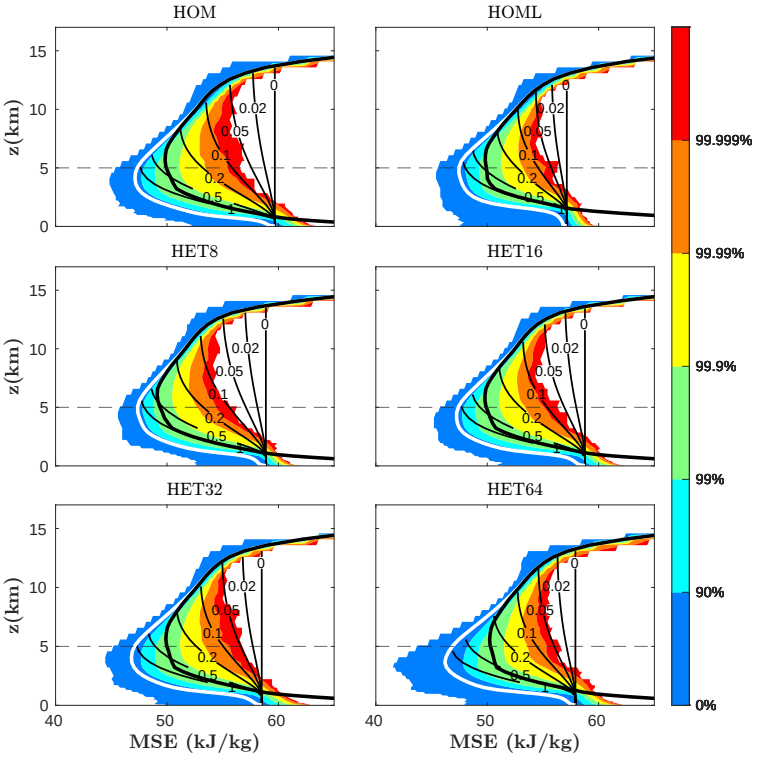

FIGURE 3.5: Cumulative distribution function of Moist Static Energy (MSE) at each level (colours) in the homogenous (top row) and heterogenous (middle and bottom row) simulations as labeled. White lines give domain- and time-mean MSE $\overline{h}$, thick black lines give domain- and time-mean saturated MSE $\overline{h}^*$ and thin black lines give MSE profiles h_p for plumes with entrainment rates as given by the labels in units of km^{-1} Grey dashed line marks the 5 km level.

3.5.1 Interpretation using spectrum of entraining plumes

To begin, we interpret our simulation results within a framework in which convection is represented as a spectrum of entraining plumes. To do so, we consider the distribution of moist static energy (MSE) at each vertical level within the simulations. Here the MSE h is defined

$$h = c_p T + gz + L_v q, \tag{3.4}$$

where, c_p is the isobaric specific heat capacity of dry air, T is the temperature, g is gravity, z is the height above the surface, L_v is the latent heat of vaporization, and q is the specific humidity of water vapor. As shown in Figure 3.5, at most levels within the free troposphere, the vast bulk of the MSE distribution is concentrated close to the mean MSE $\overline{h}$, but there are some gridpoints that have relatively high MSE values, far in excess of $\overline{h}$ or even the mean saturation MSE $\overline{h}^*$ at that level, and closer to the typical MSE values in the boundary layer. Since the MSE is approximately conserved for adiabatic motions, we may interpret these high-percentile MSE values as occurring in air that has experienced a relatively low amount of entrainment as it has risen through clouds from the boundary layer.

To quantify the entrainment experienced by air parcels with different values of MSE, we define a set of plumes with moist static energy h_p governed by the equation

$$\frac{dh_p}{dz} = -\epsilon(h_p - \overline{h}) \tag{3.5}$$

with lower boundary conditions given by the mean MSE at the lowest model level, and with a variety of different entrainment rates ϵ. For simplicity, we use constant values of the entrainment rate in the free troposphere and set $\epsilon = 0$ within the boundary layer. We may now define an effective entrainment rate for air parcels within the free troposphere based on the value of ϵ that gives $h_p(z;\epsilon) = h(z)$ at a given height z. The value of $h_p(z;\epsilon)$ for a range of entrainment rates is shown by the thin black lines on Figure 3.5.

Examination of Figure 3.5 reveals that different simulations have differing distributions of the effective entrainment rate. For example, the 99.99th percentile of the MSE distribution has an effective entrainment rate of roughly 0.2 km^{-1} over the lower troposphere in HOM, whereas for the same percentile the effective entrainment rate is closer to 0.15 km^{-1} in HET64. The variation in SBR, and the associated variations in boundary-layer depth and cloud size, appear to induce a change in the distribution of entrainment across the simulations. Why does this not lead to larger changes in updraught velocity?

To answer this question, we note that cloud buoyancy depends on the density of a cloud compared to its environment, which is approximately a monotonic function of the difference $h^* - \overline{h}^*$, where h^* is the in-cloud saturation MSE. Cloud buoyancy therefore depends not only on high-percentiles of the MSE distribution but also the

saturation MSE of the mean profile, and a model for both is needed to understand convective intensity.

Singh and O'Gorman (2013) provided a model for the mean saturation MSE $\overline{h}^*$ in RCE based on the assumption that convection remains neutrally buoyant relative to an entraining plume initialized within the boundary layer. However, this zero-buoyancy plume model cannot be used to estimate convective intensity, because it neglects cloud buoyancy entirely and assumes $h^* - \overline{h}^* = 0$. To remedy this, Zhou and Xie (2019) extended the zero-buoyancy plume model to a spectrum of plumes, with $\overline{h}^*$ set by the plume that becomes neutrally buoyant at level z. Here we follow Singh and O'Gorman (2015) and consider the simplest possible spectral approach that considers only two entraining plumes. In this two-plume model, one plume represents the bulk of the convective mass flux; the mean profile is assumed to be neutrally buoyant to this plume with entrainment rate ϵ_{mean}. The second plume represents high-percentile updrafts and has a correspondingly lower entrainment rate.

We estimate these two entrainment rates for each of our simulations at a mid-tropospheric level $z_m = 5$ km. The entrainment rate ϵ_{mean} is given by the entrainment rate such that $h_p(z_m; \epsilon_{\text{mean}}) = \overline{h}^*(z_m)$. This may be visualized as the entrainment rate for which the thin black curves on Figure 3.5 intersect the saturated MSE (thick black) curve at $z_m = 5$ km. The entrainment rate of high-percentile updrafts $\epsilon_{99.99}$ is given by the entrainment rate such that $h_p(z_m; \epsilon_{99.99}) = h_{99.99}(z_m)$, where $h_{99.99}$ is the 99.99th percentile MSE. This may be visualized as the intersection of the thin black curves on Figure 3.5 and the boundary separating yellow and orange at the 5 km level. It is important to note that non-entraining plumes are essentially absent in our simulations, since even for the highest MSE percentiles, the effective entrainment rates remain substantial.

3.5.2 Cloud size and entrainment

Having diagnosed the bulk entrainment rate ϵ_{mean} and the high-precentile entrainment rate $\epsilon_{99.99}$, we may now evaluate how they vary across the simulations. As shown in Figure 3.6c, both ϵ_{mean} and $\epsilon_{99.99}$ decrease with increasing patch size in the heterogeneous cases. The bulk entrainment of HET8 is roughly double that of HET64. On the other hand, for the homogenous cases, ϵ_{mean} is slightly larger in HOML compared to HOM, while $\epsilon_{99.99}$ has the opposite trend.

TABLE 3.2: Analysis of key environmental parameters from the simulations. The vertical mean relative humidity averaged between 2 to 3 km RH_{23}, the pseudo-adiabatic CAPE, the entrainment rate for the bulk of the convective mass flux ϵ_{mean}, the high-percentile entrainment rate $\epsilon_{99.99}$, and scalings for the CAPE and square of the updraught velocity w^2 according to the two-plume model.

Case	RH_{23}	CAPE (kJ kg^{-1})	ϵ_{mean} (km^{-1})	$\epsilon_{99.99}$ (km^{-1})	$\epsilon_{\text{mean}}(1 - RH_{23})$ (km^{-1})	$\delta\epsilon(1 - RH_{23})$ (km^{-1})
HOM	0.81	1.79	0.432	0.192	0.082	0.047
HOML	0.82	1.14	0.455	0.171	0.082	0.051
HET8	0.84	1.94	0.548	0.239	0.088	0.049
HET16	0.80	1.60	0.437	0.185	0.087	0.050
HET32	0.78	1.45	0.388	0.170	0.085	0.048
HET64	0.74	1.24	0.301	0.135	0.078	0.043

Since the size of clouds increases with patch size, the entrainment variations in the heterogenous cases are consistent with the hypothesis that wider clouds are more protected from the environment and entrain less (Williams and Stanfill, 2002). For example, in the heterogenous cases, the bulk entrainment rate ϵ_{mean} monotonically decreases with an increase in the size of clouds, as measured by the 99.9th percentile (Figure 3.6d). In the homogenous cases, the relationship between cloud size and entrainment depends on the part of the cloud-size distribution that is examined. HOML has fewer moderate sized clouds ($\sim$ 5 km^2), but a larger number of large clouds in excess of 10 km^2. This is consistent with the hypothesised relationship between cloud size and entrainment if one supposes that the entrainment rate for the bulk of the convective mass flux is set by the more numerous but relatively small sized clouds, while the entrainment rate of the most intense updrafts is set by the largest clouds.

3.5.3 Effects of entrainment on CAPE and updraught velocities

According to the two-plume model of Singh and O'Gorman (2015), the entrainment rates ϵ_{mean} and $\epsilon_{99.99}$ respectively control the lapse rate and updraft distribution of convection in RCE. Specifically, for a constant mean temperature and depth of troposphere, the two-plume model suggests that the convective available

potential energy (CAPE) scales as

$$CAPE \sim \epsilon_{\text{mean}}(1 - RH), \tag{3.6}$$

where RH is a measure of the tropospheric relative humidity. The equation above is based on the fact that the deviation of the lapse rate from that of a moist adiabat is due to the mixing of dry air into clouds as they rise toward the tropopause. The effect of this mixing is proportional to the entrainment rate ϵ_{mean} and the subsaturation of the free troposphere (see Eq. (4) of Singh and O'Gorman, 2013).

To test the scaling (Equation 3.6), we diagnose CAPE in each simulation as the integral of the positive buoyancy of a parcel lifted pseudoadiabatically and initialised with the mean temperature and specific humidity at the lifting condensation level in each simulation. Ice processes are treated with a mixed-phase range between 233.15 and 273.15 K. The parcel buoyancy is then calculated with respect to the domain-and time-mean virtual temperature.

In our heterogenous simulations, the CAPE, ϵ_{mean}, and the lower tropospheric RH all decrease marginally with increasing patch size (Figure 3.6). Interpreting this through the lens of the two-plume model, this suggests that changes in relative humidity and entrainment have opposite influences on the CAPE, although the effect of changing entrainment wins out, causing CAPE to decrease with patch size. Indeed, as shown in table 2, the value of $\epsilon_{\text{mean}}(1 - RH_{23})$ where RH_{23} is the mean relative humidity between 2 and 3 km does decrease with patch size, although the fractional decrease is smaller than that of the CAPE.

In the homogenous simulations, the CAPE decreases considerably as the SBR increases, but the entrainment rate and relative humidity change only marginally and in ways that would affect the scaling for CAPE in opposite directions. The two-plume model therefore does not capture the behaviour of the CAPE in response to a change in boundary layer depth. We do not at present have a full explanation for this result, but we speculate that changing the depth of the boundary layer affects turbulence characteristics within it, thereby affecting the properties of air parcels that leave the boundary layer in clouds. Our calculation of CAPE, however, neglects such effects; it assumes that the relevant parcel has the mean properties of the lowest model level in all cases.

Finally, we turn to convective intensity itself. According to the two-plume model, the buoyancy within the strongest updrafts depends on the difference between the

entrainment rate relevant to the bulk of convection and the entrainment rate relevant to high-percentile updrafts. Singh and O'Gorman (2015) derive an equation for the temperature excess within such strong updrafts [see their Eq. (10)]. Based on this, we may write a scaling relation for updraft velocity given by

$$w^2 \sim \delta\epsilon(1 - RH). \tag{3.7}$$

Here w is a measure of updraft strength and $\delta\epsilon = \epsilon_{\text{mean}} - \epsilon_{99.99}$. This scaling relation assumes that the free tropospheric temperature and the depth of convection are invariant; owing to our free-tropospheric temperature relaxation approach, these are good approximation in our simulations.

Consistent with the results for vertical velocity presented in the previous section, the scaling (Equation 3.7) varies little across both the homogenous and heterogenous simulations (table 2) except in the case of HET64. This is despite variations in the entrainment rates ϵ_{mean} and $\epsilon_{99.99}$ and the subsaturation $(1 - RH_{23})$ of the order of 100%. The reason for this is two-fold. Firstly, in the heterogenous simulations, ϵ_{mean} and $\epsilon_{99.99}$ vary together, and so their difference has relatively small variations. As the patch size increases, all clouds become larger, reducing the amount of entrainment into clouds. On its own, this would act to strengthen the strongest updrafts. However, because the lapse rate itself is dependent on entrainment, the atmosphere becomes more stable, reducing the instability. These two effects offset each other and their effect on the updraft speed. Notwithstanding the above offsetting effect, the simulations do exhibit some changes in the entrainment difference $\delta\epsilon$, particularly for the homogenous cases. However, we also find that the environmental relative humidity tends to vary in such a way as to offset some of these changes, resulting in weak changes in the vertical velocity scaling across all simulations.

The scaling Equation 3.7 provides a mechanistic explanation for the insensitivity of updraft velocity to SBR variations found in this and previous work (e.g., Hansen and Back, 2015). Countervailing changes in entrainment and relative humidity conspire to keep updrafts at a similar strength despite changes in cloud size and changes in diagnosed entrainment rates. Whether this cancellation of the effect of changes in entrainment and relative humidity across our simulations represents a more fundamental control of updraft speed in moist convection is a tantalising question that we hope to pursue in future work. Figure 3.7a shows the relationship

of the undiluted undiluted CAPE calculated from mean profiles of the RCE simulations, and the scaling of CAPE (ϵ_{mean}(1-RH)) from the two-plume model. The relationship of the square of mid-tropospheric mean vertical velocity (w_2) and the two-plume scaling of updraught velocity ($\delta\epsilon$ (1-RH)) is also shown on Figure 3.7b.

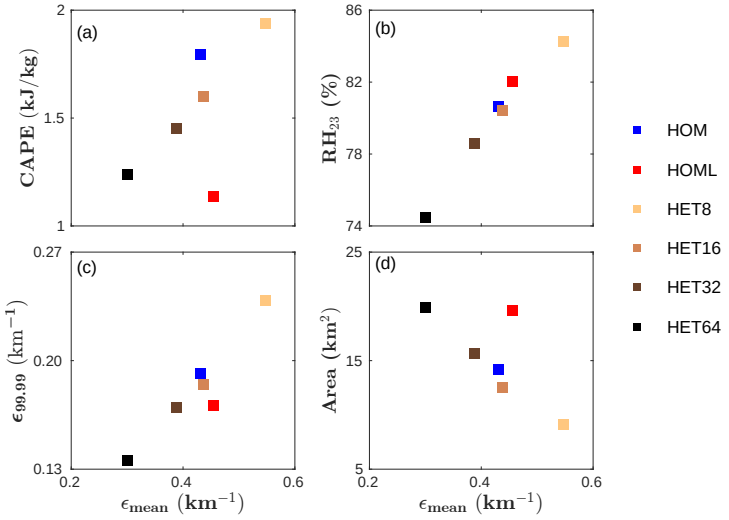

FIGURE 3.6: (a) CAPE, (b) Relative Humidity averaged between 2 and 3 km (RH_{23}), (c) the high-percentile entrainment rate $\epsilon_{99.99}$, and (d) the 99.9th percentile of the cloud size distribution between 2 and 5 km plotted as a function of the bulk entrainment rate ϵ_{mean}.

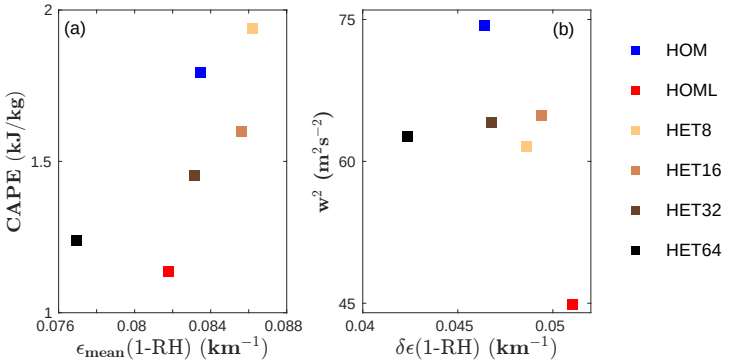

FIGURE 3.7: Plot of the relationship between (a) undiluted CAPE and the simple scaling of CAPE (ϵ_{mean}(1-RH)) and (b) squared mid-tropospheric mean vertical velocity and the simple two-plume scaling of updraught strength ($\delta\epsilon$(1-RH))

3.6 Summary and conclusions

This study explores the effect of two characteristic features of the land surface on the intensity of storms in idealized RCE simulations using a cloud resolving model.

Simulations of high and low SBR over both homogeneous and heterogeneous surfaces are run to test the hypothesis that the high SBR and heterogeneous nature of the land surface controls the intensity of thunderstorms that form over land. It is shown from the simulations that varying the SBR over a homogeneous surface and on a surface with checkerboard pattern of varying SBR with different patch sizes does not lead to significant changes in the intensity of storms as measured by both the highest percentile in the vertical velocity and the in-cloud vertical velocity.

Consistent with the hypothesis by Williams and Stanfill (2002), a deeper boundary layer depth results in a shift toward more clouds of large spatial extent, eventually leading to differences in the distribution of entrainment, since wider clouds tend to entrain less environmental air. However, in contrast to the hypothesis and consistent with Hansen and Back (2015), the intensity of the convection does not significantly change with changing boundary layer depth. Indeed from our simulations, the cloud core vertical velocity is marginally higher in the case with shallow boundary layer depth. For the heterogeneous simulations, cloud size increases with increasing heterogeneity patch size, and therefore entrainment rate decreases with increasing patch size, but as above, this has negligible effect on measures of convective intensity such as updraft velocity.

In contrast to updraft velocity, CAPE does vary across the simulations, with the highest CAPE found in the heterogenous simulation with the smallest patch size, with CAPE systematically decreasing with increasing patch size. The disconnect between the strong variations in CAPE and the lack of variation in convective updraft velocity suggests that, consistent with previous modelling studies (e.g., Romps, 2011) undiluted cloud updrafts are virtually non-existent in our simulations.

To understand the above results, we adopted a theoretical model of convection in RCE as a spectrum of entraining plumes (Zhou and Xie, 2019). For simplicity, we limited the spectrum to only two plumes, one representing the bulk of the convective mass flux and the other representing the strongest updrafts. According to this conceptual model, the CAPE and environmental relative humidity are set by a characteristic "bulk" entrainment rate, while strong updrafts are maintained by entraining plumes with relatively low values of the entrainment rate. The magnitude of these strong updrafts are then dependent on the difference in the

rate of entrainment between the bulk of convection and the strongest updrafts (Singh and O'Gorman, 2015).

According to the two-plume model, the lack of variations in updraft velocity in our simulations was a result of similar changes in the entrainment rates for the bulk of the convective mass flux and for the strongest updrafts. In addition, variations in relative humidity that offset changes the effects of a changing entrainment distribution also contributed to the insensitivity of updrafts to varying SBR and varying patch size.

While the two-plume model gives a parsimonious explanation for updraft variations among our simulations, it should be noted that it failed to account for variations in CAPE in our homogenous simulations. We speculate that this is because our measure of CAPE did not sufficiently account for differences in the properties of cloudy air parcels as they left the boundary layer that occur as the boundary layer deepens.

Our results point to a limited effect of heterogeneity and boundary-layer depth in invigorating convection in the setting of RCE. Based on our plume-spectrum model, this insensitivity of updraft strength may be partially explained by the sensitivity of the lapse rate (and therefore CAPE) in RCE to convective entrainment. In the tropics, the lapse rate is not set locally but is rapidly homogenized over large regions through the action of waves and the large-scale flow (Charney and Eliassen, 1964). This may provide a mechanism by which spatial variations in cloud entrainment, driven by spatial variations in surface properties, may be translated into more intense cloud updrafts. Exploring this mechanism using methods to parameterize the large-scale flow (e.g., Sobel and Camargo, 2011; Kuang and Bretherton, 2006) is a possible avenue for future work.

Finally, we note that while we have examined two possible surface properties that may drive the observed land-ocean contrast in convective intensity, there are many a number of other hypotheses for the origin of this contrast that are relevant. For example, the large diurnal cycle of temperature over land compared to that of ocean has been suggested as a possible reason for enhanced convective intensity over land. However, a recent paper by Hansen *et al.* (2020) found this mechanism not to be effective in explaining the land-ocean contrast in storm intensity. Additionally, the effects of aerosols on invigorating convection have long been hypothesized to contribute to the land ocean contrast because of the higher aerosol

loading over land (Williams and Stanfill, 2002; Abbott and Cronin, 2021). A comprehensive account of the factors that control the land-ocean convective intensity contrast therefore remains elusive.

Chapter 4

Diurnal cycle of temperature control on intensity of thunderstorms

4.1 Background

In this chapter, we investigate how the large diurnal cycle of surface temperature is connected to the intensity of convective storms that form over land. The set of experiments in this chapter are designed to address parts of research questions one and two of this thesis. Idealized RCE simulations are run over two different configurations of a land-like surface, and over an ocean surface. In line with the objectives of the first two research questions of this thesis, we assessed differences in updraught velocity, CAPE, and precipitation among the three simulations. We show that differences in updraught velocity over land and ocean surfaces in our simulations can be linked to a measure of CAPE, if only the parcels with the strongest updraught are considered, and more importantly when the measure of CAPE considers entrainment. The results from our set of simulations provide some evidence that the large diurnal cycle of surface temperature has physical connections with the intensity of continental thunderstorms but may not be the main surface feature controlling the intensity of these storms.

We first review the basis for the hypothesis that links the large diurnal cycle of the land surface to the intensity of continental storms in Section 4.2, we then describe the model setup and experimental design for these simulations that test the connection of the diurnal cycle of surface temperature to the intensity of storms in Section 4.3, the key results and analysis of this experiment are presented in Section 4.4, and the main conclusions of this experiment are discussed in Section 4.5.

4.2 Introduction

The characteristic large diurnal cycle of surface temperature over land surfaces has been mentioned as a plausible control of the intensity of storms that form over land, and possibly a physical explanation to the observed land - ocean contrast in intensity of storms over the tropics (Williams and Stanfill, 2002; Christian *et al.*, 2003; Romps *et al.*, 2018).

Diurnal cycle is a generic term usually used to describe any pattern that recurs over a 24 hour period. In this context, the diurnal cycle of surface temperature is just the daily variation of high and low surface temperatures of the land surface. Surface and atmospheric variables such as temperature, wind, and sometimes precipitation over land surfaces seem to exhibit a near consistent diurnal pattern in terms of when they peak and when they are minimal (Betts, 2003). Naturally, how high or low the surface temperature over land surfaces is dependant on the on the amount of solar energy received and the nature of the land surface (Sobel *et al.*, 2001). For example, diurnal variation of surface temperature over humid surfaces are more moderated than over dry surfaces. Over deserts and arid land surfaces where the land surfaces are dry and the air above are less humid, the diurnal temperature range is greater compared to a more humid. land surface. The state of the atmosphere also plays a key role in determining the total radiation that reaches or leaves the earth's surface, and the partitioning of the incoming solar radiation into different heat fluxes depends on the nature of the surface. Comparatively, the land surface has a larger diurnal temperature range than the ocean surface. This is as a result of the difference in heat capacity between the land and ocean surfaces(Betts, 2003). The ocean has a large effective heat capacity because the energy absorbed in the surface skin layer is rapidly mixed downwards through the mixed layers. Again insolation penetrates tens of meters into the ocean. This reduces the variability of the skin temperature of the ocean surface. The land surface

however has a low heat capacity and minimal mixing within its layers, therefore the skin temperature at the land surface increases rapidly in response to incoming solar radiation that strikes the surface. Indeed, the extent of variability of the the surface temperature over land depends greatly on the geographical state of the land surface; whether it is a desert, forested, humid or dry (Sharifnezhadazizi *et al.*, 2019).

Over tropical land surfaces, there is an overall scientific agreement on the diurnal pattern of surface temperature and near surface air temperature during the day. In response to incoming solar radiation, near - surface temperature begins to rise during sunrise as thermal fluxes of the surface interacts with the atmosphere above it. Usually near surface air temperature peaks after noon and falls after sunset establishing a significant temperature range during the day (Yang and Slingo, 2001; Betts, 2003; Zhao *et al.*, 2021). Such large range in surface temperature is not seen over ocean surfaces. Betts (2004) in an observation study found that under light wind conditions, the diurnal temperature range over tropical ocean surfaces can go up to 1 K, but this is rarely achieved, and even if it is, the temperature range is insignificant when compared to the large diurnal temperature range observed over different land surfaces.

The idea that the large diurnal cycle of temperature could be the surface feature that controls the intensity of storms over land is premised on the thermal difference between land and ocean surfaces, and how the thermal fluxes interacts with the relatively colder lower free-troposphere (Williams and Stanfill, 2002). As noted by Charney (1963), there is a weak gradient in free-tropospheric temperature over the tropics, as a result, the free-tropospheric temperature over land and ocean surfaces are faily similar. Convection over the tropical ocean surfaces are said to induces gravity waves that modulate the free tropospheric temperature over land, maintaining a weaker gradient of free-tropospheric temperature over the tropics (Sobel *et al.*, 2001). According to the physics that support the large diurnal cycle of surface temperature as a plausible candidate that controls the intensity of continental storms, the warmer land surface continually interacts with the relatively cold lower free troposphere during the day as surface temperature gets to its maximum, this interaction between the surface and the lower free-troposphere would result in a build up of CAPE that would support convection over the land surface provided the relative humidity in the boundary layer does not become too low (Hansen *et al.*, 2020). The general expectation is that CAPE will continue to

build up during the day until peak surface temperature is achieved, and that the CAPE over land will be significantly higher than CAPE over the ocean surface. However, observational analyses generally show no evidence to suggest larger values of CAPE over land compared to the ocean surface (Lucas *et al.*, 1994; Matsui *et al.*, 2016). Indeed some studies (e.g.: Williams and Renno, 1993) found their measure of storm intensity to be independent on mean CAPE.

A number of observation studies have shown a consistent diurnal cycle of precipitation over land. Over tropical land surfaces, precipitation is seen to peak in the late afternoon, while peak precipitation over tropical ocean surfaces are mostly observed at night and early mornings (Betts and Jakob, 2002; Collier, 2004; Guichard *et al.*, 2004; Wei and Pu, 2022). Enhancement of precipitation and convection in general have been reported in some studies with imposed diurnal cycle in their experimental design. Using an idealized island experiment with a diurnal cycle of insolation, Cronin *et al.* (2015) showed enhancement in the high percentiles of vertical velocity at 500 hPa level and precipitation over the island region with a low heat capacity relative to the ocean in their experimental setup. Lee *et al.* (2018) and Harvey *et al.* (2022) both showed enhanced precipitation over the dry regions of their heterogeneous domain in modelling simulations with imposed diurnal cycle. They imposed heterogeneity in a checkerboard pattern of alternating low and high Bowen ratios. Given that updraught strength have been shown to be independent on boundary layer depth in both homogeneous (Hansen and Back, 2015) and heterogeneous domains (Chapter 3 of this thesis), one can infer that the imposed diurnal cycle in these studies may be a contributory factor for the enhanced updraught velocity and precipitation in these studies. Therefore to better understand the relative effect of the different land surface features on the intensity of continental storms, the surface features must first be tested individually.

There is a general thought that diurnal cycle of temperature enhances convection over land surfaces. However, this enhancement has mostly been in the context of enhanced precipitation rather than the a real measure of the updraft strength for example; updraught velocity. Only a handful of studies have been dedicated to establishing a physical link between the diurnal cycle of temperature and the updraught strength of convective storms. Hansen *et al.* (2020) using a cloud-permitting model simulation over an idealized island, a statistical sampling technique, and analysis of satellite and reanalysis data, studied the relationship between the diurnal cycle of temperature and intensity of deep convection and made

the following conclusions;
1. Convective intensity is not affected by the diurnal cycle after controlling the effect of large scale precipitation which appears enhanced over the island.
2. The intensity of the convective clouds did not increase because boundary layer quasi equilibrium (BLQE) prevented CAPE from increasing in response to heating of the land surface.
3. CAPE calculated from reanalysis data did not show a significant land-ocean contrast to explain the contrast in the intensity of storms as observed over the two surfaces.

Hansen *et al.* (2020) therefore suggests that the diurnal cycle of temperature over islands does not impose strong control on thunderstorm storm intensity over land. It is important to note that their study defined updraught intensity as the high percentiles of vertical velocity at 500hPa level. However idealized modeling studies on the response of updraught velocity to warming over tropical ocean surfaces (e.g.: Singh and O'Gorman, 2015; Seeley and Romps, 2015; Muller and Takayabu, 2020) have shown that updraught velocity increases more rapidly at the upper troposphere than the lower troposphere and middle troposphere when the surface temperature increases. A look into how vertical velocity across all vertical levels differ between land and ocean surfaces could perhaps give a different perspective into this land surface feature in relation to the convective intensities of continental storms.

A key finding of Hansen *et al.* (2020) was the mismatch between the peak times of CAPE and updraught velocity during the day. They found that over the island, CAPE peaks in the early morning but updraught velocity and precipitation peaks some hours later. They concluded that the marginal difference in updraught velocity between the land and ocean surfaces could not be attributed to difference in CAPE between the two surface. Their estimation of CAPE was based an undiluted parcel lifted pseudo-adiabatically from the surface to 500 hPa level. However, knowledge from the two-plume theory (Singh and O'Gorman, 2015) suggests that the strongest updraughts are always associated with plumes that are weakly entrained compared to the bulk of the convective mass flux. Perhaps a different approach to the calculation of CAPE would give a different perspective of this mismatch.

In this study we aim to seek further answers on the influence of the large diurnal cycle of temperature on the intensity of convective storms by exploring some of

the outstanding questions from previous studies. Specifically, we take a similar approach to Hansen *et al.* (2020) but rather than an island, we consider idealised RCE simulations with a spatially uniform but temporally varying temperature. Further, instead of only looking at the vertical velocity at 500 hPa, we are interested in knowing how much additional information can be obtained if we assess vertical velocity across all vertical levels. We are also interested in exploring other theories of CAPE and buoyancy available in literature and how it applies to the mechanism being tested.

4.3 Experiment design and simulation

The general model description and setup discussed in Chapter 2.4 is applied here with some adjustments made to suit the land surface feature being examined. The approach is similar to the experimental design by Hansen *et al.* (2020) in terms of the imposition of the diurnal cycle, and the diurnal temperature range but deviate from their approach by imposing diurnal cycle of temperature over the entire domain in our case. The goal here is to assess how much of the results of Hansen *et al.* (2020) are still captured in our highly idealized configurations of the boundary surface in our simulations.

Two different configurations of the land-like surface are explored in this experiment; a case where we impose diurnal cycle of surface temperature over an ocean surface (hereinafter DC), and a case where the ocean surface has both imposed diurnal cycle of temperature and reduced surface moisture (hereinafter HBR). These two configurations represent the land-like cases in this study. The HBR configuration is primarily a surface with high Bowen ratio and imposed diurnal cycle of temperature. The high surface Bowen ratio was achieved by introducing an evaporative conductance parameter (α) into the bulk equation of latent heat flux in the CRM model, details of how this was done is seen in Section 3.3.1. An α value of 0.5 was used in this particular experiment. As discussed in Section 3.3.1, increasing the surface Bowen ratio (SBR) without a corresponding adjustment to the surface temperature result in cooling of the free troposphere. In our experiment that tested the response of thunderstorm intensity to changes in boundary layer depth (Chapter 3), a temperature adjustment approach was implemented in the CRM model to keep a similar free tropospheric profile for all simulations by

a time-step increment in surface temperature until the free tropospheric temperature profile was adjusted to a reference profile taken from simulations over an ocean surface. Here we deliberately ignore this approach in order not to break the setting of how the diurnal cycle is modelled. However, we set two extreme cases of a land-like surface, with a much colder free-tropospheric temperature and one with a relatively warmer free troposphere in comparison to an ocean surface. Since the imposed diurnal cycle is over the entire domain, the free troposphere in our case is not influenced by remote regions as would be the case in the real tropics. Moreover, in the real world, land surfaces affect the atmosphere in a number of ways. The goal here is not to reproduce real world scenarios but to test the response of updraught strength to a single physical feature of the land surface.

All simulations are run with an initial mean surface temperature of 300 K. Since our approach involves imposition of surface temperature, insolation is kept fixed, and the simulations are non-rotational as Coriolis parameter is kept to zero. In these simulations we use the single-moment microphysics scheme, the first-order Smagorinsky SGS closure is used to parameterize sub-grid scale turbulence and radiation is parameterized using the Rapid Radiative Transfer Model (RRTM: Clough *et al.*, 2005) as highlighted in Chapter 2. Simulations are run for a total of 100 days, data from the last 30 days of the simulations are used in all analysis. The domain size and resolution used in the previous chapter are retained for these sets of experiments.

The SST of the ocean is made to be interactive across the model domain using a coupled slab ocean but a mean SST of 300 K is retained at each time step, hence there is no imposed diurnal cycle in simulations where the boundary surface is considered as ocean in this study. For the DC and HBR cases, we impose diurnal cycle of temperature over the lower boundary domain. Although the interactive slab-ocean option was not turned off for the land-like cases, the modeling approach of diurnal cycle of surface temperature make the surface domain far less interactive. The imposed diurnal cycle in our simulations and the diurnal temperature range are comparable to Hansen *et al.* (2020) in terms of the modeling of the imposed diurnal cycle and the diurnal temperature range. Surface temperature is modelled to vary sinusoidally and peak at the 1200 local standard time (LST). The surface temperature varies between 295 K at midnight and 305 K at noon with a mean of 300 K during the day at 0600 LST and 1800 LST. The sinusoidal cycle of SST is modelled as follows;

$$SST_{\mathrm{xy}} = \overline{SST_t} - A\cos(\pi D/H) \tag{4.1}$$

where SST_{xy} is the domain mean surface temperature at every timestep, $\overline{SST_t}$ is the time-mean SST of 300 K, A is the amplitude of surface temperature which peaks at noon, D is the time of the day and, H is the the time step at which maximum surface temperature is achieved (12 hours in this case). Figure 4.1 shows the diurnal composite of the surface temperature as modelled.

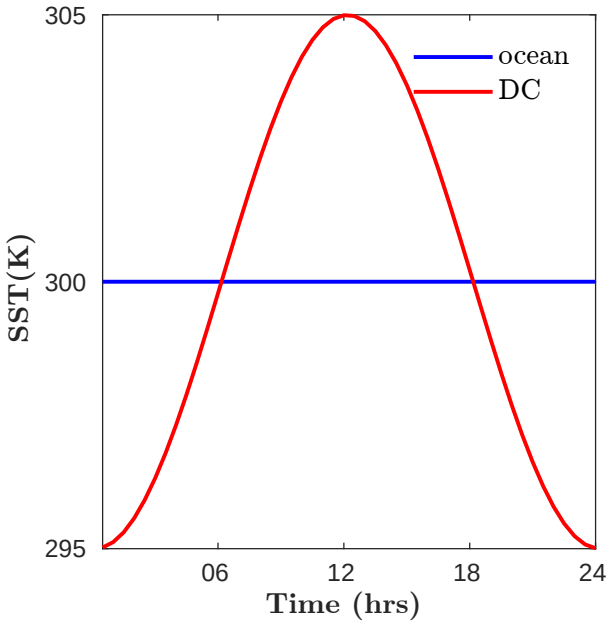

FIGURE 4.1: Diurnal variation of surface temperature for the land-like case (red line) as modelled. Surface temperature reaches maximum at noon and minimum at night times. The ocean case (blue line) retains a mean of SST 300 K.

4.4 Results

4.4.1 Thermodynamic structures at the lower and mid-troposphere

In this section we examine some boundary layer thermodynamic variables from the different simulations to formulate a basis for how CAPE and overall updraught would be expected to vary during day over the DC and HBR cases. We specifically consider the moist static energy (MSE), specific humidity(q), near surface air temperature, and the mid-troposphere environmental relative humidity. We assess

the diurnal variation of these thermodynamic variables and how it relates to the physics behind the large diurnal cycle of surface temperature's connection to the intensity of continental storms.

We present a perspective of how domain- and time-mean of these thermodynamic variables differ from their high percentile and what the difference represent in terms of setting a conducive environment within which convection could thrive in the atmosphere. Essentially we highlight on some key similarities of some thermodynamic variables from our idealization of the land surface to the case of Hansen *et al.* (2020) who had a well defined island and ocean surfaces setup over their simulation domain.

We start by considering the simulated time-mean temperature profiles and their 99th percentile. Figure 4.2 shows the temperature difference of the DC (red line) and the HBR (black line) cases relative to the ocean's temperature profile. The differences are calculated from the time-mean temperature profiles (Figure 4.2a), and from the 99th percentile of temperature profile (Figure 4.2b) at noon. The two plots are important for two reasons. First it shows the biases in our experimental setup in terms of how different the free-tropospheric temperatures of the idealized land cases are from a typical ocean's free-tropospheric temperature. Secondly, it represents two different cases; a colder free-tropospheric temperature of a tropical atmosphere as one would expect over a typical dry land surface (HBR: black line), and how the ocean surface would behave if it had land surface characteristics like the large diurnal cycle of surface temperature (DC: red line). Figure 4.2a is therefore the temperature profile of the bulk of convecting parcels represented through the time-mean in the DC and HBR cases relative to the ocean case, and Figure 4.2b represents the temperature profile of the strongly convecting parcels in the land-like simulations relative to the ocean from the two-plume model perspective. It is important to note that the mean and high percentiles of temperature profile of the DC case relative to the ocean is very comparable to the domain-mean temperature profile, and temperature perturbation found over the island region in the study by Cronin *et al.* (Figure 10-11; 2015) which involved a well defined island and ocean regions, and a diurnal cycle of insolation. This gives us confidence that that our idealization of the land surface is not in isolation and that the results shown here is comparable to previous studies with island-ocean configurations.

A significant feature on these two plots is the transitioning of the HBR temperature profile into a warmer phase relative to the ocean's profile at the upper troposphere

(∼15 km), it is marginally seen in the mean profiles but is significantly enhanced in the 99.99th percentile profile. This has an effect on the shape of profile of buoyancy as we will see later in subsequent sections.

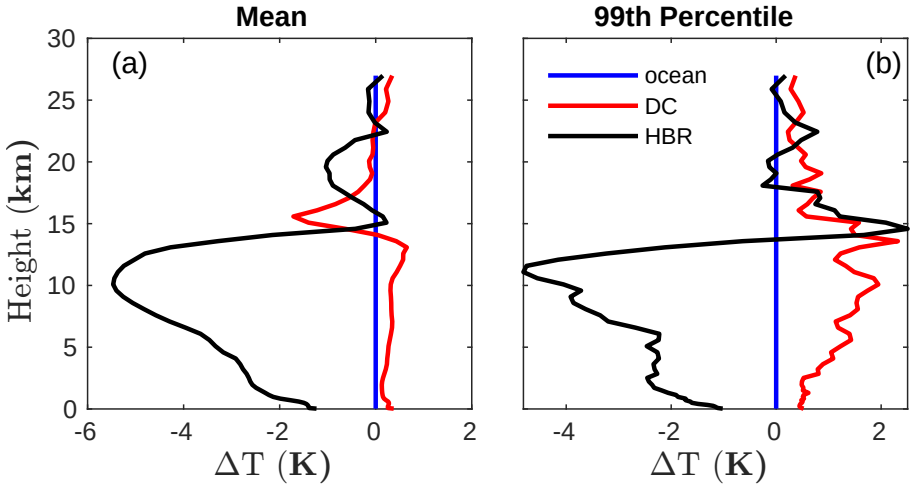

FIGURE 4.2: Plot showing how the simulated temperature profiles of the land-like cases, DC (red line) and HBR (black line) vary from the (a) time-mean and (b) 99th percentile of the ocean's temperature profile (blue line) in our simulations. The simulated ocean's temperature profile is subtracted from the profile of the two land cases in both instances.

4.4.1.1 Diurnal variation of thermodynamic variable

We interpret our results from the perspective of the two-plume theory of Singh and O'Gorman (2015), and as highlighted in Chapter 3. Here the domain- and time-means of the thermodynamic variables represent the strongly entraining parcels in our simulations and the high percentiles represent the thermodynamic structure of the strongly convecting parcels. Figure 4.3 shows near surface air temperature (T), near surface moist static energy (MSE) and specific humidity (q), and mid-troposphere relative humidity in the mean state (Figure 4.3a-d) and their 99th percentile (Figure 4.3a-d) for the different simulations. The thermodynamic variables (except the mid-troposphere relative humidity) in the ocean and the DC cases are significantly higher than the HBR case because of the differences in temperature profiles as seen in Figure 4.2. The HBR case is a typical of dry land case with a much colder atmosphere compare to the ocean and DC case.

As notice by Hansen *et al.* (2020) in their island experiment, the boundary layer domain- and time-mean MSE and specific humidity in our land simulations fails to increase correspondingly to increasing surface temperature during the day. In

such conditions, CAPE is not expected to increase as the near surface MSE and humidity clearly decrease during the day, with their minimum occurring in the afternoon when surface temperature peaks. Hansen *et al.* (2020) attributed the lack of increase in the MSE and CAPE over the island region in their studies to boundary layer quasi-equilibrium (BLQE) resulting from convective downdrafts and entrainment. In our simulations, the idealization of the land surface captures similar diurnal patterns of mean boundary layer thermodynamic variables as those found over the island region in the study by Hansen *et al.* (2020) in terms of peak times of this variables and and how they fade off during the day. This is evident that similar pattern of mean thermodynamic variables could exist over both wet and dry land surfaces and results in mean CAPE peaking in the early morning (more on this in later sections) and fading off during the day as surface temperature increases. Hansen *et al.* (2020) found evidence of BLQE in their analysis of observation data. In the midst however is the contribution of the high percentiles of these thermodynamic variables to the debate of the large diurnal cycle of temperature as a surface feature that controls intensity of convective storms. Questions of how different the CAPE of the strongest convective parcels are from their mean, and the possible effect of entrainment becomes important in unraveling the actual contribution of the large diurnal cycle of surface temperature to the intensity of continental storms. We address some of these questions in subsequent sections.

A general look at the 99th percentiles of boundary layer MSE and humidity (also true for higher percentiles) suggest a scenario where CAPE could increase during the day as hypothesized. As seen in Figure 4.3f-g, MSE and specific humidity at the boundary layer increases correspondingly to increasing boundary layer air temperature in both the DC and HBR land cases. On a first guess, the diurnal pattern of the mid-tropospheric environmental relative humidity in the mean state (Figure 4.3d) and the 99th percentile (Figure 4.3h) gives an ideal of how CAPE would vary through the day in the two states if one thinks of the effect of entrainment and saturation deficit in the estimation of CAPE. In the mean state, mid-tropospheric environmental relative humidity (RH) peaks in the morning around 0900 LST for both DC and HBR cases, with the HBR case being slightly higher than the DC case. At noon where the diurnal maximum temperature is achieved as modelled, the RH is at its lowest, indeed it decreases immediately after peaking at 0900 LST. At certain times in the afternoon, the mid-tropospheric RH over the ocean is seen to be higher than the DC case.

On the argument of saturation deficit contribution to CAPE, once can infer that CAPE over the land surface would peak just around the time of peak RH and significantly reduce as the surface temperature increases during the day. Conversely, the higher percentiles tells a different story, in this instance the mid-troposphere environmental RH of the two land cases increases from the early morning, remains fairly constant during the day and decreases later in the evening with the HBR case being marginally higher than the DC case. Again, from the same argument of saturation deficit and CAPE relationship, CAPE would be expected to peak around 0900 LST and remain fairly constant during the day and reduce later in the evening. We investigate how this is true in subsequent sections by considering different theories of CAPE and how it explains the differences in the mean state and the high percentile state as seen in our simulations.

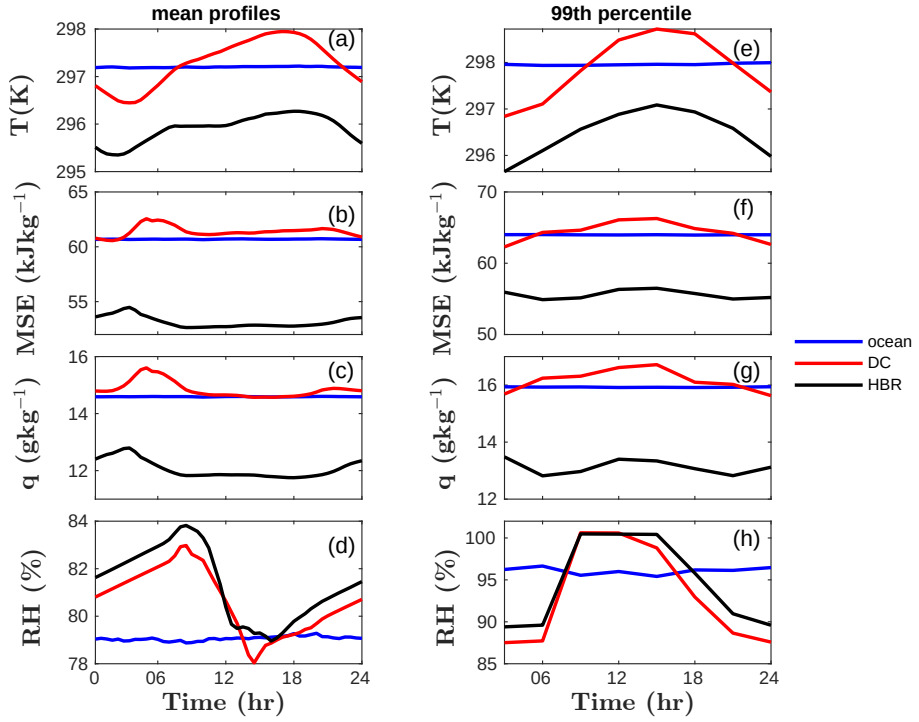

FIGURE 4.3: Diurnal composite of domain-mean profiles (a-d) and 99.9th percentile (e-h) of thermodynamic variables from the simulations with imposed diurnal cycle (DC: red line), imposed diurnal cycle and high Bowen ratio (HBR: black line), and the simulation without diurnal cycle (ocean: blue line). Composites are for the first model level (a&e) near-surface air temperature, (b&f) moist static energy (MSE), (c&g) specific humidity, and (d&h) are the mid-tropospheric (2-5 km) mean environmental relative humidity (RH). The 99th percentiles are calculated from instantaneous 3D outputs from the simulations.

4.4.2 Diurnal variation of updraught velocity in the different simulations

To get a clearer picture of how the diurnal patterns of the different thermodynamic variables shown earlier are actually reflected in the buoyancy of the convective storms, we assess the evolution of vertical velocity during the day in the different simulations. Here we show how the 99.99th percentile of vertical velocity changes through time. We consider vertical velocity across all vertical levels to get a fair perspective of the real influence the diurnal cycle of surface temperature on the intensity of the storms. Only vertical velocities greater than 1 ms^{-1} are used in these analyses.

Figure 4.4 shows a time-height plane of the 99.99th percentile of vertical velocity ($w_{99.99}$) for the different cases. The simulation over the ocean surface by their design has no diurnal cycle hence deep convection is assume to be occurring at every time of the day. We have plotted the time-height plane of it just for comparison with the land-like cases. For the two land cases, $w_{99.99}$ peaks in the afternoon just around the time of maximum surface temperature. There is a visible difference in $w_{99.99}$ between the land-like cases and the ocean case at this time of the day. At the height in the troposphere where $w_{99.99}$ is maximum ($\approx$ 12 km into the troposphere), $w_{99.99}$ in the land-like cases is about 10 ms^{-1} higher than the ocean case. At the 500 hPa level (marked as dash lines on Figure 4.4), the the 99.99th percentile of vertical velocity (w_{500}) over land is about 4 ms^{-1} greater than that of ocean surface. Cronin *et al.* (2015) and Hansen *et al.* (2020) found similar w_{500} difference between the island and ocean surfaces in their island experiments. Between the DC and the HBR cases, $w_{99.99}$ at the upper troposphere is marginally ($\sim$2 ms^{-1}) higher in the HBR case. The DC case however has a marginally ($\sim$1 ms^{-1}) higher w_{500} compared to the HBR case. Although the three case are happening in relatively different environment by virtue of the different setups, it is still significant that the land-like cases have significantly higher vertical velocities than the ocean case.

Considering the difference in higher percentiles of boundary layer temperature and humidity as seen in Figure 4.3e&g, one would expect the DC case and indeed the ocean case to have larger CAPE and result in stronger updraught if the parcels were to remain moist adiabatic throughout their ascent according to the parcel theory of CAPE. However, we see a situation where the HBR case with significantly

lower temperature and humidity having higher updraught velocity at least at the upper troposphere. A visual view of the $w_{99.99}$ in the different simulations reveal that vertical velocity in the HBR goes deeper into the atmosphere than the DC case, suggesting clouds in the HBR case could grow deeper and taller into the tropopause.

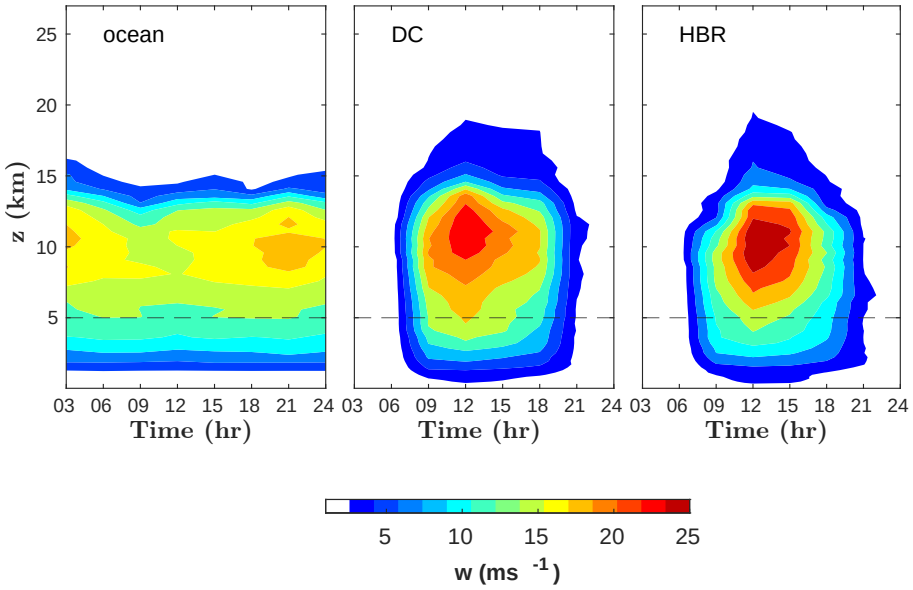

FIGURE 4.4: Time-height plane of 99.99th percentile of vertical velocity from the ocean and land-like simulations. Composite show the diurnal variation of 99.99th percentile vertical velocity (w) at all vertical levels. Percentiles are calculated from 3D output of vertical velocity of the last 30 days of the simulations. Plots are for w≥1.

4.4.2.1 Buoyancy and updraght velocity at specific times of the day.

To get a better perspective of how the high percentiles of vertical velocity differ during the day, we assess the vertical profiles of the 99.99th percentiles of MSE, buoyancy and vertical velocity at different times of the day, here we consider three hours before and after the peak times of the vertical velocity as shown in Figure 4.4. We therefore assess how the profile changes from 0900 LST through to noon, and 1500 LST in the afternoon. These times essentially capture the evolution of the strongly convecting parcels during the day in the DC and HBR cases in comparison to the ocean case.

As shown in Figure 4.5, there are visible differences in buoyancy and vertical velocity for different times of the day considered. At 0900 LST (Figure 4.5a-c), the buoyancy and vertical velocity are visibly greater in the DC case compared to

the HBR case, with the difference much apparent at the upper troposphere. This is expected since the DC case has no restriction of moisture and hence respond immediately to the imposed diurnal cycle. As surface temperature begins to increase, the response time of the interaction between the surface and the lower troposphere in the DC case is expected to be faster than the HBR case. At 1200 LST when the surface of the HBR case has been warmed enough, the buoyancy of the convective region relative to their environment increases, and it's reflected in the much enhanced vertical velocity compared to the ocean case with no imposed diurnal cycle. A similar feature is seen at 1500 LST. At this point the difference in buoyancy and vertical velocity between the DC and HBR case is more visible. One can only infer that the potential energy actually converted to kinetic energy by the strongly convective region in the HBR case is higher and much sustained during the day than the ocean and the DC case.

From the profiles of buoyancy and vertical velocity at the different times of the day, it is shown that surfaces with imposed diurnal cycle of temperature would have strongly convecting clouds that grows deeper into the troposphere, reaching the tropopause. It can therefore be speculated that the imposed diurnal cycle of temperature has a significant connection with the intensity of convective clouds that form in our land-like simulations.

It can also be inferred that the mechanisms preventing the build up of CAPE as suggested by the diurnal pattern of the mean MSE may be self-induced by the few convective clouds that grow deeper into the troposphere and reach the tropopause. The buoyant convecting parcels that reach the stable layers of the tropopause result in anvil clouds that are known to produce drowndraft which eventually dry the surface and suppress further development of clouds. Hansen *et al.* (2020) found downdrafts to be the main reason for the decrease in mean MSE during the day.

4.4.3 Diurnal pattern of diluted and undiluted CAPE in the different simulations

The analysis of the simulation results of the different cases have so far revealed that the land-like cases have stronger updraughts compared to the ocean case. However,

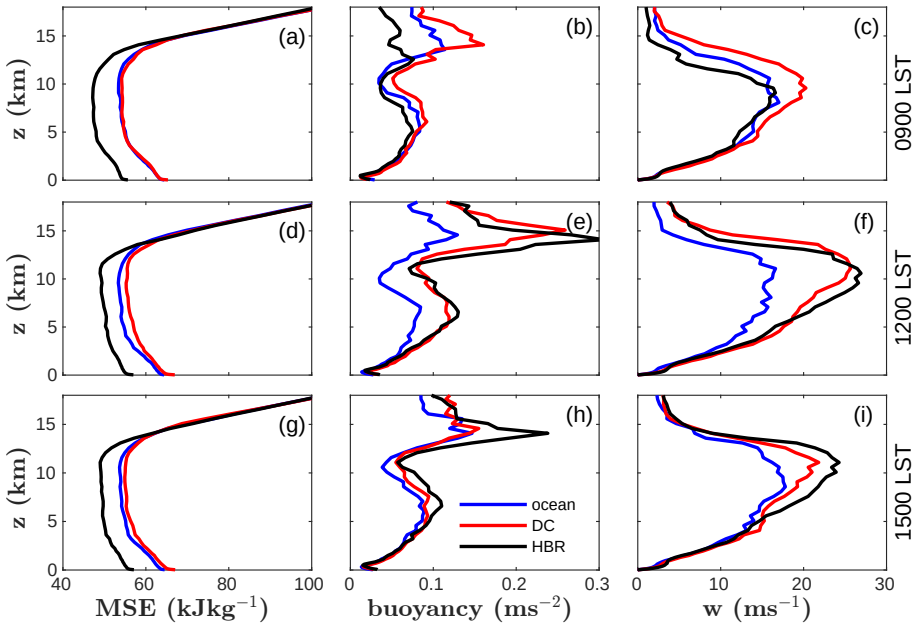

FIGURE 4.5: Profiles of the 99.99th percentiles of (a,d&g) MSE, (b,e,&g) buoyancy, and (c,f,&i) vertical velocity from the different simulations and at different times of the day. Plots shown here are the 99.99th percentile of the profiles at 0900 LST (a-c), 1200 LST(d-f), and 1500 LST (g-i). Percentiles are calculated from instantaneous 3D outputs from the ocean (blue line), DC(red line), and HBR (black line) simulations.

there exist significant differences in the diurnal variation of the thermodynamic structure for both the mean state and the high percentiles. To get a clearer view of these results, we attempt to find a physical link between the intensity of the convective storms as seen in the different simulations and CAPE. We start by thinking generally of CAPE as the integral of positive buoyancy of a parcel lifted pseudo-adiabatically with ice processes treated with a mixed-phase range between 233.5 and 273.15 K. To stay consistent to our analysis of mean and high percentiles, we initialize the parcel in the CAPE calculation with; first the domain- and time-mean temperature and specific humidity at the surface, and also with the temperature and humidity at each grid point within the first model level. Here the buoyancy is integrated across all vertical levels. In our simulation, the 3D instantaneous snapshots were output every three hours, and the data of the last 30 days from the simulations are used in all analysis. The second approach therefore gives a horizontal map of CAPE at each time from which we calculate the 99.99th percentile.

As show in Figure 4.6a-b, the undiluted mean CAPE and 99.99th percentile CAPE reflects what we expected from assessing the mean and higher percentiles of the

different thermodynamic variables (Figure 4.3). The mean CAPE over the land-like simulations peak in the morning around the same time as the time-mean boundary layer MSE and specific humidity. The diurnal variation of mean mid-troposphere environmental RH (Figure 4.6c) also has a similar diurnal pattern as the mean CAPE.

Similarly, the 99.99th percentile CAPE in the land-like simulations show a similar diurnal pattern as the high percentiles of MSE, specific humidity and mid-tropospheric environmental relative humidity. This clearly shows that the strongly convecting parcels as captured by the higher percentiles have a different CAPE from the weakly convecting parcels. It can also be inferred that the physics supporting the large diurnal cycle of temperature as a surface feature with potential to influence the intensity of convective storms can be confirmed in our simulations when the diurnal pattern of the high percentiles of undiluted CAPE and vertical velocity are considered. The question that arises is, how much of the potential energy available at the surface is actually translated as kinetic energy by the convecting parcels. As seen from both the mean and 99.99th percentile of CAPE, the HBR case has the least undiluted CAPE in both instances. However, as shown in Figure 4.6, it has the strongest updraught during the day. The effect of entrainment on the buoyancy of convective parcels is an obvious candidate in explaining this mismatch between parcel buoyancy and attainable potential energy. We investigate how entrainment affect the buoyancies of the different simulations by exploring some other theories of CAPE.

We follow a similar approach discussed earlier in Section 3.5.1 of this thesis to estimate the entrainment rates of the bulk of the convective clouds and the strongly convecting clouds. The approach is based on the the two-plume model (Singh and O'Gorman, 2015) which argues that the updraught velocity of clouds is set by the width of distribution of entrainment on a rising parcel. Here we determined the entrainment rates of the strongly entraining parcels which represent the means state of convection (ϵ_{mean}) and the entrainment rates of the strongly convecting parcels ($\epsilon_{99.99}$). As seen in Figure 4.6e-f, ϵ_{mean} which represents the entrainment rate of the bulk of the parcels is highest in the morning and decreases as the land surface temperature increases during the day. $\epsilon_{99.99}$ in the HBR and DC cases is also high in the early morning but decreases sharply before the time of maximum surface temperature. Putting the two together and relating it to how the diurnal cycle of temperature was modelled, it is seen that the transitioning time of the peak

entrainment rate is around 0600 LST, this is the time where mean temperatures of the land cases and ocean case are equal (300 K). After this period of the day, both the entrainment rates of the mean convecting parcels and the strongly convecting parcels begin to decrease, and are lowest at the in the afternoon. $\epsilon_{99.99}$ however decreases at a faster rate compared to ϵ_{mean}. This can be understood from the view point that, entrainment is highest over land during the morning when surface temperature of the land surface are relatively low compared to the ocean surface. In the morning when relative humidity over land peaks, and surface temperature begins to rise, a favourable condition is set for the build up of CAPE. However, there is a competition between entrainment and relative humidity in setting the CAPE during the day. Entrainment eventually wins as environmental relative humidity decreases and hence the mean CAPE decreases during the day as the effect of further drying of atmosphere by downdrafts increases. The caveat here however is, the strongly convecting parcels retains their buoyancy and are less entrained, hence they develop into stronger storms that reach the tropopause as seen in Figure 4.5. Downdrafts from these deep clouds with anvils over the land surface further induce dryness over the land surface and suppress the buoyancy of smaller clouds. Since the smaller cloud dominate compare to the deeper ones, any estimation of the mean buoyancy in the different simulations would be appear to be weak during the day due to the effect of downdrafts on convection over land surfaces. This corroborates earlier findings that downdrafts play a leading role in decreasing MSE and eventually CAPE over land (Hansen *et al.*, 2020).

4.4.3.1 A simple scaling of CAPE and buoyancy using the two plume model

Following the estimation of the mean and weakly entraining rates in the different simulations, we test a simple scaling relationship for the strength of updraughts and CAPE of the different simulations. This scaling relations are in tune with the two-plume model (Singh and O'Gorman, 2015) which relates the buoyancy of the strongly convecting parcels to the difference in entrainment rates of the strongly entraining parcels (ϵ_{mean}) and the weakly entraining parcels ($\epsilon_{99.99}$) and the subsaturation at the mid troposphere. The scaling of CAPE also relates CAPE to the product of the bulk entrainment rate (ϵ_{mean}) and the mean mid-troposphere subsaturation . These scaling approaches have been used in Chapter 3 of this thesis

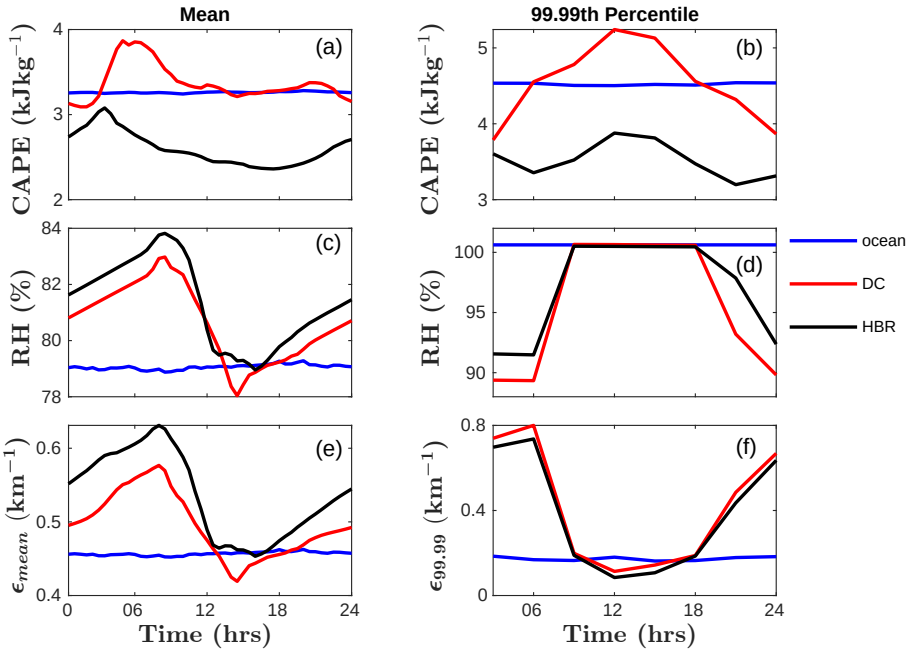

FIGURE 4.6: Diurnal composites of (a) mean CAPE, (b) 99.99th percentile of CAPE, (c) mean mid-troposphere environmental RH, (d) 99.99th percentile of RH, (e) entrainment rate of the strongly entraining parcel, and (f) entrainment rate of the strongly convecting parcels.

to assess the strength of convective storms and CAPE over heterogeneous land-like surfaces, and on homogeneous surface with different surface Bowen ratio.

The simple scaling relationships are giving as follow;

$$w^2 \sim \delta\epsilon(1 - RH), \ \delta\epsilon = \epsilon_{mean} - \epsilon_{99.99} \tag{4.2}$$

$$CAPE \sim \epsilon_{mean}(1 - RH), \tag{4.3}$$

where w^2 is a measure of buoyancy of the convecting parcel, $\delta\epsilon$ is the difference in the two entrainment rates ($\epsilon_{mean} - \epsilon_{99.99}$), RH is the mean mid-troposphere environmental relative humidity (2 - 5 km) and CAPE is the convective available potential energy.

The results of the scaling relations are shown in Figure 4.7. As expected the scaling of CAPE (Figure 4.7a) shows a similar diurnal pattern as the mid-troposphere relative humidity (Figure 4.6b) and the bulk entrainment rate (Figure 4.6c). Although the predicted CAPE from the two-plume scaling approach shows similar diurnal pattern as the conventional undiluted CAPE (Figure 4.6a), there are significant physical differences where the scaled CAPE of the HBR case is seen to

be larger than the DC and ocean cases at least in the morning. This underscores the significance of entrainment in the estimation of CAPE. There is a visible difference in the measure of buoyancy (Figure 4.7b) between the land-like cases and the ocean case during the day with the HBR case being the highest. Most importantly, the buoyancy scaling confirms the diurnal pattern of updraught velocity as seen in Figure 4.4. Therefore the difference in updraught velocity among the different simulations are as a result of strongly convecting cloud parcels that are less affected by entrainment.

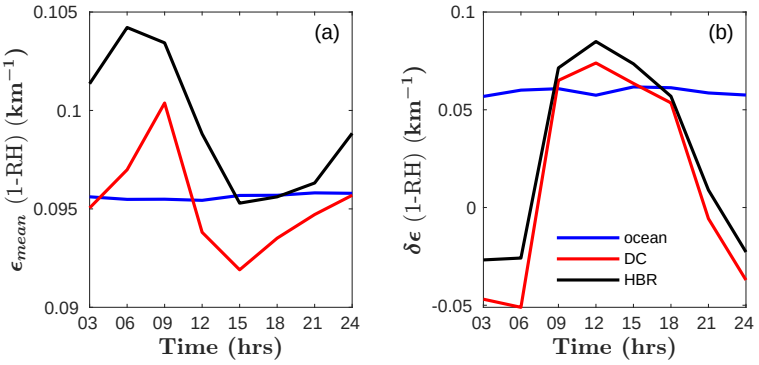

FIGURE 4.7: Simple scaling of (a) CAPE and (b) buoyancy from the two-plume model. The buoyancy scaling relates the buoyancy of plumes to the difference in entrainment rates of the strongly entraining plume (ϵ_{mean}) and the weakly entraining plume ($\epsilon_{99.99}$), and the subsaturation of the mid-troposphere. The CAPE scaling also relates CAPE to ϵ_{mean} and the mid-troposphere saturation deficit (1-RH).

4.4.3.2 Entraining CAPE from the spectral plume model

We have seen so far that the high percentiles of CAPE support the idea that the large diurnal cycle of surface temperature has some relationship with the updraught velocity of the DC and HBR cases. We have also shown that although the high percentiles of CAPE give a picture of the available energy required for convection in the land-like simulations, it does not necessarily mean stronger updraughts as the effect of entrainment and relative humidity controls the actual buoyancy of the of the convective clouds. The scaling of buoyancy with the two-plume model seem to provide an explanation for the difference in updraught velocity as seen in the different simulations.

To better understand the relative importance of entrainment in setting the buoyancy of the convecting parcels, we use a spectral plume model (Zhou and Xie,

2019) to investigate the effect of entrainment and relative humidity in the different simulations. The model predicts properties of updraughts from a spectrum of entraining rates at different levels of the troposphere. In this model the environment is assumed to be neutrally buoyant to the entraining plumes and as such MSE decreases monotonically with height in the lower troposphere. The model therefore predicts changes in environmental temperature(ΔT) as a function of change in MSE (Δh) between the undiluted parcels (calculated from the mean temperature and specific humidity from the simulations) and the MSE of the entraining plume at every height. The model therefore predicts the undiluted buoyancy integral and the buoyancy of each entraining plume within the spectrum. A significant feature in the spectral plume model is its ability to estimate the buoyancy of the weakly entraining plumes.

According to this plume spectrum model, changes in temperature and MSE at different heights in the atmosphere is given by the following equations (equations: 8 &19 Zhou and Xie, 2019):

$$\Delta T = \frac{1}{1 + \frac{L_v}{R_v \overline{T^2}} \frac{L_v \overline{q^*}}{C_p}} \Delta h \tag{4.4}$$

$$\frac{d\Delta h}{dz} = \lambda \Delta h - \epsilon[z](1 - RH)\frac{L_v \overline{q^*}_v}{C_p} \tag{4.5}$$

where $\frac{\Delta h}{dz}$ is the change in MSE with height for a particular plume with entrainment $\epsilon[z]$ at a particular height, Δh is the change in MSE of the entraining plume relative to the mean (undiluted) MSE, λ is a parameter which controls the changes in MSE at different altitudes in response to the different entrainment plumes and thus set the deviation of temperature of the plume from the environment, RH is the environmental relative humidity, $\overline{q^*}$ is the mean environmental saturation humidity, L_v is the latent heat of vaporization and C_p is the isobaric specific heat capacity of air.

The spectral plume model is used to calculate the buoyancy integrals (CAPE) in the different simulations to fully understand the effect of entrainment on CAPE in the different cases. To also see the effect of relative humidity on the buoyancy of the different simulations, we first initialize the spectral plume model with mean temperature, specific humidity, and relative humidity from the different simulations. We next initialize the model with mean temperature and specific humidity

from the different simulations and a constant relative humidity of 80 %. This gives the relative effect of just entrainment (when RH is fixed), and the coupled effect of entrainment and RH (when model is initialized with RH from the simulations).

Figure 4.8 shows the results of the positive buoyancy integral of the undiluted air parcel ($CAPE_u$) and the positive integral of buoyancy of the weakly entraining plume ($CAPE_w$) calculated from the spectral plume model. When the relative humidity is kept fixed, $CAPE_u$ (Figure 4.8a) and $CAPE_w$ (Figure 4.8b) show a situation where the undiluted CAPE of the DC and ocean cases are higher than the HBR case, and both $CAPE_u$ and $CAPE_w$ are similar to the diurnal pattern of undiluted CAPE calculated from parcel theory (Figure 4.6a). Conversely, when the mean surface temperature, specific humidity and relative humidity profiles from the RCE simulation is used to initialize the spectral plume model, both $CAPE_u$ and $CAPE_w$ show a diurnal pattern of increasing CAPE during the day time similar to what is seen in the 99.99th percentile of CAPE (Figure 4.6b), $CAPE_w$ in the HBR case is now seen to be marginally higher the DC and the ocean case, which supports our initial scaling of buoyancy. This sets the premise to link the updraught velocity differences seen in our simulations to entraining CAPE.

Figure 4.9 shows the profiles of buoyancy from the RCE simulations of the different cases and that of the spectral plume model. The spectral plume model effectively predicts the buoyancy of the different RCE simulations. The buoyancy of the weakly entraining plume (Figure 4.9c) reveals the difference in the various simulations and essentially predicts the marginal difference between the 99.99th percentile of buoyancy of the HBR case (black line) and the DC (red line) case (Figure 4.9a) as seen from the RCE simulations. The undiluted buoyancy calculated from parcel theory (Figure 4.9b) initialized with mean thermodynamic profiles from the RCE simulation is also largely predicted by the spectral plume model (Figure 4.9d).

The entraining plume model therefore places focus on the effect of entrainment in reducing the the buoyancy of convecting parcels than might be stated by the undiluted CAPE. It can be concluded that the large diurnal cycle of surface temperature indeed lead to enhancement of CAPE. However, entrainment is key to determining the buoyancy and eventual updraught strength of the convective storms.

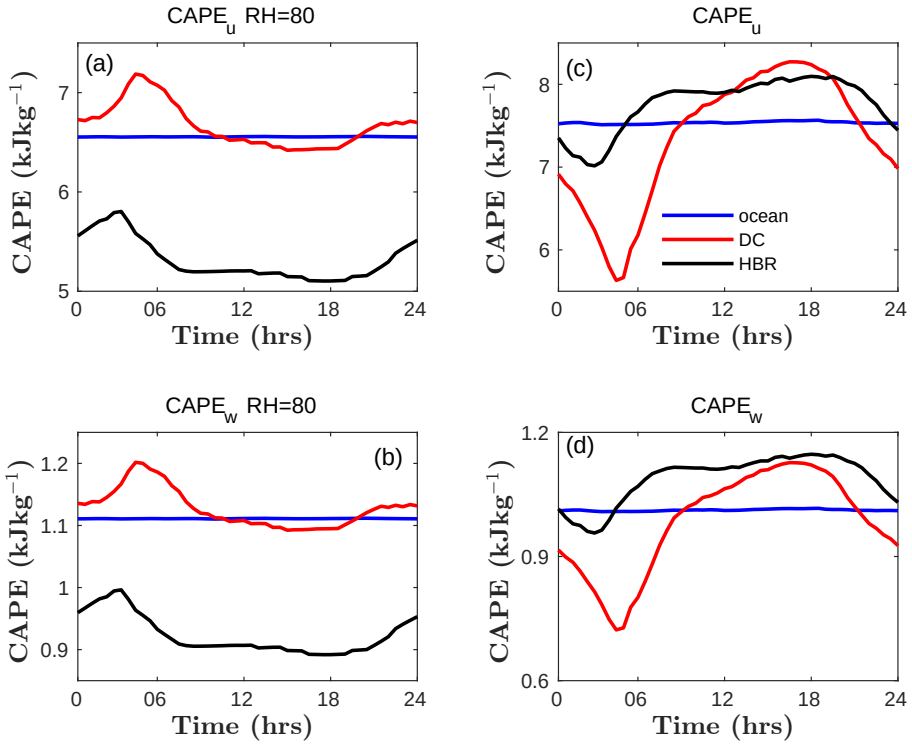

FIGURE 4.8: Diurnal variation (a,c) undiluted CAPE and (b,d) weakly entraining CAPE calculated from the spectral plume mode initialized with mean profiles from the simulations. (a,b) are calculated assuming a fixed RH of 80% for all simulations and (c,d) are initialized with mean RH from the simulations.

4.4.4 Precipitation increases in response to the diurnal cycle of temperature

Finally, we assess the diurnal precipitation rates in the different simulations. As shown in Figure 4.10a, there is a stark difference in precipitation rate between the land-like cases and the ocean case. As expected, the DC case with readily available moisture at the surface has enhanced evaporation represented through the latent heat flux, and as a result records the highest precipitation few hours after local noon. The peak precipitation rate for the DC case is 9.7 mmday^{-1}, with a daily-mean of 2.9 mmday^{-1}, the HBR case follows in terms of the maximum precipitation rate during the day with a peak of 8.2 mmday^{-1} and a daily-mean of 2.1 mmday^{-1}. The ocean case has a mean precipitation of 2.8 mmday^{-1}. The daily-mean precipitation rates do not vary much between the land-like cases and the ocean case. As seen in Figure 4.10a, precipitation over the land only start after 0600 LST when it has the same mean surface temperature as the the ocean. The diurnal pattern of the vertical mean cloud fraction (Figure 4.10b) shows that large number of clouds form over the land-like surfaces during the day as compared

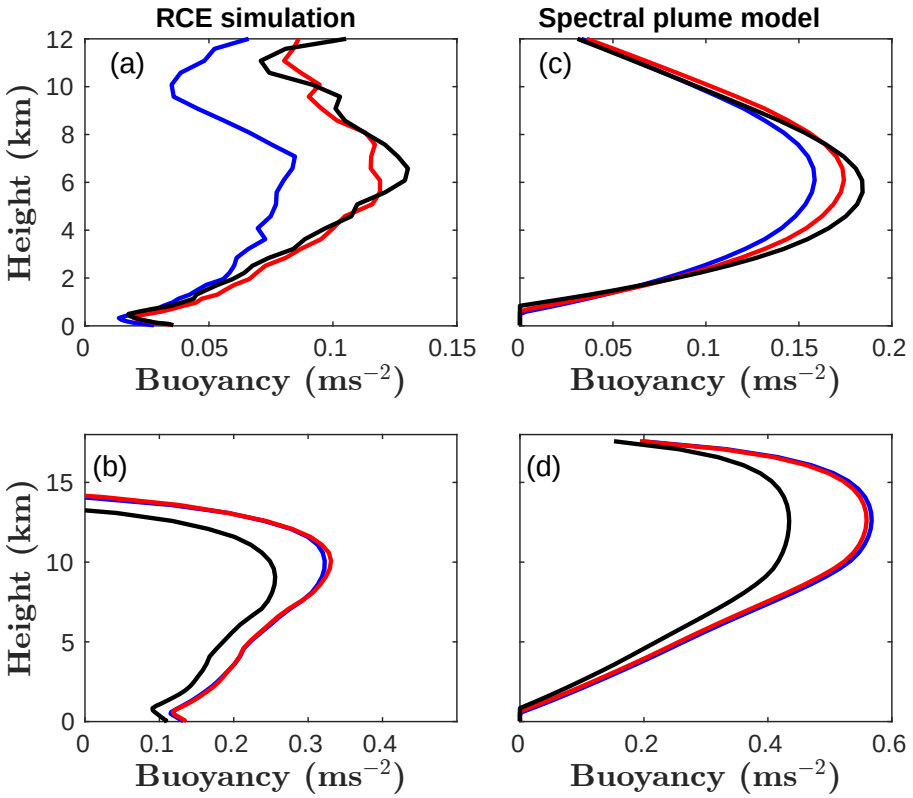

FIGURE 4.9: Buoyancy profiles from the RCE simulations and and the spectral plume model. (a) 99.99th percentile of buoyancy from the simulations, (b) undiluted buoyancy calculated as a pseudo-adiabatic parcel with mean profiles from the RCE simulations (c) buoyancy of the weakly entraining plume, (d) undiluted buoyancy calculated by the spectral plume model.

to the ocean surface. Figure 4.10c shows the mean cloud fraction at noon. The land-like cases clearly have enhanced anvil clouds during the day which supports the argument that downdrafts could be enhanced over land.

4.5 Discussion and chapter conclusion

The linkage between the large diurnal cycle of surface temperature and updraught strength of convective storms that form over land surfaces has been explored with a set of highly idealized RCE simulations using a cloud resolving model (CRM). The approach involved imposing a sinusoidal diurnal cycle of temperature over the lower boundary of the simulation domain, where surface temperature is forced to peak at noon and be minimum at midnight. Simulations were run over a surface with only the imposed diurnal cycle of surface temperature (DC case), and over a surface with both imposed diurnal cycle of temperature and high surface Bowen

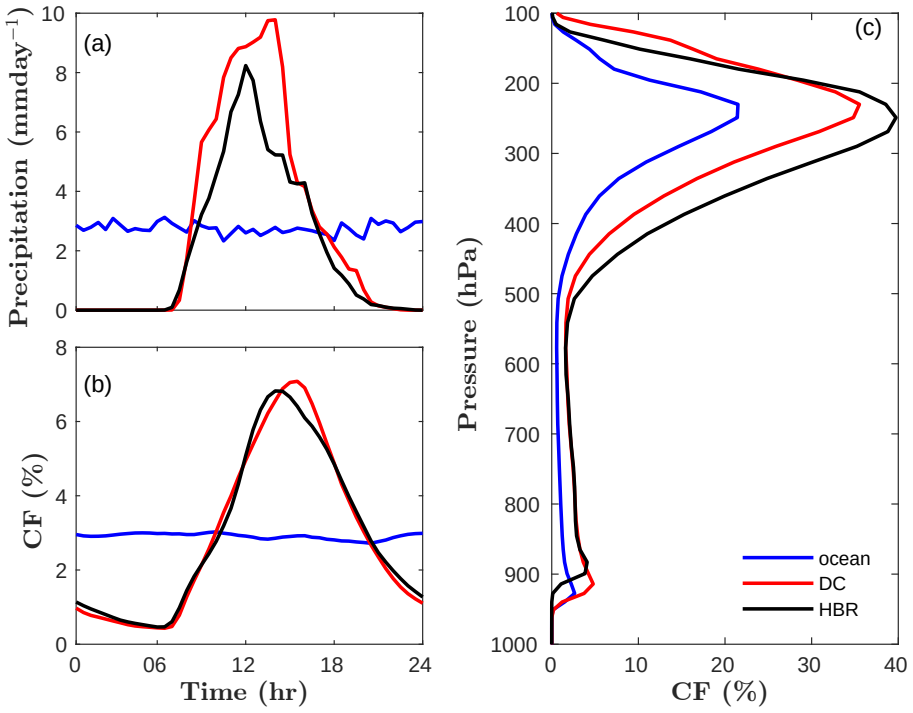

FIGURE 4.10: Plots showing the (a) domain -and time-mean precipitation, (b) vertical mean cloud fraction, and (c) the vertical profile of cloud fraction at noon. Cloud fraction is calculated from cloudy grids with non-precipitating condensate greater than 0.01 gkg^{-1}

ratio (HBR case). Simulation results of these two land-like configurations are compared to a simulation over an ocean surface with no imposed diurnal cycle of temperature. This approach deviates from the usual island configuration that has been used to explore differences in convection over land and ocean surface (e.g., Cronin *et al.*, 2015; Hansen *et al.*, 2020). Instead we impose the diurnal cycle of temperature over the entire domain for the different land configurations (DC and HBR), this allows us to study the surface temperature diurnal cycle mechanism from two extremes. The HBR case with deep boundary layer has a relatively colder free-tropospheric temperature profile compared to the ocean, and the DC case has a marginally higher free-tropospheric temperature profile relative to the ocean case, and is comparable to the mean free-tropospheric temperature profile over the island region in the study by Cronin *et al.* (2015).

Guided by earlier argument by Williams and Stanfill (2002) on the inaccuracies of parcel theory in estimating the buoyancies of convective clouds, and the study of Hansen *et al.* (2020) who found no evidence of daytime increases in CAPE over the island region in their study. We approach the analysis of our simulations from the standpoint that a different measure of CAPE or buoyancy would be required

to establish any connection between the diurnal cycle of surface temperature and the intensity of convective storms. In view of this, we assessed the simulation results by comparing the diurnal pattern of the domain-and time-mean of different thermodynamic variables to their high percentiles. This allowed for a two-point argument and investigation of the dynamics that favor or deny the connection between the large diurnal cycle of temperature and the intensity of continental storms.

Firstly, analysis of the simulation output for the two land-like cases showed a similar diurnal pattern of mean boundary layer MSE and specific humidity as that seen in Hansen *et al.* (2020), the mean boundary layer MSE peaked in the early morning as near surface air temperature begins to rise and continues to decrease during the daytime. As a result the mean undiluted CAPE assumes a similar pattern, peaking in the morning and decreasing during day. However, when an argument is made based on the two-plume theory, we find a situation where the land-like simulations show the strongest updraught velocity and high percentiles of undiluted CAPE that peak as the surface temperature peaks, in line with the hypothesis that supports the large diurnal cycle of temperature's control of continental storms.

To answer the question of whether the highest percentile of undiluted CAPE should be main focus when estimating the relationship between the large diurnal cycle of temperature and the intensity of convective storms. We presented two cases of simulations over land-like surfaces; the DC case with only the imposed diurnal cycle of temperature, and the HBR case with both imposed diurnal cycle of temperature and deeper boundary layer. Comparing the highest percentiles of undiluted CAPE, the DC case had significantly higher CAPE than the HBR case, However, the HBR case had marginally higher updraught velocity than the DC case. A scaling relation based on a two-plume model (Singh and O'Gorman, 2015) was used to show the dependance of buoyancy on entrainment. The scaling relation was able to reproduce the marginal difference in buoyancy between the two cases. Results of the scaling was confirmed by a spectrum of entraining plume model (Zhou and Xie, 2019) that calculates both the undiluted CAPE and the CAPE of the entraining plume which represents the parcels with strongest buoyancy. This highlights the importance of entrainment to the overall debate on thunderstorm intensity. Since entrainment is such a complex parameter to study in the real

world, it becomes increasingly difficult to make a solid claim for any surface mechanisms whose connection to the intensity of convective storms is centred around the build up of CAPE.

The evidence of boundary layer quasi-equilibrium (BLQE) in the real world as found by Hansen *et al.* (2020) largely suggests that the lack of contrast in CAPE found in real world might be self induced by convection over the land surface itself. As shown earlier, the few strongest storms in the land-like simulations represented through the high percentiles of buoyancy, grow deeper into the troposphere reaching the tropopause and forming anvil clouds. Enhanced downdrafts from these anvil clouds could essentially suppress the buoyancy of other developing clouds by drying the surface and enhancing entrainment. Hence the bulk of the convecting parcels would have weaker buoyancy. This is a plausible reason for the largely observed contrast in updraught strength between land and ocean surface, but little evidence of a contrast in CAPE between the two surfaces.

It is still possible that some other land surface features may have a stronger control on the intensity of continental storms than the mechanism tested in this study. Abbott and Cronin (2021) for example found significant invigoration of convective storms in response to increasing aerosol concentration in a WTG experiment, and explained that the high concentration of aerosols increased environmental humidity leading to more buoyant clouds. The results of our study largely support the significance of environmental humidity in the debate of how buoyancy is sustained over the tropics and the eventual updraught strength of convective clouds over tropical land surfaces.

Finally, we conclude on the note that from a modeling perspective, the large diurnal cycle of surface temperature as tested in this experiment has some physical connections to the intensity of convective storms in terms of providing the potential available energy required for convection. However, the actual buoyancy of the convective clouds is determined by the environmental humidity and the entrainment. A better perspective to this work would be to replicate this diurnal cycle experiment with parameterized large-scale dynamics based on the weak temperature gradient (WTG) approximation.

Chapter 5

Response of updraught intensity of thunderstorms to surface warming over a conceptual land surface in RCE.

5.1 Background

In this chapter we investigate the response of moist convection to different temperature regimes using RCE simulations over a highly idealized land surface. This chapter seek to address the third research question which asks: **How does the intensity of convective storms over a conceptual land surface respond to different temperature regimes?** Here, our idealized land surface is only loosely defined as a surface with imposed diurnal cycle of surface temperature, and a high boundary layer. This idealization of the land surface follows earlier findings in Chapter 4 of this thesis where we found some connections between the large diurnal cycle of surface temperature and the intensity of storms that formed over the idealized land surfaces. The high surface Bowen ratio is employed to make a distinction between a wet and dry land surface. This allows for a side-by-side comparison of the response of convection over an idealized wet and dry land surfaces.

For warming simulations over both wet and dry land surfaces, we assess changes in precipitation, udraught velocity and CAPE. We also explore how some known lightning proxies respond to warming over wet and dry land surfaces. Specifically, the CAPE ×P, PW10, ICET (IFLUXT) and I×G are assessed in this study. We show how these different metrics differ in the various simulations. Detailed description of these metrics, and how they are calculated in this study is given in Section 5.3.1.

5.2 Introduction

Moist convection is a significant aspect of the earth's climate. It is the main mechanism for the distribution of energy and momentum between the earth's surface and the atmosphere. Thunderstorms resulting from convective processes produce a significant percentage of precipitation across different climatic zones, especially the tropics and the subtropics. Notwithstanding the strategic importance of moist convection, it remains one of the most complicated and least understood part of the earth's climate (Bony *et al.*, 2015) primarily because they occur at scales too fine to be resolved by conventional global climate models (GCMs). This places considerable restraint on our ability to fully understand and predict storms formed out of these convective processes. The clearest pathway around this conundrum is presented by the continues improvement in the abilities of cloud reserving models (CRMs). Most CRMs are now set on geographical grids and can be used to study moist convection on global scales. Full scale studies of convective processes on global scale with the so-called global cloud resolving models (GCRM) are now emerging. However, the so-called small domain configuration of CRMs has been used to great effect in studying different aspect of convection over the tropics, and over different surfaces.

Muller *et al.* (2011) for example, used a relatively high resolution CRM simulations to study the response of precipitation extremes to increases in mean sea surface temperatures (SST). In their warming simulations, they found significant increases in extreme precipitation in response to warming over a tropical ocean surface. They identified three factors that contributed to the increase in magnitude of the extreme precipitation. In order of relative importance they identified that the extreme precipitation increase roughly scales with; changes in concentration of water at the surface, changes in vertical velocity at the convection region and

precipitation efficiency. These features represent the thermodynamic, dynamic, and microphysics contributions respectively. They contended that the microphysical contribution represented through the precipitation efficiency remains largely unchanged with warming, but there are significant changes in the concentration of surface water vapour and updraft velocity to enhance precipitation as temperature increases. Their results corroborated findings of a similar study by Romps (2011), who also showed that the increases in precipitation scales with increases in water vapour gradient in response to warming. Romps (2011) approach used a higher resolution over a much smaller domain compared to the domain size and resolution used in the case of Muller *et al.* (2011). Again their warming approach was by increasing the concentration of carbon di-oxide (CO_2), which is different from the case of Muller *et al.* (2011) where the warming approach was by increasing the mean SST. Notwithstanding the marked differences in the two studies, their results agreed on many grounds in respect to how moist convection over tropical ocean surfaces response to warming. Romps (2011) posited that fluxes of global and local precipitation obeys the Clausius-Clapeyron (CC) approximation at a fractional rate of 3% K^{-1} and 7% K^{-1} respectively. Similar increases in precipitation in response to warming have been reported in a number of studies (e.g, Jeevanjee and Romps, 2018; Meredith *et al.*, 2019).

The intensity of convective storms is mostly tied to the potential danger the storm poses to life and property. High percentiles of vertical velocity within a convective storm is a simple but yet direct measure of the storm's intensity (Del Genio *et al.*, 2007). The vertical velocity within convective clouds form the basis of the dynamic contribution to the enhancement of precipitation extremes (Muller *et al.*, 2011). The vertical flow of air within convective clouds especially at the mixed ice-liquid phase level speeds up the collision of ice particles, and thus enhance electrical charges within clouds which are represented as lightning flashes in thunderstorms. A vertical velocity threshold of about 10 ms^{-1} is known to trigger significant cloud to ground lightning (Zipser and Lutz, 1994). Lightning from intense storms is a perpetual danger to the natural habitat of plants and human alike. Therefore central to the study of moist convection is to understand the mechanisms that influences the intensity of convective storms and to investigate how these intensities might change in the future.

There have been substantial progress made towards understanding how updraught intensity might change in response to warming especially over tropical ocean

surfaces. Singh and O'Gorman (2015) for example investigated the response of updraught velocity to warming and found that updraught velocity of convective storms and CAPE increases with mean SST. They found that, the largest fractional increase in the updraught velocity were more noticeable at the upper atmosphere. They argued that the vertical velocity increases at a lower magnitude than might be implied by CAPE, and attributed this to the effect of entrainment on updraft within the convective clouds. Their explanation was based on a two-plume model where the weakly entrained plume represented the strongest updraughts, and the strongly entraining plumes represented parcels with weaker updraughts. The CAPE increment in their study was also attributed to saturation deficit which also increases with warming. Romps (2011) also found similar increases in CAPE and vertical velocity in their warming studies. They found a 6% - 7% increase in CAPE in response to doubling the concentration of CO_2 in their simulations. Again, most of these warming studies and theories that focuses on convective updraughts have mainly been explored over tropical oceans, and not much have been done over land mainly because of the complicated nature of the land surface.

Most studies on extreme precipitation changes to warming over these small-domain CRM simulations have mostly focused on the ocean surface, and not much have been done over land surfaces. Given that extreme precipitation are mostly from intense thunderstorms, which are more prevalent over land surfaces, it becomes extremely important to replicate some of these studies over land surfaces. Zhang and Zhou (2019) have shown that, there has been significant increases in precipitation over the global land monsoon regions in the last decade attributable to global warming during this period. The question of how much these changes will vary going into a warmer future still remain to be explored in GCRMs or understood in simple frameworks using CRMs.

There is a growing scientific interest to isolate the main features of the land surface that are key to enhancing convection over land. Identifying this features would allow for simplification of the land surface for such warming simulations. There has however not been enough consensus amongst studies that investigate these land surface features and their connection to the intensity of convective clouds. For studies that have found some of these surface features of the land surface to be connected to continental storm intensity (cloud base height: Williams *et al.*, 2005a), (aerosol concentration: Abbott and Cronin, 2021), these connections have

not been explored over warming simulations to know how the relationship of such surface features hold under different temperatures.

In the previous Chapter 4 of this thesis, we found the large diurnal cycle of surface temperature over the land surface to have some physical connections with the intensity of convection over land. Based on this, we explore how a conceptual land surface defined by its anomalous diurnal heating responses to warming. To give a better perspective, we assess these warming simulations over wet and dry idealized land surfaces. We make comparison of how the different surfaces respond to warming.

The rest of the chapter is structured as follows: We highlight the specific experiment design for the RCE simulations run towards addressing the third research question in Chapter 5.3. We discus come common metrics used as proxies for lightning in some studies and how they have being applied in this study. The different proxies of lightning considered in this study and their governing equations are presented in Section 5.3.1. The main findings of the warming simulations and analysis are presented in Chapter 5.4. We discuss our findings further and make conclusions of this chapter in Chapter 5.5.

5.3 Experiment design and simulations

We run simulations to radiative-convective equilibrium (RCE) over a land-like surface with imposed diurnal cycle of temperature and high surface Bowen ratio. The high surface Bowen ratio is only forced over our conceptual land surface to establish how wet and dry surfaces of the land surface respond warming. We maintain the general model setup describe in Section 2.4 with little alterations to suit the objectives of this experiment. Here the imposed diurnal cycle of temperature is the same as the approach described in Section 4.3, where a sinusoidal variation of surface temperature as imposed by Equation 4.1. For this warming experiment, all simulations are run over a doubly periodic homogeneous domain. We used the SAM one-moment microphysics scheme. All simulations are run for a total of 100 days with time-mean statistics collected every 30 minutes and 3D instantaneous snapshots collected every 3 hours. The same radiation and sub-grid parameterization schemes used in the previous chapters are unchanged. We also maintain the same domain size and resolution as previous chapters of this thesis. The last

30 days of the simulations are considered in the analysis shown in the subsequent sections.

To distinguish between wet and dry land surface, we moderate the available moisture at the boundary surface by using two different evaporative conductance parameter (α) values in the bulk latent heat equation of the CRM model. This approach is already explored in this thesis as detailed in Section 3.3.1. We use α of 0.25 for simulations described as dry, and 0.5 for simulations described as wet. For each case we run simulations with mean surface temperature of 300 K, 305 K and 310 K.

5.3.1 Estimation of updraught intensity from our simulations

Consistent with the earlier chapters, the main metric for estimating the intensity of the convective storms in the various simulations is the highest percentile of updraught velocity across all vertical levels. We specifically use the 99.99th percentile of vertical velocity calculated from instantaneous 3D outputs of the last 30 days of our simulations. The 99.99th percentile calculated here represents the near-highest velocity over the entire domain at all times, and at each vertical level. In line with the diurnal configuration in this study, percentiles are calculated for each time of the day separately.

In this chapter we consider the four proxies used by Romps (2019a) in estimating lightning rates in convective storms in response to warming over ocean surface. We therefore test the response of these proxies to warming over our conceptual land surface. In line with our experiment design, we assess the diurnal variation of these proxies in response to warming. We deviate slightly from the approach of Romps (2019a) by considering both high percentiles of these proxies as well as their time-means.

5.3.1.1 Lightning proxies

The four proxies of lightning used in the work of Romps (2019a) to assess the changes in lightning rates in response to warming over tropical ocean surfaces are; CAPE×P, PW10, IFluxT (hereinafter ICET) and I×G. Here we present the

theoretical basis and the governing equations of these proxies as explained in various literature, and we highlight on how they are being used in this study.

CAPE×P

CAPE×P is simply the product of CAPE and precipitation rate at the surface as shown in Equation 5.1. It has been shown to reproduce and explain a significant percentage of variance in total lightning flash rates over continental United States (Romps *et al.*, 2014). The proxy is grounded on the idea that higher values of CAPE are required for stronger updraught and faster lofting of water into the atmosphere. In this sense, CAPE provides the energy for the lifted mass of water vapour which condenses to form clouds and later fall as precipitation. The assumption here is that there is a high conversion rate of evaporated water into condensates and the energy of the lifted mass of water vapour is transferred to the condensates. Precipitation falling from these condensates therefore assumes kinetic energy enough to trigger lightning in the atmosphere. Here, we calculate both the high percentiles and time-means of CAPE×P. High percentiles of CAPE are calculated as a pseudo-adiabatic parcel initialized with first model level temperature and specific humidity from 3D instantaneous outputs from the different simulations. The 99.99th percentile of the integrated buoyancy of this parcel is then calculated. Higher percentiles of precipitation rate (P) are also calculated from the instantaneous precipitation flux at the surface. We also calculate mean CAPE×P using CAPE calculated from mean temperature and humidity profiles, and mean P is the calculated time-average precipitation rate. In both cases, we show the diurnal composite of CAPE×P. The simple governing equation of the CAPE×P proxy is as detailed below:

$$CAPE \times P = CAPE(x, y, t)P(x, y, t), \tag{5.1}$$

Here, CAPE is the convective available potential energy, P is precipitation rate in energy units. x, y, z, and t are domain horizontal, vertical dimension, and time respectively.

PW10

The PW10 proxy is very similar to the CAPE×P in terms of the theoretical meaning and underlying physics. It is defined as the average precipitation rate in regions where the maximum vertical velocity in a column is greater than 10 ms^{-1}. This proxy is similar to the theory for CAPE × P, if one assumes that higher

vertical velocity is as a result of higher CAPE. The CAPE should be high enough to produce vertical velocity of at 10 ms^{-1} somewhere in the atmospheric column above the surface domain. High values of vertical velocity have been linked to precipitation extremes (Muller *et al.*, 2011), and vertical velocity of about 10 ms^{-1} appears to be the good threshold for the generation of lightning in the atmosphere (Zipser and Lutz, 1994). We therefore calculate high percentiles of PW10 from the instantaneous precipitation flux at the surface scaled by the 10 ms^{-1} vertical velocity threshold. We also calculate domain- and time-mean of PW10 guided by the equation below:

$$PW10 = P(x, y, t)\big[w \geq 10ms^{-1}\big], \tag{5.2}$$

where PW10 is precipitation rate (P) at the horizontal surface (with dimensions x and y) constrained by vertical velocity (w) of 10 ms^{-1} or higher within the cloud column over the domain.

I×G

The I×G is the product of mass concentration of ice and graupel in the atmosphere. This proxy is premised on the fact that electrical charges in the atmosphere are as a result of collision of hydrometeors particularly ice particles and graupel in the atmosphere. The general assumption is that, a higher concentration of ice and graupel in a particular cloud would have a high collision rate to release enough electrical charges that are represented in the atmosphere as lightning. As shown in Equation 5.3, I×G is calculated as the integral of the product of the mass concentration of ice and graupel in the entire cloud column. Similar to other proxies, we calculate high percentiles and mean of I×G from instantaneous profiles of ice and graupel integrated from the surface to the top of the cloud, and the time-means are calculated from mean ice and graupel output from the simulations.

$$I \times G = \int_0^\infty dz \rho_i(x, y, z, t)\rho_g(x, y, z, t), \tag{5.3}$$

where I×G is the product of concentration of ice and graupels, ρ_i and ρ_g are densities of ice and graupels respectively, and dz is the vertical column of the atmosphere being integrated.

ICET

The ICET (IFLUXT) proxy is based on the relationship between ice and electrification and subsequent lightning of the atmosphere. As the name suggests, it is a measure of the mass flux of ice at a particular temperature "T". This proxy has evolved from studies (e.g., Finney *et al.*, 2016) that considered the mass flux of ice pegged at a particular isobar, to estimation of ice flux at a particular isotherm (e.g., Romps, 2019a). The argument in support of the estimation of ICET at a particular isotherm instead of isobar is that, as the atmosphere warms in response to increasing temperature at the surface, isotherms are shifted further upwards and the mixed-phase level where ice are expected to be concentrated shifts accordingly. Restricting the estimation of the ice flux to a particular isobar would therefore risk the ability of the proxy to capture the level where ice are concentrated and may underrepresent lightning as the atmosphere warms. As shown in Equation 5.4, the updraft flux of ice is calculated as the product of density of ice and vertical velocity at the 260 K isotherm in a particular simulation. The caveat here is that vertical velocity should be greater than 1 ms^{-1} since we are only interested in updraft flux of ice. From the temperature profiles in our individual simulations, we loop through to identify 260 K isotherm level, we then calculate the high percentiles and mean updraft flux of ice at that particular level in the different simulations.

$$ICET = \rho_i(x, y, z\prime, t)w(x, y, z', t)\big[w(x, y, z', t) \geq 1\big], \tag{5.4}$$

Here ICET is the updraft flux of ice at 260 K isotherm level z′, ρ_i is the density of ice at the specific isotherm level and w the vertical velocity.

5.3.1.2 Calculation of fractional rates of change

In this chapter, the fractional rate of change (δX) has been used to estimate changes in different variables in response to warming. We test how much a variable, X_2 at a new temperature, T_2 has changed from its initial state, X_1 and previous temperature, T_1. This gives a measure of the change in the variable (X) per unit change in temperature. The fractional change is mostly expressed in percentage terms and is always written as $\delta X\%\ K^{-1}$.

The fractional change is given by the equation below:

$$\delta X = \frac{log(X_2) - log(X_1)}{T_2 - T_1} \tag{5.5}$$

5.4 Results

5.4.1 Response of convective storms to warming over wet land surface

In this section we present results of various aspects of convection in response to warming over a wet land surface. Here the wet land surface is loosely defined as a surface with a relatively low surface Bowen ratio, and with imposed diurnal cycle of temperature. An evaporative conductance parameter (α) value of 0.5 is used in the wet case as described in Section 5.3. Changes in precipitation, updraught velocity and CAPE are assessed for the individual idealized simulations run at different temperatures. The key differences and basis for the changes are highlighted. We finally present results for an alternative metric for assessing the intensity of convective storms. Here four proxies of lightning known in literature are explored and their response to warming described.

5.4.1.1 Precipitation increases in response to warming over wet land surface.

TABLE 5.1: Summary of domain-mean precipitation and evaporation rates from the simulations over wet land surface. P_{max} and E_{max} the daily maximum precipitation and evaporation rates respectively, P_{mean} and E_{mean} are the daily mean precipitation rate and evaporation rates respectively.

Case (K)	P_{max} ($mmday^{-1}$)	P_{mean} ($mmday^{-1}$)	E_{max} ($mmday^{-1}$)	E_{mean} ($mmday^{-1}$)
305 wet	8.2	2.1	4.2	2.1
305 wet	11.4	2.7	5.7	2.7
310 wet	15.5	3.4	8.0	3.4

Changes in precipitation and evaporation rates in response to warming in simulations with a relatively wet surface are presented here. As shown in Figure 5.1a,

hourly precipitation rates increases significantly with warming. The peak times of precipitation are mostly in the afternoon, and it does not change much across the different temperatures. Precipitation starts just around the same time in all temperature regimes except for the case run with the highest mean temperature (310 K) which have a few hours delay in the start time of precipitation. The increases in precipitation are mainly as a result of enhanced evaporation with warming.

As seen in Figure 5.1c, mean evaporation rates increase at almost the same fractional rate as precipitation and peak at the same time as surface temperature maxima. However as shown in Table 5.1 the daily maximum precipitation rate far exceeds the daily maximum evaporation rate at their peak times (noon) which suggest that precipitation minus evaporation (P-E) increases during the day in response to warming. Increases in P-E during day time is a common feature over wet land surfaces (Koster and Suarez, 2001). The daily change in mean P-E is almost zero across the different temperatures as expected, given that simulations are run to steady-state RCE.

We also see significant increases in extreme precipitation rates with warming over the wet land surface. Figure 5.1b shows the 99.99th percentile of instantaneous precipitation from the warming simulations over the wet land surface. The extreme precipitation across the different temperatures peaks around noon and has very similar start and end times. At their peak times, the 99.99th percentile of precipitation increases at a fractional rate of about 8%-9% K^{-1}, Muller *et al.* (2011) found a fractional increase of 7.4% K^{-1} in their assessment of the high percentiles of precipitation extremes over tropical ocean surfaces.

The fractional changes in daily mean and daily maximum precipitation rates are shown in Figure 5.1d. Both the daily mean (red colour) and the daily maximum precipitation (blue line) increases linearly with temperature. The daily mean precipitation increases at a fractional rate of about 5% K^{-1}, while the daily maximum precipitation also increases at a fractional rate of 8% K^{-1}. A summary of the daily-maximum and daily-mean precipitation and evaporation rates are shown in Table 5.1.

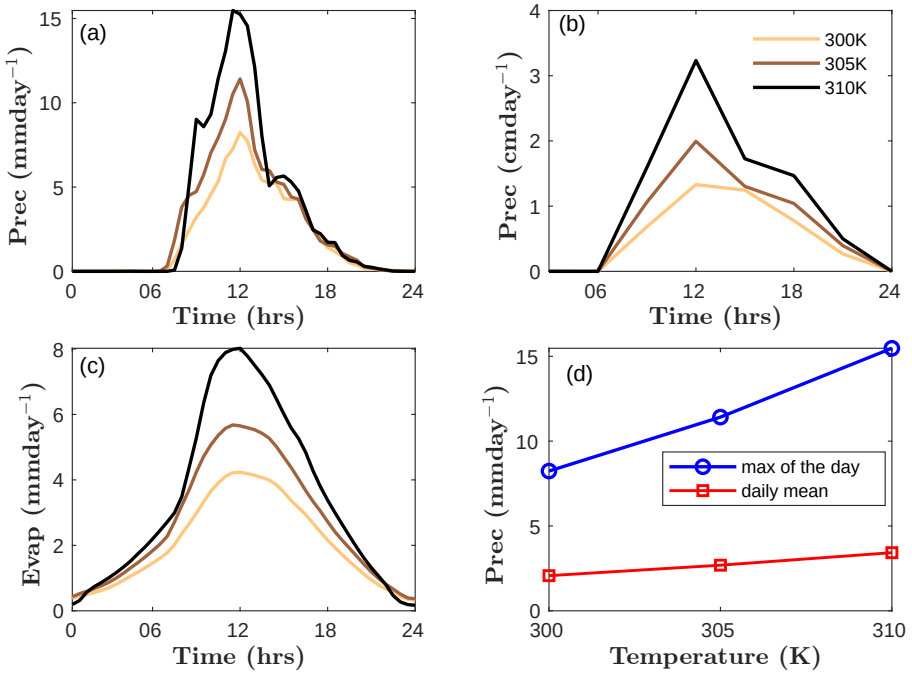

FIGURE 5.1: Diurnal composite of (a) domain- and time-mean precipitation rate, (b) 99.99th percentile of precipitation, and (c) domain- and time-mean evaporation rates from the warming simulations over wet land surface. Plot (d) shows the relationship between daily mean (red line), daily maximum precipitation (blue line) and mean surface temperature.

5.4.1.2 Updraught velocity increases with warming in RCE simulations over wet land surfaces

We now present results for the analysis of the high percentiles of updraught velocity across the different temperatures. First we assess the diurnal variation of the 99.99th percentiles of vertical velocity ($w_{99.99}$) across all vertical levels in response to warming in a time-height plane. We also make a determination of the changes in vertical velocity at the upper troposphere where they are maximum (w_{max}) and the daily-maximum of the 99.99th percentile of vertical velocity at the 500 hPa level (w_{500}) in response to warming.

Figure 5.2 shows a time-height plane of the 99.99th percentile of vertical velocity ($w_{99.99}$) in warming simulations over a relatively wet land surface with relatively low surface Bowen ratio (SBR). It is clearly seen that the $w_{99.99}$ increases significantly with warming. When the mean surface temperature is 310 K, its vertical velocity in the upper troposphere is about twice ($\sim 2\times$) as high as in the case with mean surface temperature of 300 K. In addition, the vertical velocities reach higher altitudes in the troposphere possibly overshooting into the stratosphere as

mean surface temperature over the wet land surface increases. There is also a visible increase in w_{500} (estimated at the point of the dash lines on the plot) with warming. At the peak time of the maximum velocity across the different mean temperatures, w_{500} in the 310 K case is about 5 ms^{-1} higher than the 300 K case.

It has already been shown in idealized modeling simulation studies (e.g., Singh and O'Gorman, 2015) over tropical ocean surfaces that vertical velocity increases in response to warming, and the fractional increase is most noticeable at the upper troposphere. The marginal increase in vertical velocity at the lower troposphere in warming simulations has been shown to only play a secondary role in the overall contributions of extreme precipitation over tropical ocean surfaces (Muller *et al.*, 2011). For the warming simulations shown here, the apparent increases in vertical velocity at the middle troposphere could mean an increase in the dynamic contribution to precipitation extremes. The visible vertical depth reached by the vertical velocities in the different cases also suggests clouds overshooting into the tropopause might be prevalent in the future over wet land surfaces, this might have implications for the thermodynamic structure of the tropopause as noted by previous studies done over tropical ocean surfaces (e.g., Singh and O'Gorman, 2015).

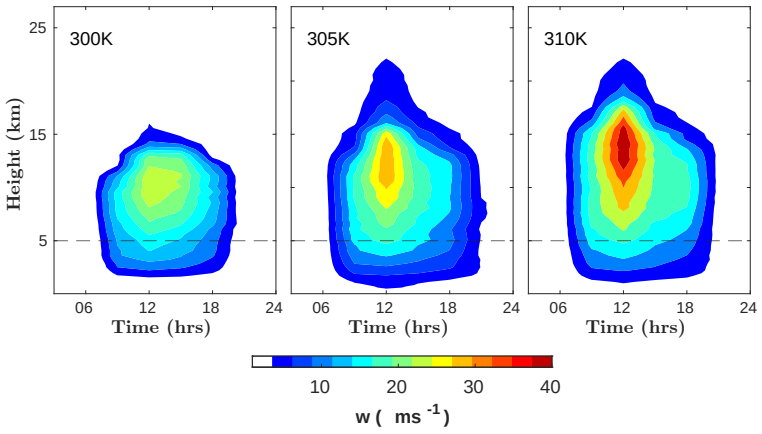

FIGURE 5.2: Time-height plane of the 99.99th percentile of vertical velocity in warming simulations over a wet surface with imposed diurnal cycle of temperature. Plots shown here are for simulations run with mean surface temperature between 300 K to 310 K as labeled on the plots.

A clearer picture is shown in Figure 5.3 where we compare the maximum vertical velocity profiles during the day and a diurnal pattern of the maximum vertical velocity everywhere in the troposphere at a particular time of day. Figure 5.3a shows the vertical profile of $w_{99.99}$ at noon. The 310 K case clearly has the strongest updraught, followed by the 305 K case, with the 300 K having the lowest updraught

speed. A similar picture is revealed by the diurnal pattern of vertical velocity estimated across all vertical levels at a particular time of the day (Figure 5.3b). In the early morning, the maximum vertical velocity across the different temperatures remain largely similar, at noon there is almost an exponential increase in the maximum vertical velocity between the 300 K case and the 310 K case. The maximum $w_{99.99}$ retains a fairly similar diurnal pattern with warming. This might be as a result of how the imposed diurnal cycle of temperature is modelled but essentially the plots show increases in updraught velocity in the day in response to warming.

We finally show how the maximum $w_{99.99}$ estimated across all vertical levels and at their peak time changes with warming (Figure 5.3c: red line). The daily maximum $w_{99.99}$ which is starkly seen at the upper troposphere increases at a fractional rate of about 4-6% K^{-1}. The maximum w_{500} (Figure 5.3c: blue line) increase at relatively lower fractional rate of 1-3% K^{-1}.

It is seen from these plots that the vertical velocity of convective storms increases significantly with warming over an idealized land surface with a relatively lower boundary layer (wet case), and the fractional increases are more noticeable in the upper troposphere where there is almost an exponential increase in vertical velocity with warming. It can also be inferred that deeper and taller clouds would form over relatively wet land surfaces in the future.

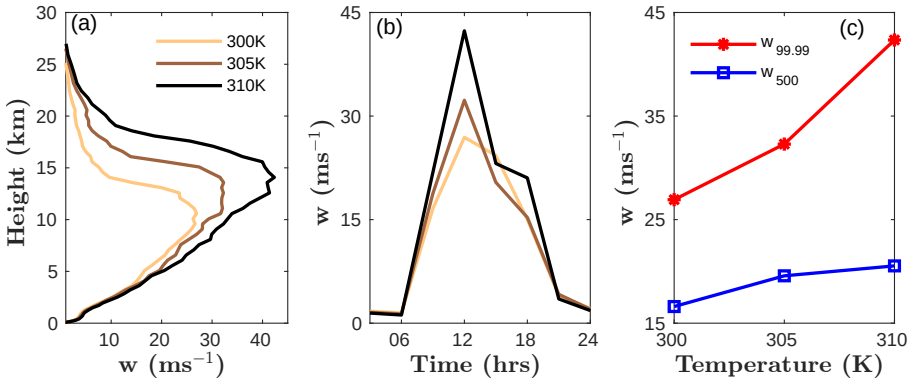

FIGURE 5.3: Plots of daily maximum of the 99.99th percentile of vertical velocity ($w_{99.99}$) shown as; (a) profile of $w_{99.99}$ at each vertical level of the atmosphere for the different temperatures, (b) the diurnal variation of maximum $w_{99.99}$ with respect to warming. Plot (c) shows how maximum $w_{99.99}$ (red line) and maximum w_{500} (blue line) changes with temperature.

5.4.1.3 Increases in CAPE with warming in simulations over a wet land surface

In Figure 5.4a we show the diurnal variation of the buoyancy integral estimated from the 99.99th percentile of buoyancy from the simulations. First we calculate the 99.99th percentile of buoyancy from the instantaneous 3D outputs from the simulations, and integrate across all vertical levels of the troposphere. There is an almost uniform increment in the maximum buoyancy integral with warming as seen in Figure 5.4b. Across the different temperatures, the integrated buoyancy peaks at noon. At the peak time, the buoyancy integral from the simulations increases at a fractional rate of 4-5% K^{-1}, and scales fairly well with the maximum updraught speed from the simulations.

We also show the undiluted CAPE (buoyancy integral) calculated from the spectral plume model. As shown in Figure 5.4c, undiluted CAPE increases significantly with warming and at all times of the day. The daily maximum undiluted CAPE calculated from the spectral plume model also increases at a fractional rate of 4-5% K^{-1} with warming as seen in Figure 5.4d.

The results so far points towards enhancement in convection over wet land surfaces in response to warming. There is a visible increase in precipitation, updraught velocity, and CAPE in response to warming over the idealized land surface with relatively lower surface Bowen ratio. Although the approach to these simulations are highly idealized, The results here gives a fair view of how convection might behave over wet land surfaces.

5.4.1.4 Lightning proxies response to warming over wet land surface

We assess how the different lightning proxies described in Section 5.3.1.1 respond to warming over the wet land surfaces. The 99.99th percentiles and domain- and time-mean of the proxies are shown for the different simulations. As shown in Figure 5.5, all the proxies except the ICET proxy point towards increases in lightning flash rates with warming over the wet land surface in our simulations. The CAPE $\times$ P proxy that relies on CAPE and precipitation showed significant increase with warming in both the time-mean and highest percentile. This is expected because both undiluted CAPE and precipitation increases significantly with warming. Similarly to the CAPE $\times$ P proxy, the PW10 which is premised on

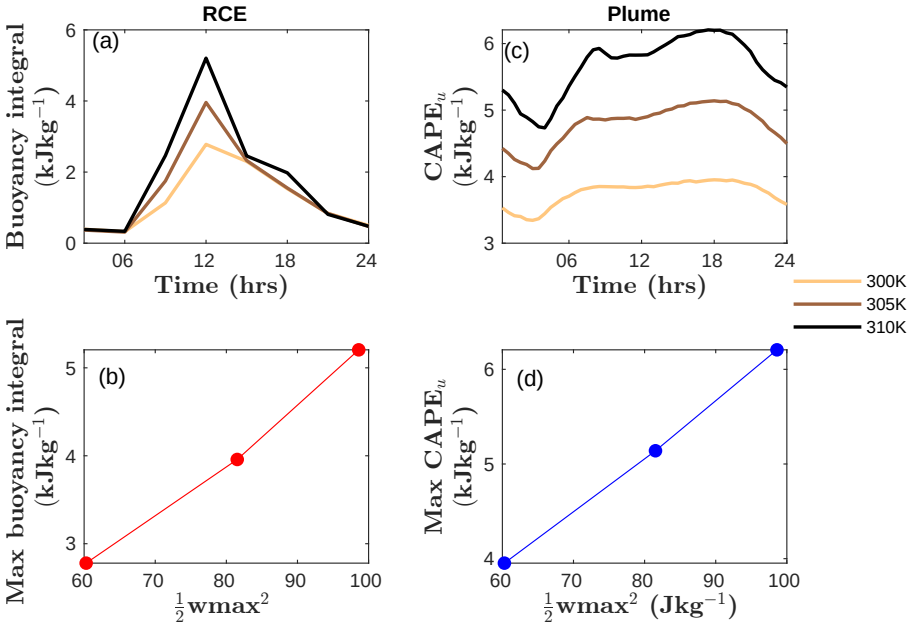

FIGURE 5.4: Diurnal composite of the (a) integral of the 99.99th percentile of buoyancy from simulations, (b) undiluted CAPE calculated from the spectral plume model. (c) shows the relationship between the maximum buoyancy integral of the day and the maximum updraught speed found for the different simulations. (d) show similar relationship between maximum undiluted buoyancy calculated from the spectral plume model and the maximum updraught speed from the simulations

precipitation constraint by vertical columns in the troposphere with a minimum updraught velocity of 10 ms^{-1} also increases with warming. As seen earlier, the vertical velocities in our simulations increases significantly with warming, hence it is easy to find precipitating regions with the 10 ms^{-1} vertical velocity threshold .

The I×G proxy which is the integral of the product of mass concentration of of ice and graupel also increases with warming in our simulations. The increase is however more noticeable in the 99.99th percentile compared to the mean. In the study of Romps (2019b), the mean I×G proxy showed a decreasing tendency in response to warming over tropical ocean surfaces. It can therefore be inferred that there might be more ice and graupel in storms over wet land surfaces in the future.

Finally, as found by Romps (2019b) over tropical ocean surfaces, the ICET (IFLUXT) proxies show a decreasing trend with warming in our simulations. The ICET proxy is founded on the ice flux at the 260 K isotherm.

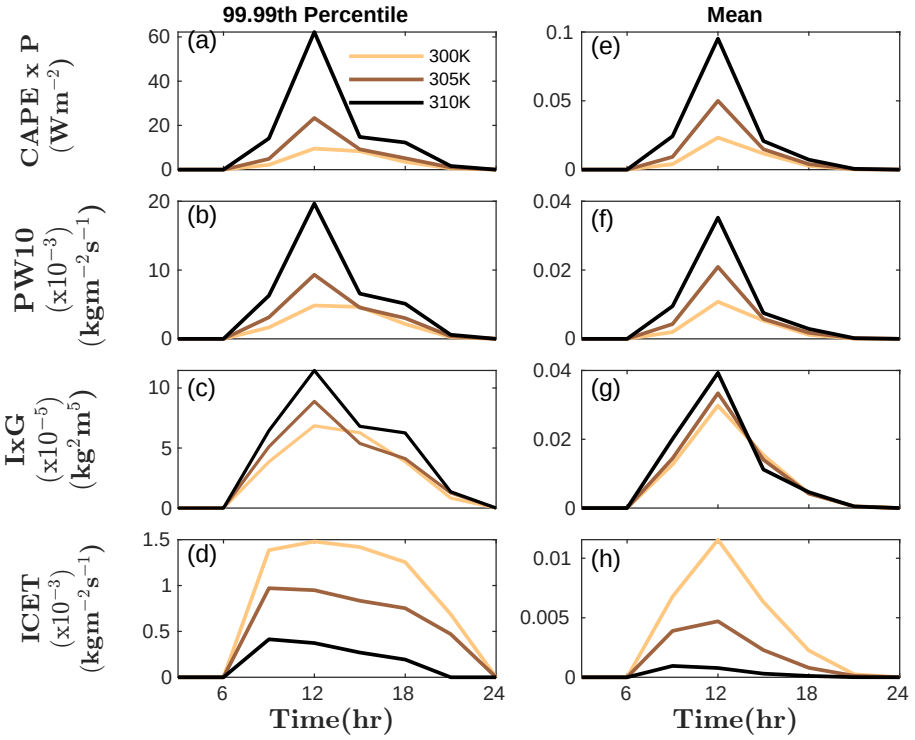

FIGURE 5.5: Diurnal composite of CAPE × P for simulations over the ocean (blue line) and the land - like simulations with increasing maximum temperature from 305 K (red line) to 311 K (black line). CAPE × P is the product of entraining CAPE (ECAPE) and mean precipitation rates in energy units.

5.4.2 Response of convection to warming over a dry land surface

We also assess the response of convection to warming over dry land surface. Here, the dry land is defined as a surface with relatively higher surface Bowen ratio (deeper boundary layer), and an imposed diurnal cycle of surface temperature. Similar to the approach described earlier for the wet case, an evaporative conductance parameter (α) value of 0.25 is used to give the dry cases a significantly higher surface Bowen ratio compared to the wet case. We assess the response of precipitation, updraught velocity and CAPE to simulations with mean surface temperature of 300 K, 305 K and 310 K. We highlight the differences seen in these parameters in response to warming over our idealized dry land surface.

TABLE 5.2: Summary of domain-mean precipitation and evaporation rates from the simulations over dry land surfaces. P_{max} and E_{max} the daily maximum precipitation and evaporation rates respectively, P_{mean} and E_{mean} are the daily mean precipitation rate and evaporation rates respectively.

Case (K)	P_{max} (mmday^{-1})	P_{mean} (mmday^{-1})	E_{max} (mmday^{-1})	E_{mean} (mmday^{-1})
305 dry	5.2	1.4	2.7	1.4
305 dry	6.0	1.8	3.6	1.8
310 dry	8.5	2.6	4.8	2.5

5.4.2.1 Changes in precipitation rates in response to warming over dry land surfaces

Over the idealized dry land surface, the hourly precipitation rate does not vary much across the different temperatures, at their peak times, the precipitation rate of the 310 K case is is only about 3 mmday^{-1} higher than the 300 K case. There are also visible differences in the start and peak times of the domain- and time-mean precipitation rate. The precipitation rate in the warmest case (310 K) appears to start earlier than the colder cases, and the 300 K case has the latest start time (Figure 5.6a). The extreme precipitation rates shown in Figure 5.6b also shows a similar diurnal pattern, although the extreme precipitation rates show larger increment in response to warming than the domain- and time-mean precipitation rates. In terms of the fractional changes, the daily maximum precipitation rate in the dry land case changes at a rate 3-6% K^{-1}, while the daily mean precipitation rate changes by 5-7% K^{-1} in response to warming. A summary of daily maximum and daily mean precipitation and evaporation rates are shown in Table 5.2.

The fractional increases in daily mean precipitation rates in the dry cases are largely comparable to the fractional changes in the wet cases. However, the fractional increase in the maximum precipitation in the dry cases is significantly lower than the wet cases. This suggests that at warmer temperatures precipitation would be much enhanced over wet land surface than a dry surface with deeper boundary layer depth. The difference in precipitation rates between the wet and dry case is mainly as a result of the available surface moisture in the wet case. At the same surface temperature, one would expect enhanced evaporation over wet land surfaces and eventual enhancement of precipitation.

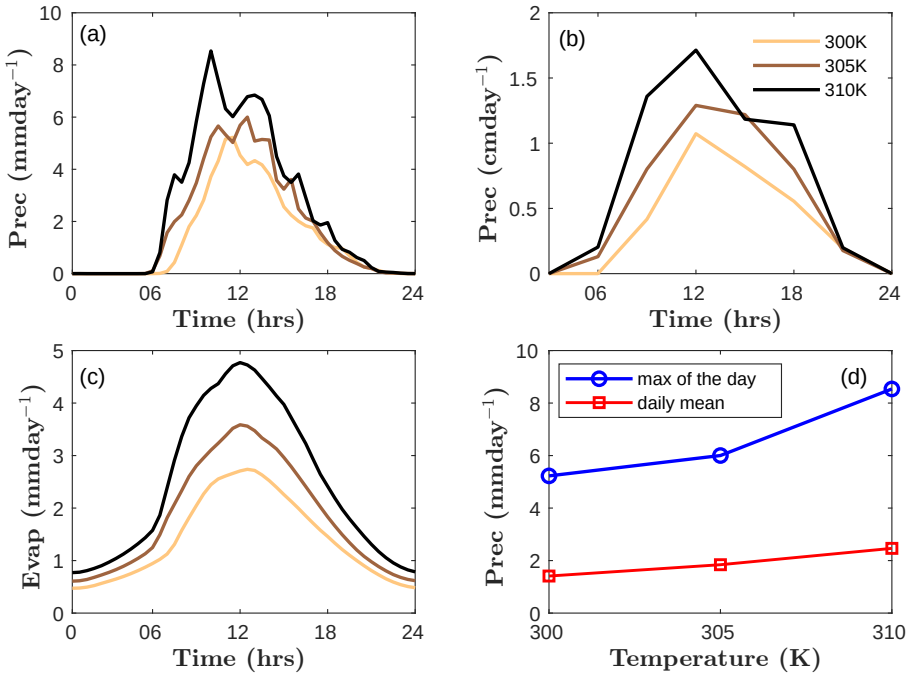

FIGURE 5.6: Same as Figure 5.1 but for warming simulations over dry land surfaces.

5.4.2.2 Changes in updraught velocity in response to warming over dry land surfaces

We also assess the diurnal evolution of the higher percentile of vertical velocity found in the warming simulations over the dry land surfaces by first looking at the diurnal pattern and later focusing on the maximum profiles and their fractional changes in response to warming.

Figure 5.7 shows the time-height plane of the 99.99th percentile of vertical velocity in the different simulations. While the vertical velocities of the warmer cases reach into deeper levels in the troposphere suggesting deeper clouds that reaches the tropopause, the differences in the vertical velocities at their peak levels in the upper troposphere are very marginal. The maximum updraught velocity in the 310 K is only about 2 ms^{-1} higher than the 300 K case, and almost the same as the 305 K case.

As earlier seen in the time-height plane, the maximum profiles of the higher percentiles of vertical velocity changes only marginally with warming as seen in Figure 5.8a-b. The 310 K and 305 K cases have almost the same maximum velocity at

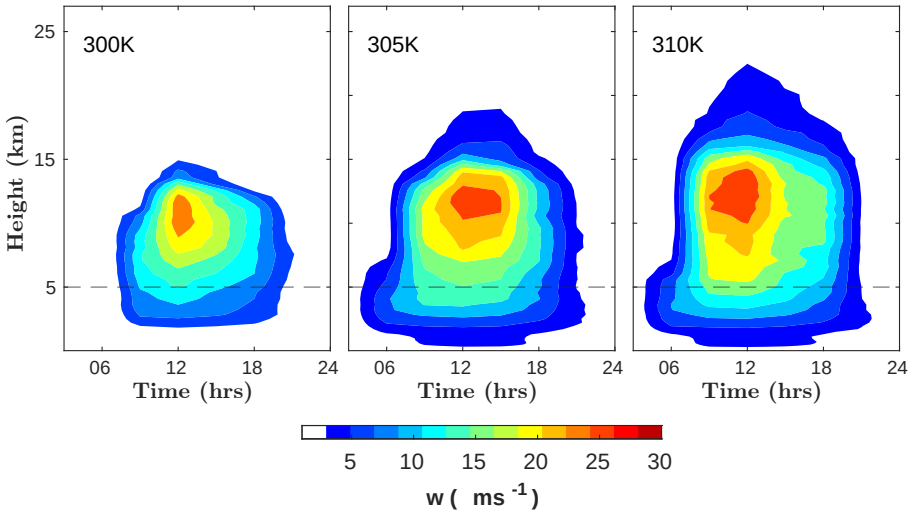

FIGURE 5.7: Same as Figure 5.3 but for warming simulations over dry land surfaces.

the upper troposphere, and are only marginally higher than the 300 K case. There are also marginal differences in the 99.99th percentile of vertical velocity at the 500 hPa level (w_{500}), as shown in Figure 5.8c. w_{500} increases at a fractional rate of about 2% K^{-1}. The peak vertical velocity at the upper troposphere increase just about the same fractional rate as w_{500}, and begins to decrease with further warming.

The dry cases largely appear to have relatively weaker storms in comparison to the wet cases. While the 99.99th percentile of vertical velocity increases significantly in response to warming over the wet surfaces, there is only a marginal increase in the dry cases.

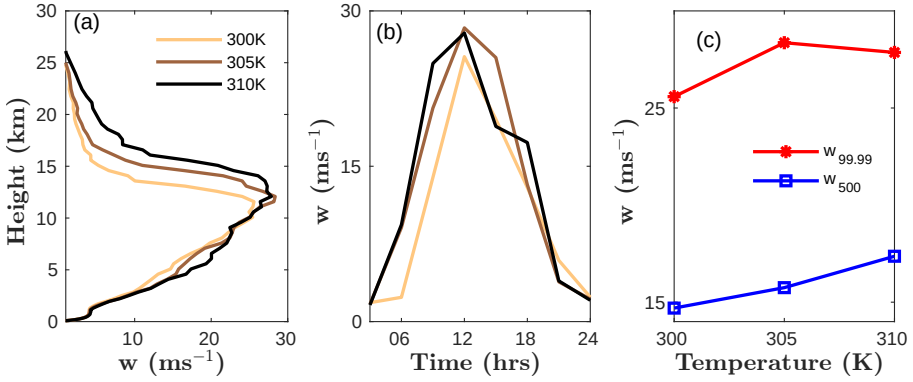

FIGURE 5.8: Same as Figure 5.4 but for warming simulations over dry land surfaces.

5.4.2.3 Changes in CAPE in response to warming over dry land surfaces

We also assess the response of CAPE to warming over dry land surfaces. As shown in Figure 5.9a, the buoyancy integral calculated from the 99.99th percentile of buoyancy from the RCE simulations increases with warming over the dry land surface. The increases are largely seen in the early morning and a noon when they peak. There are periods in the afternoon where the 305 K case had marginally higher buoyancy than the 310 K case.

The undiluted CAPE in the dry cases are very comparable to the wet cases in terms of the huge increases in CAPE in response to warming. Given that at the same temperature, the wet cases have significantly higher updraught than the dry case can only be explained by the presence of mechanisms that that acts to reduce buoyancy of convective parcels in the atmosphere. As seen in Figure 5.9a, the dry cases have significantly lower buoyancies compared to the wet cases (Figure 5.4a). Entrainment and downdrafts are the two most likely candidates for the reduced buoyancy in the dry cases.

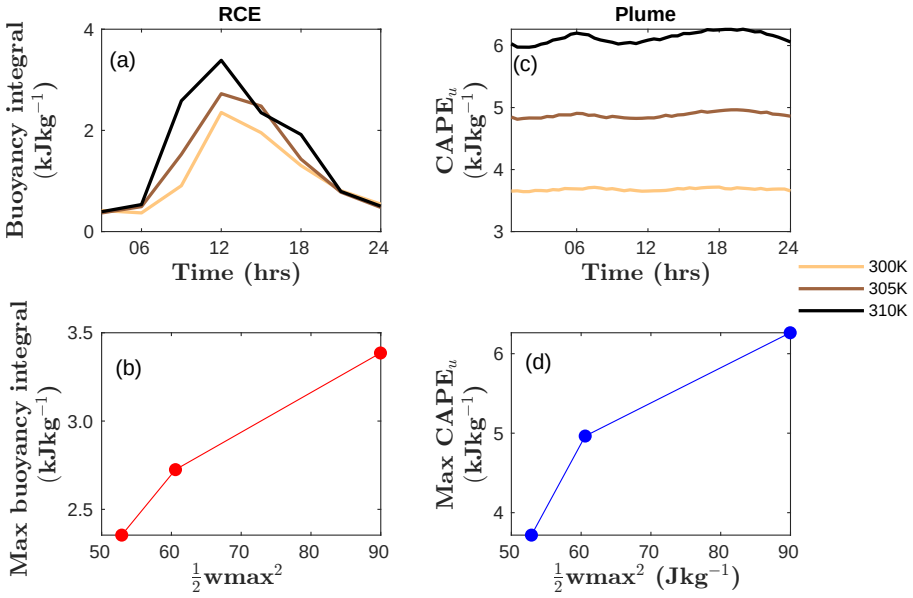

FIGURE 5.9: Same as Figure 5.5 but for warming simulations over dry land surfaces.

5.4.2.4 Lightning proxies in warmer over dry land surfaces

Finally, we assess how the high percentiles and domain- and time-means of the different proxies respond to warming over dry land surfaces. As shown in Figure 5.10, both CAPE ×P and PW10 show a possibility of enhanced lightning over dry land surfaces in response to warming. The high percentiles and time-mean of I×G however points towards different directions. While the high percentile suggest increase in lightning in response to warming, the time-mean suggests a decrease in lightning flash rates over dry land surfaces at higher temperatures. This is different from the wet surface case, where both the high percentile and time-mean of the I×G proxy predicted increases in lightning in response to warming. Just like the wet case, the ICET predicted decreases in lightning over dry land surface in response to warming.

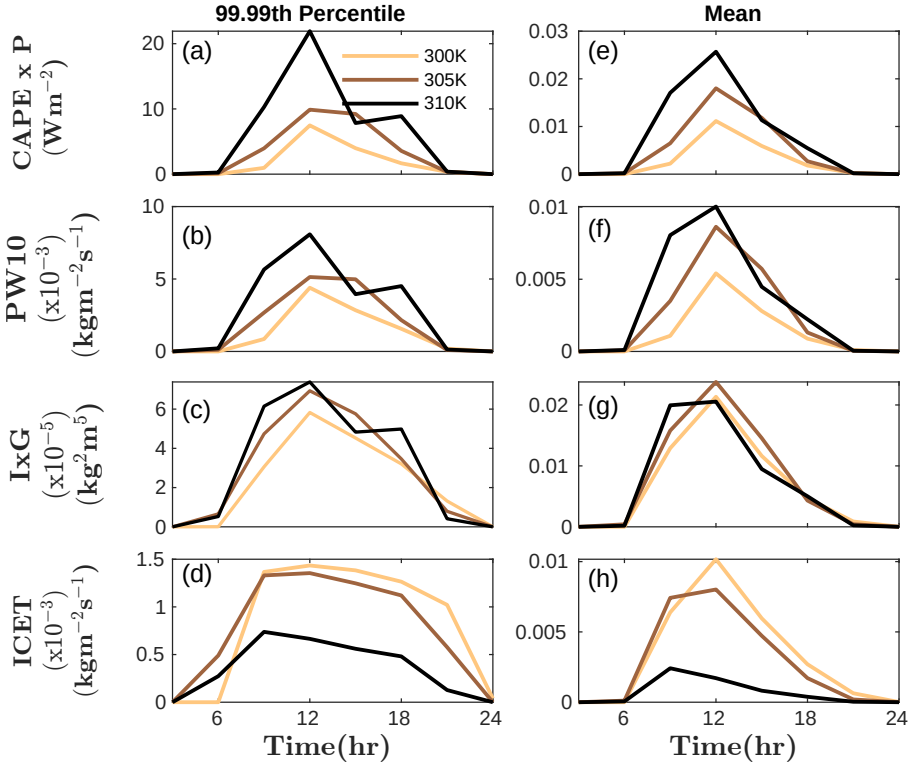

FIGURE 5.10: Same as Figure 5.5 but for warming simulations over dry land surfaces.

5.5 Discussion and summary of chapter

In this chapter, idealized RCE simulations were run to assess the response of thunderstorm intensity to warming over an idealized wet land and dry land surfaces with imposed diurnal cycle of temperature. The wet and dry surfaces were set by controlling the moisture available to the surface. This was achieved by introducing an evaporative conductance parameter (α) into the bulk equation of latent heat in the simulation model. In line with this, an α value of 0.5 and 0.25 were used to represent two conceptual land surfaces with relatively lower surface Bowen ratio (wet case), and relatively higher surface Bowen ratio (dry case) respectively. This approach was motivated by findings in previous chapters of this thesis where we found the high Bowen ratio of the land surface to be unrelated to continental storms (Chapter 3), and some increases in updraught velocity in simulations with imposed diurnal cycle of temperature (Chapter 4). The goal of this chapter was therefore to assess how different aspects of moist convection respond to warming over our highly idealized land surfaces.

We showed that in both the dry and wet cases in our simulations, hourly precipitation rates and extreme precipitation increase with warming. In both the wet and dry case, the daily mean precipitation increases at a fractional rate of 5-7% K^{-1}. However, the daily maximum precipitation rate in the wet case increases at a fractional rate of 8-9% K^{-1} compared to the dry case which only increase at a rate of 3-6% K^{-1}

Again, we found that over the idealized wet land surface, the high percentiles of velocity increases significantly with warming, and with more noticeable difference at the upper troposphere consistent with earlier findings over tropical ocean surfaces (Singh and O'Gorman, 2015). The dry cases on the other hand showed only marginal increase in the high percentiles of vertical velocity in response to warming. An assessment of the undiluted CAPE and the integral of the 99.99th percentile of buoyancy revealed that, at the same temperature, both the dry and wet cases have comparable undiluted CAPE but significantly different buoyancies. We conclude that mechanisms such as entrainment and downdrafts, may be the potential cause for the reduced buoyancies in the dry case. These mechanisms could be explored further in future research to ascertain the apparent difference in precipitation rates and updraught strength between the wet and dry cases.

Some proxies that have been used to predict lightning over tropical ocean surfaces (Romps, 2019b) were also explored in this study. Here we tested how these proxies predict lightning in our idealised simulations. We found that all the proxies explored predicted enhanced lightning with warming except the ICET(IFLUXT) proxy which predicted a decrease in lightning. In the study of Romps (2019b) , the IFLUXT proxy also predicted a decrease in lightning flash rates in response to warming over tropical ocean surfaces.

While this study only sought to compare convection over highly idealized wet and dry land surfaces, the results presented here provide grounds for further research. Further investigation is required to ascertain the reasons for the reduced buoyancy in the dry cases, and why there are only marginal differences in their updraught velocities. It will also be interesting to fully study the coupled effect of the large diurnal cycle of temperature and the land surface Bowen ratio, to determination the points at which they result in enhancement of convection and at which point convection is slowed.

Chapter 6

Thesis discussion and conclusions

This thesis had two main objectives all aimed at understanding moist convection over tropical land surfaces. The first objective was to investigate the physical connections between some land surface features and the intensity of convective storms that form over land. The lead to this objective was founded on some hypotheses that link the intensities of continental storms to characteristic features of the land surface. The second objective was to test the response of the intensity of moist convection over land to changes in mean surface temperature, synonymous to a warming climate. These objectives were explored through idealized model simulations of deep convection with a high resolution cloud resolving model (CRM) run in the radiative-convective equilibrium (RCE) framework. The surface features tested in this thesis are; the high boundary layer depth of the land surface (high surface Bowen ratio), the heterogeneity of surface fluxes, and the large diurnal cycle of surface temperature. We have tested these surface features individually in idealized RCE model simulations where our conceptual land surface is defined only by the specific surface feature being tested, and their linkages to updraught intensity have been assessed.

The thesis was structured around three broad research questions. The first and second research questions formed the basis for the third research question. Research questions one and two sought to identify and establish physical connections between the surface features studied in this thesis and the intensity of storms that form over land in our idealized simulations. The third question broadly sought to find how the intensity of convective storms over our idealized land surface response to warming. In this sense, the results captured in this thesis are mainly to

understand convectively processes over land surfaces but not a true reflection of convection in the real world.

In this chapter, we present how the research questions one and two were addressed with respect to the individual surface features investigated in this thesis, we describe how the third research question was addressed, and the key inferences made. We highlight the significance and limitations of this thesis and give a general conclusion of the processes studied in this thesis.

6.1 Addressing the first and second research questions

The first and second research questions were addressed concurrently in Chapter 3 and Chapter 4 of this thesis. The first research question was; **Which of the land surface features considered in this study is connected to the intensity of storms that form over land?**. This fact-finding question simply sets a first condition for the surface feature being tested. For a surface feature to be considered as having any connection with the intensity of continental storms in our simulations, it should be able to show increases in updraught intensity. We use the 99.99th percentile of vertical velocity as a measure of the intensity of the convective storms. Here, we compare high percentiles of vertical velocities in our idealized land surface cases to that of a control case (simulation over an ocean surface) to make a determination of the success or failure of the land surface feature tested.

The second condition is then set by the second research question which asks; **Are there physical linkages between the surface feature and large-scale environmental parameters like CAPE, known to favour thunderstorm development?**. The second condition that a surface feature being tested must meet is; it should be able to physically result in higher CAPE in comparison to the ocean simulation (control case). These two conditions of having stronger updraught velocity and higher CAPE in comparison to the ocean case is used as a threshold to decide on the relative connection between the surface features we tested and the intensity of convective storms in our simulations.

We present below conclusions drawn from the different surface features tested in an attempt to address research questions one and two.

6.1.1 The homogeneous high boundary layer perspective

Based on the conditions set by research questions one and two in this thesis, the high boundary layer over the homogeneous land surface failed the test in terms of its connection to the intensity of convective storms over land surface.

As detailed in Chapter 3, simulations over the idealized homogeneous land surface with higher Bowen ratio (hereinafter HOML) failed to show stronger updraughts than the ocean case. The ocean simulations on the other hand, had marginally stronger updraughts than the HOML case. We found evidence of larger clouds in the HOML case relative to the ocean case. A key argument that supports the deeper boundary layer of the land surface, as a surface feature that controls the intensity of continental storms is premised on the fact that, clouds that form over such surfaces with deeper boundary layer are relatively bigger, and have higher cloud base height. These big clouds experience minimal entrainment leading to sustained buoyancy and stronger updraught Williams and Stanfill (2002). While our simulation in the HOML case showed bigger clouds than the ocean case, it did not result in stronger updraughts as earlier hypothesized. Our analysis of entrainment also showed comparable entrainment rates between the HOML and the ocean case. We also found the ocean case to have higher CAPE and marginally higher precipitation rates than the HOML case.

One the grounds of the lack of increase in updraught velocity and CAPE in the HOML case in comparison to the ocean case, we concluded that the intensity of convective storms in our idealized simulations is insensitive to the boundary layer depth over a homogeneous land surface. Our results therefore corroborate the earlier study by Hansen and Back (2015) who also found the intensity of continental storms to be independent of the high surface Bowen ratio.

6.1.2 The heterogeneity of surface fluxes perspective

The heterogeneity of surface fluxes over land surface also failed to meet the conditions set by this thesis to assess the connection between surface features and the

intensity of convective storms found in our simulations.

As detailed in Chapter 3 of this thesis, heterogeneity was imposed in a checkerboard pattern of alternating high and low surface Bowen ratios over the surface boundary. This approach imposed a heterogeneous pattern of dry (hot) and wet (cold) patches over the simulation domain. Such horizontal gradient in surface fluxes is hypothesized to result in more buoyant clouds with stronger updraughts. Our set of heterogeneous simulations however did not show such invigoration of convection. The widely known effect of land surface heterogeneity inducing mesoscale circulations over the hot patches was found in our heterogeneous simulations, as clouds mainly formed on the dry patched regions of the simulation domain. However when the higher percentiles of vertical velocity over these heterogeneous surfaces were assessed, it had similar values as the ocean case and were not significantly stronger than the homogeneous land surface with high surface Bowen ratio. Again, the heterogeneous cases failed to show larger CAPE values when compared with the ocean case.

We also explored the argument that larger patch sizes of heterogeneity would lead to stronger storms over continental surfaces. By using idealized simulations with imposed heterogeneity of different patch sizes, we found no invigoration of convection over domains with relatively large heterogeneity patch size. But we did find increases in cloud sizes with increasing heterogeneity patch size.

Since the heterogeneous simulations with different patch sizes did not show increases in the high percentile of vertical velocity in comparison to the ocean case, we concluded that the intensity of thunderstorms over land is insensitive to the heterogeneity of surface fluxes over land within the RCE framework.

6.1.3 The large diurnal cycle of temperature perspective

For the surface features tested in this thesis, only the large diurnal cycle of surface temperature showed some physical connections with the intensity of thunderstorms in our idealized simulations.

We investigated the connection between the intensity of thunderstorms and the large diurnal cycle of surface temperature in Chapter 4 of this thesis using idealized RCE simulations over surfaces with imposed diurnal cycle of surface temperature. We analyzed the results of the simulations by identifying conditions by

which cloud buoyancy could be enhanced. We showed that the high percentiles of boundary layer temperature, moist static energy (MSE) and specific humidity set a favourable condition for enhancement of buoyancy of the convective clouds. We also showed that the high percentiles of undiluted CAPE increased during the day in response to the diurnal evolution of surface temperature as earlier hypothesized. We found significant differences in the high percentiles of vertical velocity between the idealized land surfaces and the ocean surface, the difference was most noticeable at the upper troposphere. A conceptual model of CAPE was used to show the effect of entrainment in setting the mean CAPE which had a different diurnal pattern from the high percentile of CAPE.

Since simulations with imposed diurnal cycle of surface temperature showed stronger updraught and relatively larger CAPE when the high percentiles of CAPE are considered, we concluded that the large diurnal cycle of surface temperature has some physical connections with the intensity of thunderstorms in our idealized simulations. We however make note of the effect of entrainment and downdrafts which affect the bulk of the convective parcels, resulting in reduced buoyancy of the mean cloud parcels during the day.

6.2 Addressing the third research question

The third research question broadly asks; **How does the intensity of convective storms over a conceptual land surface respond to different temperature regimes?** We addressed this question in Chapter 5 of this thesis. Following our investigation of land surface features and their connection to thunderstorm intensity in Chapter 3 and Chapter 4 of this thesis. We run warming simulations over two idealized land surfaces with an imposed diurnal cycle of surface temperature. We explored the response of convection over idealized wet land and dry land surfaces to changes in mean surface temperature. We distinguish between wet land and dry land surfaces by controlling the available surface moisture over the model domain. The wet and dry surfaces only differed by the evaporative conductance parameter used to imposed different surface Bowen ratios for the two cases. We found that the precipitation increased significantly with warming over the idealized wet land surface at much higher fractional rates as compared to the increases in the dry land surface.

We also found that updraught velocity increased significantly with warming over the wet surface, with more noticeable fractional increase at the upper troposphere. The dry surface on the other hand, showed marginal increases in updraught velocity in response to warming. We noticed that the wet cases had similar undiluted CAPE as the dry case, but at the same temperature, the wet cases had stronger buoyancy than the dry case. We concluded that mechanisms like entrainment and downdraft could be the reason for the reduced buoyancy in the dry cases.

6.3 Implication of the study

The results presented in this thesis has potential impact on the overall understanding of the controls of intensity of thunderstorms over land. It also sets the basis for more refined approach to predict future thunderstorms over land surfaces.

6.3.1 The diurnal cycle of temperature of the land surface has physical connection to the intensity of land thunderstorms

It is the position of this study that, from a modeling perspective, the large diurnal cycle of surface temperature over land exerts significant control on the intensity of continental thunderstorms. While it might not be the main or only feature controlling the intensity of continental thunderstorms, it could be a key lead to understanding the differences in the intensity of thunderstorms over land and ocean surfaces.

6.3.2 Significant increase Updraught velocity and precipitation

The idealized warming simulations explored in this thesis point towards enhanced convection over wet land surfaces, and an almost suppressed convection over dry land surface in the future. Although this findings are from a highly idealized perspective, it plays into the wet-get-wetter paradigm. Future thunderstorms over islands and wet land surfaces could be stronger than they currently are. This

could mean more lightning, heavier precipitation and enhanced gusty winds which could be detrimental to human life and property.

6.4 Limitations of the study

This study investigates only three land surface features and their connection to the intensity of storms over land. There are still a number of land surface features that could be key to the intensity of convective storms over land. Our work here is therefore incomplete from the view point of the number of land surface features not considered in this thesis.

The results presented in this thesis are those of a very idealized land surface which only captures the specific land surface feature been tested. Essentially, what we call land or land-like in this thesis is only an ocean surface made to assume land surface characteristic. Since we study each surface feature individually, the lower boundary in our simulations may still retain some ocean-like characteristics that could introduces biases in our results.

Finally, the land surface features and processes tested in this thesis have not been replicated in realistic model simulations to assess their realism in the earth's land surface, hence the results highlighted in this thesis are only to broaden our theoretical understanding of land surface mechanisms and their connections with thunderstorm intensity over land surfaces. It is very possible that other parallel studies that test the same surface features tested here may have comparable or contradicting results from the ones presented here. This is because, idealization studies such as the one adopted in this thesis can be sensitive to the experimental design and setup, the numerical framework used and even the metric for assessing the intensity of the convective storms. .

6.5 Concluding points of the study

The two main points that sums up findings in this thesis are:

1. The large diurnal cycle of temperature exerts some control on the intensity of thunderstorms, and this control could be further amplified in a future warmer

climate. While this surface feature might not be able to entirely explain the land-ocean intensity contrast in thunderstorm intensity, it is key to understanding land surface processes and convection over land. Therefore, there should be further investigation of this land surface feature to better understand its connections with convection over land.

2. The second point which is loosely posited is that, future thunderstorms over island regions and wet land surfaces would be much enhanced. Hence, the dangers thunderstorms pose to life and property could be severer.

Chapter 7

Future outlook

The focus of this thesis was to identify land surface features that are physically connected to the intensity of convective storms that form over land, and to investigate how the intensity of storms that form over land changes under different temperature regimes. The fact finding approach adopted in this thesis presented us with the opportunity to focus on only surface features found to exert some control on the intensity of thunderstorms in our simulations. In this sense, the land surface features considered in this study were investigated individually in simplified idealized simulations. For the three surface features studied (High boundary layer depth, heterogeneity of surface fluxes, and diurnal cycle of temperature) only the diurnal cycle of temperature was able to show significant increases in updraught velocity and as well show increase in CAPE. The result in this thesis in only a motivation to further explore the connections between the land surface and the intensity intensity convective storms to address some of the shortcomings of this thesis, and to enrich our understanding of land surface properties and their connection to moist convection.

Findings in this thesis are far from being conclusive on the surface features that could potentially control the intensity of storms over land. It is important to study all the different land surface features mentioned in literature as potential candidates for the invigoration of convective storms over land. It is also important to explore the relationship of some of these surface features and convective intensity in current observation data. This will form the basis to link some of these idealized studies back to real world scenarios and present a better perspective to the results found in idealised simulation studies as the one employed in this thesis.

We therefore present a future outlook of this research area broadly in three sections.

7.1 Storm intensity and other land surface features

The hypotheses linking the features of the land surface to thunderstorm intensity inadvertently makes every single distinguishing feature of the land surface a potential candidate for controlling of the intensity of continental storms. So far only a handful of the characteristic features of the land surface have been studied in literature and in this thesis. Perhaps some of these features not yet explored are key to the enhancement of convection over land. Features such as orography, surface roughness have seen less attention in this current debate. There are still unresolved questions on some of these surface features explored in different studies. Contrasting results have been found in studies that examine the same surface feature using perhaps different models and experimental setups. There might be a number of reasons for these contrasting results. Indeed basic details such as the metric of assessing the intensity of the convective storm can influence the results of these studies. A more consistent approach would be to study at least all the main surface features with the same model and numerical framework, and with the same intensity metric. This is a slow but necessary process to understanding the relationship between features of the land surface and storms that form over land. Aerosol loading for example was not studied in this thesis, but there are studies (e.g., Abbott and Cronin, 2021) that report increases in the intensity of thunderstorms at higher concentration of aerosols. There are other studies that contradict this conclusion.

How a land surface feature is defined in model simulations can also be a major source of bias. For example in this thesis, the heterogeneity of the land surface was imposed as a surface with checker-board pattern of alternating high and low surface Bowen ratio. Our results from this setup did not show increases in updraught intensity over the domain. However, evidence of convection being predominant on the warm and dry patch was found and there were marginal differences in the updraught velocity between the heterogeneous cases and the homogeneous case. This raises the question of how different our result would be if we increased the available moisture at the dry patch. Going forward, some of these options can be

explored further to better understand the relative role these surface features play in enhancing continental storms. It will be interesting to further investigate the diurnal cycle of temperature over land in simulations where the solar constant is made to vary instead of the fixed solar constant in this current study. Additionally, some of these theories can be assessed using different numerical frameworks. We can for example use the weak temperature gradient (WTG) framework to restudy the effect of the diurnal cycle of temperature over land. This would allow for the effect of remote regions on the tropospheric temperature profile, an effect that is neglected in this thesis.

7.2 Realistic model simulations

A key approach to understanding the results in this thesis is to compare results of the idealized simulations explored in this thesis to a more realistic simulation study of convection in the real world. The design and objective of this realistic simulations would be to find a replication of the ideas tested in the idealized simulations in the real world. In the context of the findings of this thesis, a realistic simulation can be run to assess the connection between updraught intensity, CAPE and the large diurnal cycle of surface temperature. The availability of surface moisture which have been found to be key in defining both CAPE and precipitation amounts can also be explored in this realistic simulations. In terms of moisture availability, two simulations can be run over two different climatic regions of the tropics; for example, an island region where moisture is readily available and a desert region where available water at the surface is relatively low but temperatures are significantly hight. Such case studies would give an all round understanding of these land surface processes and some of the theories explored in idealized simulations.

The ultimate goal in the long term would be to run realistic global warming simulations over land surfaces guided by our understanding of continental moist convection from theories developed in idealized model simulations and confirmed in realistic case studies of convection. This approach would answer most questions of moist convection over land and help reduce the apparent difficulty in predicting future storms over land and ultimately provide evidence based explanation for the largely observed land-ocean contrast in updraught intensity.

7.3 The observation perspective

A natural next step to this process testing approach employed in this study is to find corroborating evidence of the hypothesis and theories being studied in the real world. Analysis of observation and reanalysis data can be used to characterise various aspects of convection of the past and current climate to give perspective of changes in the past decade for example. The diurnal composite of precipitation, CAPE and updraught intensity over land can be analysed from and their results compared to results of the variation of these variables as found in this thesis. This can help identify areas where the model simulation differ or is similar to observations and to make adjustments to the model setup if necessary.

Bibliography

Abbott, T. H. and Cronin, T. W. (2021). Aerosol invigoration of atmospheric convection through increases in surface humidty. *Science*, 85 (January), 83–85.

Abbott, T. H., Cronin, T. W. and Beucler, T. (2020). Convective Dynamics and the Response of Precipitation Extremes to Warming in Radiative–Convective Equilibrium. *Journal of the Atmospheric Sciences*, 77 (5), 1637–1660. doi:10.1175/JAS-D-19-0197.1.

Agard, V. and Emanuel, K. (2017). Clausius-Clapeyron scaling of peak CAPE in continental convective storm environments. *Journal of the Atmospheric Sciences*, 74 (9), 3043–3054. doi:10.1175/JAS-D-16-0352.1.
URL http://journals.ametsoc.org/doi/10.1175/JAS-D-16-0352.1

Anber, U. M., Wang, S., Gentine, P. and Jensen, M. P. (2019). Probing the response of tropical deep convection to aerosol perturbations using idealized cloud-resolving simulations with parameterized large-scale dynamics. *Journal of the Atmospheric Sciences*,, 2885–2897.doi:10.1175/jas-d-18-0351.1.

Avissar, R. and Schmidt, T. (1998). An evaluation of the scale at which ground-surface heat flux patchiness affects the convective boundary layer using large-eddy simulations. *Journal of the Atmospheric Sciences*, 55 (16), 2666–2689. doi:10.1175/1520-0469(1998)055¡2666:AEOTSA¿2.0.CO;2.

Bao, J., Stevens, B., Kluft, L. and Jimenez-de-la Cuesta, D. (2021). Changes in the tropical lapse rate due to entrainment and their impact on climate sensitivity. *Geophysical Research Letters*, 48 (18).

Betts, A. (2003). DIURNAL CYCLE. In: *Encyclopedia of Atmospheric Sciences*, pp. 640–644.
URL https://linkinghub.elsevier.com/retrieve/pii/B0122270908001354

Betts, A. K. (2004). The diurnal cycle over land. In: *Forests at the land-atmosphere interface*. No. January 2003, UK, pp. 73–93.
URL http://www.cabidigitallibrary.org/doi/10.1079/9780851996776.0073

Betts, A. K. and Jakob, C. (2002). Evaluation of the diurnal cycle of precipitation, surface thermodynamics, and surface fluxes in the ECMWF model using LBA data. *Journal of Geophysical Research: Atmospheres*, 107 (20), LBA 12–1–LBA 12–8. doi:10.1029/2001JD000427.

Bony, S., Stevens, B., Coppin, D., Becker, T., Reed, K. A., Voigt, A. and Medeiros, B. (2016). Thermodynamic control of anvil cloud amount. *Proceedings of the National Academy of Sciences of the United States of America*, 113 (32), 8927–8932. doi:10.1073/pnas.1601472113.

Bony, S., Stevens, B., Frierson, D. M., Jakob, C., Kageyama, M., Pincus, R., Shepherd, T. G., Sherwood, S. C., Siebesma, A. P., Sobel, A. H., Watanabe, M. and Webb, M. J. (2015). Clouds, circulation and climate sensitivity. *Nature Geoscience*, 8 (4), 261–268. doi:10.1038/ngeo2398.
URL http://dx.doi.org/10.1038/ngeo2398

Bretherton, C. S., Blossey, P. N. and Khairoutdinov, M. (2005). An energy-balance analysis of deep convective self-aggregation above uniform SST. *Journal of the Atmospheric Sciences*, 62 (12), 4273–4292. doi:10.1175/JAS3614.1.

Brooks, H. E. (2013). *Severe thunderstorms and climate change*.
URL http://dx.doi.org/10.1016/j.atmosres.2012.04.002

Charney, J. G. (1963). A note on large-scale motions in the tropics. *J. Atmos. Sci.*,, 6–8.doi:10.1175/ 1520-0469(1963)020,0607:ANOLSM.2.0.CO;2.
URL https://doi.org/10.1175/1520-0469(1963)020,0607:ANOLSM.2.0.CO;2.

Charney, J. G. and Eliassen, A. (1964). On the Growth of the Hurricane Depression. *Journal of the Atmospheric Sciences*, 21 (1), 68–75. doi:10.1175/1520-0469(1964)021¡0068:OTGOTH¿2.0.CO;2.
URL http://journals.ametsoc.org/doi/10.1175/1520-0469(1964)021%3C0068:OTGOTH%3E2.0.CO;2

Cheng, W. Y. Y. and Cotton, W. R. (2004). Sensitivity of a Cloud-Resolving Simulation of the Genesis of a Mesoscale Convective System to Horizontal Heterogeneities in Soil Moisture Initialization. *Journal of Hydrometeorology*, 5 (5), 934–958. doi:10.1175/1525-7541(2004)005¡0934:soacso¿2.0.co;2.

Christian, H. J., Blakeslee, R. J., Boccippio, D. J., Boeck, W. L., Buechler, D. E., Driscoll, K. T., Goodman, S. J., Hall, J. M., Koshak, W. J., Mach, D. M. and Stewart, M. F. (2003). Global frequency and distribution of lightning as observed from space by the Optical Transient Detector. *Journal of Geophysical Research: Atmospheres*, 108 (1). doi:10.1029/2002jd002347.

Clough, S. A., Shephard, M. W., Mlawer, E. J., Delamere, J. S., Iacono, M. J., Cady-Pereira, K., Boukabara, S. and Brown, P. D. (2005). Atmospheric radiative transfer modeling: A summary of the AER codes. *Journal of Quantitative Spectroscopy and Radiative Transfer*, 91 (2), 233–244. doi:10.1016/j.jqsrt.2004.05.058.

Collier, J. C. (2004). Diurnal cycle of tropical precipitation in a general circulation model. *Journal of Geophysical Research*, 109 (D17), D17105. doi:10.1029/2004JD004818.
URL http://doi.wiley.com/10.1029/2004JD004818

Collins, W. D., Rasch, P. J., Boville, B. A., Hack, J. J., McCaa, J. R., Williamson, D. L., Briegleb, B. P., Bitz, C. M., Lin, S.-J. and Zhang, M. (2006). The Formulation and Atmospheric Simulation of the Community Atmosphere Model Version 3 (CAM3). *Journal of Climate*, 19 (11), 2144–2161. doi:10.1175/JCLI3760.1.
URL https://journals.ametsoc.org/view/journals/clim/19/11/jcli3760.1.xml

Cronin, T. W. and Emanuel, K. A. (2013). The climate time scale in the approach to radiative-convective equilibrium. *Journal of Advances in Modeling Earth Systems*, 5 (4), 843–849. doi:10.1002/jame.20049.

Cronin, T. W., Emanuel, K. A. and Molnar, P. (2015). Island precipitation enhancement and the diurnal cycle in radiative-convective equilibrium. *Quarterly Journal of the Royal Meteorological Society*, 141 (689), 1017–1034. doi:10.1002/qj.2443.

Das, S. (2017). Severe Thunderstorm Observation and Modeling – A Review Types Gust Wind Squally Wind Light Nor ' wester Moderate Nor ' wester Severe Nor ' wester Tornado, 43 (2).

Del Genio, A. D., Yao, M. and Jonas, J. (2007). *Will moist convection be stronger in a warmer climate? Geophysical Research , .*

Diffenbaugh, N. S., Scherer, M. and Trapp, R. J. (2013). Robust increases in severe thunderstorm environments in response to greenhouse forcing. *Proceedings of the National Academy of Sciences of the United States of America*, 110 (41), 16361–16366. doi:10.1073/pnas.1307758110.

Dowdy, A. J. and Mills, G. A. (2012). Characteristics of lightning-attributed wildland fires in south-east Australia. *International Journal of Wildland Fire*, 21 (5), 521–524. doi:10.1071/WF10145.

Duda, J. D. (2004). A Review on the Uses of Cloud- (System-) Resolving Models,.

Fan, J., Rosenfeld, D., Zhang, Y., Giangrande, S. E., Li, Z., Machado, L. A. T., Martin, S. T., Yang, Y., Wang, J., Artaxo, P., Barbosa, H. M. J., Braga, R. C., Comstock, J. M., Feng, Z., Gao, W., Gomes, H. B., Mei, F., Pöhlker, C., Pöhlker, M. L., Pöschl, U. and de Souza, R. A. F. (2018). Substantial convection and precipitation enhancements by ultrafine aerosol particles. *Science*, 359 (6374), 411–418.

Finney, D. L., Doherty, R. M., Wild, O. and Abraham, N. L. (2016). The impact of lightning on tropospheric ozone chemistry using a new global lightning parametrisation. *Atmospheric Chemistry and Physics*, 16 (12), 7507–7522. doi:10.5194/acp-16-7507-2016.

Giorgi, F., Avissar, R. and Brunswick, N. (1997). Representation in Earth Experience System From of H Eterogeneity Modeling ' Effects Modeling. *American Geophysical Union*, 35 (97), 413–438.

Goody, R. M. (1949). The thermal equilibrium at the tropopause and the temperature of the lower stratosphere. *Proceedings of the Royal Society of London. Series A. Mathematical and Physical Sciences*, 197 (1051), 487–505. doi:10.1098/rspa.1949.0076.
URL https://royalsocietypublishing.org/doi/10.1098/rspa.1949.0076

Gora, E. M., Burchfield, J. C., Muller-Landau, H. C., Bitzer, P. M. and Yanoviak, S. P. (2020). Pantropical geography of lightning-caused disturbance and its implications for tropical forests. *Global Change Biology*, 26 (9), 5017–5026. doi:10.1111/gcb.15227.

Grabowski, W. W. and Smolarkiewicz, P. K. (1999). CRCP: A Cloud Resolving Convection Parameterization for modeling the tropical convecting atmosphere. *Physica D: Nonlinear Phenomena*, 133 (1-4), 171–178. doi:10.1016/S0167-2789(99)00104-9.

Guichard, F. and Couvreux, F. (2017). A short review of numerical cloud-resolving models. *Tellus, Series A: Dynamic Meteorology and Oceanography*, 69 (1), 1–36. doi:10.1080/16000870.2017.1373578.
URL http://doi.org/10.1080/16000870.2017.1373578

Guichard, F., Petch, J. C., Redelsperger, J. L., Bechtold, P., Chaboureau, J. P., Cheinet, S., Grabowski, W., Grenier, H., Jones, C. G., Köhler, M., Piriou, J. M., Tailleux, R. and Tomasini, M. (2004). Modelling the diurnal cycle of deep precipitating convection over land with cloud-resolving models and single-column models. *Quarterly Journal of the Royal Meteorological Society*, 130 C (604), 3139–3172. doi:10.1256/qj.03.145.

Hannah, W. M. (2017). Entrainment versus dilution in tropical deep convection. *Journal of the Atmospheric Sciences*, 74 (11), 3725–3747. doi:10.1175/JAS-D-16-0169.1.

Hansen, Z. R. and Back, L. E. (2015). Higher surface Bowen ratios ineffective at increasing updraft intensity. *Geophysical Research Letters*, 42 (23), 10503–10511. doi:10.1002/2015GL066878.

Hansen, Z. R., Back, L. E. and Zhou, P. (2020). Boundary Layer Quasi-Equilibrium Limits Convective Intensity Enhancement from the Diurnal Cycle in Surface Heating. *Journal of the Atmospheric Sciences*, 77 (1), 217–237. doi:10.1175/JAS-D-18-0346.1.
URL https://journals.ametsoc.org/view/journals/atsc/77/1/jas-d-18-0346.1.xml

Harvey, N. J., Daleu, C. L., Stratton, R. A., Plant, R. S., Woolnough, S. J. and Stirling, A. J. (2022). The impact of surface heterogeneity on the diurnal cycle

of deep convection. *Quarterly Journal of the Royal Meteorological Society*,, 1–25.doi:10.1002/qj.4371.
URL https://onlinelibrary.wiley.com/doi/10.1002/qj.4371

Held, I. M., Hemler, R. S. and Ramaswamy, V. (1993). Radiative-Convective Equilibrium with Explicit Two-Dimensional Moist Convection. *Journal of Atmospheric Sciences*, 50 (23), 3909–3927. doi:10.1175/1520-0469(1993)050¡3909:RCEWET¿2.0.CO;2.
URL https://journals.ametsoc.org/view/journals/atsc/50/23/1520-0469_1993_050_3909_rcewet_2_0_co_2.xml

Hong, G., Heygster, G., Notholt, J. and Buehler, S. A. (2008). Interannual to diurnal variations in tropical and subtropical deep convective clouds and convective overshooting from seven years of AMSU-B measurements. *Journal of Climate*, 21 (17), 4168–4189. doi:10.1175/2008JCLI1911.1.

Jakob, C., Singh, M. S. and Jungandreas, L. (2019). Radiative Convective Equilibrium and Organized Convection: An Observational Perspective. *Journal of Geophysical Research: Atmospheres*, 124 (10), 5418–5430. doi:10.1029/2018JD030092.

Jeevanjee, N. and Romps, D. M. (2018). Mean precipitation change from a deepening troposphere. *Proceedings of the National Academy of Sciences of the United States of America*, 115 (45), 11465–11470. doi:10.1073/pnas.1720683115.

Jungmin M. Lee, M. K. (2016). Journal of Advances in Modeling Earth Systems. *Journal of Advances in Modeling Earth Systems*, 8, 1180–1209. doi:10.1002/2014MS000419.Received.

Kang, S. L. (2016). Regional bowen ratio controls on afternoon moist convection: A large eddy simulation study. *Journal of Geophysical Research*, 121 (23), 14,056–14,083. doi:10.1002/2016JD025567.

Kang, S.-L. and Bryan, G. H. (2011). A Large-Eddy Simulation Study of Moist Convection Initiation over Heterogeneous Surface Fluxes. *Monthly Weather Review*, 139 (9), 2901–2917. doi:10.1175/mwr-d-10-05037.1.

Kang, S. L. and Ryu, J. H. (2016). Response of moist convection to multi-scale surface flux heterogeneity. *Quarterly Journal of the Royal Meteorological Society*, 142 (698), 2180–2193. doi:10.1002/qj.2811.

Keenan, T. D., Ferrier, B. and Simpson, J. (1994). Development and structure of a maritime continent thunderstorm. *Meteorology and Atmospheric Physics*, 53 (3-4), 185–222. doi:10.1007/BF01029612.

Khairoutdinov, M. and Randall, D. (2006). High-Resolution Simulation of Shallow-to-Deep Convection Transition over Land. *Journal of the Atmospheric Sciences*, 63 (12), 3421–3436. doi:10.1175/JAS3810.1.
URL http://journals.ametsoc.org/doi/abs/10.1175/JAS3810.1

Khairoutdinov, M. F., Blossey, P. N. and Bretherton, C. S. (2022). Global System for Atmospheric Modeling: Model Description and Preliminary Results. *Journal of Advances in Modeling Earth Systems*, 14 (6), 1–23. doi:10.1029/2021MS002968.

Khairoutdinov, M. F. and Randall, D. A. (2001). A cloud resolving model as a cloud parameterization in the NCAR community climate system model: Preliminary results. *Geophysical Research Letters*, 28 (18), 3617–3620. doi:10.1029/2001GL013552.

Khairoutdinov, M. F. and Randall, D. A. (2003). Cloud resolving modeling of the ARM summer 1997 IOP: Model formulation, results, uncertainties, and sensitivities. *Journal of the Atmospheric Sciences*, 60 (4), 607–625. doi:10.1175/1520-0469(2003)060¡0607:CRMOTA¿2.0.CO;2.

Knist, S., Goergen, K. and Simmer, C. (2019). Effects of land surface inhomogeneity on convection-permitting WRF simulations over central Europe. *Meteorology and Atmospheric Physics*, (0123456789). doi:10.1007/s00703-019-00671-y.
URL https://doi.org/10.1007/s00703-019-00671-y

Koike, M., Kondo, Y., Kita, K., Takegawa, N., Nishi, N., Kashihara, T., Kawakami, S., Kudoh, S., Blake, D., Shirai, T., Liley, B., Ko, M. K., Miyazaki, Y., Kawasaki, Z. and Ogawa, T. (2007). Measurements of reactive nitrogen produced by tropical thunderstorms during BIBLE-C. *Journal of Geophysical Research Atmospheres*, 112 (18). doi:10.1029/2006JD008193.

Koster, R. D. and Suarez, M. J. (2001). Soil Moisture Memory in Climate Models. *Journal of Hydrometeorology*, 2 (6), 558–570. doi:10.1175/1525-7541(2001)002¡0558:SMMICM¿2.0.CO;2.
URL http://journals.ametsoc.org/doi/abs/10.1175/1525-7541%282001%29002%3C0558%3ASMMICM%3E2.0.CO%3B2

Kuang, Z. and Bretherton, C. S. (2006). A mass-flux scheme view of a high-resolution simulation of a transition from shallow to deep cumulus convection. *Journal of the Atmospheric Sciences*, 63 (7), 1895–1909. doi:10.1175/JAS3723.1. URL http://journals.ametsoc.org/doi/abs/10.1175/JAS3723.1

Lee, J. M., Zhang, Y. and Klein, S. A. (2018). The Effect of Land Surface Heterogeneity and Background Wind on Shallow Cumulus Clouds and the Transition to Deeper Convection. *Journal of the Atmospheric Sciences*, 76 (2), 401–419. doi:10.1175/jas-d-18-0196.1.

Li, Z., Rosenfeld, D. and Fan, J. (2017). *Aerosols and Their Impact on Radiation, Clouds, Precipitation, and Severe Weather Events*. No. November. : .

Lin, J.-L., Kiladis, G. N., Mapes, B. E., Weickmann, K. M., Sperber, K. R., Lin, W., Wheeler, M. C., Schubert, S. D., Del Genio, A., Donner, L. J., Emori, S., Gueremy, J.-F., Hourdin, F., Rasch, P. J., Roeckner, E. and Scinocca, J. F. (2006). Tropical Intraseasonal Variability in 14 IPCC AR4 Climate Models. Part I: Convective Signals. *Journal of Climate*, 19 (12), 2665–2690. doi:10.1175/jcli3735.1.

Liu, C., Williams, E. R., Zipser, E. J. and Burns, G. (2010). Diurnal Variations of Global Thunderstorms and Electrified Shower Clouds and Their Contribution to the Global Electrical Circuit. *Journal of the Atmospheric Sciences*, 67 (2), 309–323. doi:10.1175/2009JAS3248.1.
URL https://journals.ametsoc.org/doi/10.1175/2009JAS3248.1

Liu, C. and Zipser, E. J. (2005). Global distribution of convection penetrating the tropical tropopause. *Journal of Geophysical Research Atmospheres*, 110 (23), 1–12. doi:10.1029/2005JD006063.

Liu, C. and Zipser, E. J. (2015). The global distribution of largest, deepest, and most intense precipitation systems. *Geophysical Research Letters*, 42 (9), 3591–3595. doi:10.1002/2015GL063776.

Liu, S., Shao, Y., Kunoth, A. and Simmer, C. (2017). Impact of surface-heterogeneity on atmosphere and land-surface interactions. *Environmental Modelling and Software*, 88, 35–47. doi:10.1016/j.envsoft.2016.11.006.
URL http://dx.doi.org/10.1016/j.envsoft.2016.11.006

Lucas, C., Zipser, E. J. and Lemone, M. A. (1994). Vertical Velocity in Oceanic Convection off Tropical Australia. *Journal of the Atmospheric Sciences*, 51 (21), 3183–3193. doi:10.1175/1520-0469(1994)051¡3183:vvioco¿2.0.co;2.

Manabe, S. and Strickler, R. F. (1964). Thermal Equilibrium of the Atmosphere with a Convective Adjustment. *Journal of the Atmospheric Sciences*, 21 (4), 361–385. doi:10.1175/1520-0469(1964)021¡0361:TEOTAW¿2.0.CO;2.
URL http://journals.ametsoc.org/doi/10.1175/1520-0469(1964)021%3C0361:TEOTAW%3E2.0.CO;2

Matsui, T., Chern, J.-D., Tao, W.-K., Lang, S., Satoh, M., Hashino, T. and Kubota, T. (2016). On the Land–Ocean Contrast of Tropical Convection and Microphysics Statistics Derived from TRMM Satellite Signals and Global Storm-Resolving Models. *Journal of Hydrometeorology*, 17 (5), 1425–1445. doi:10.1175/jhm-d-15-0111.1.

Meredith, E. P., Ulbrich, U. and Rust, H. W. (2019). The Diurnal Nature of Future Extreme Precipitation Intensification. *Geophysical Research Letters*, 46 (13), 7680–7689. doi:10.1029/2019GL082385.

Morrison, H., Curry, J. A. and Khvorostyanov, V. I. (2005). A new double-moment microphysics parameterization for application in cloud and climate models. Part I: Description. *Journal of the Atmospheric Sciences*, 62 (6), 1665–1677. doi:10.1175/JAS3446.1.

Muller, C. (2013). Impact of Convective Organization on the Response of Tropical Precipitation Extremes to Warming. *Journal of Climate*, 26 (14), 5028–5043. doi:10.1175/JCLI-D-12-00655.1.
URL http://journals.ametsoc.org/doi/10.1175/JCLI-D-12-00655.1

Muller, C. and Takayabu, Y. (2020). Response of precipitation extremes to warming: what have we learned from theory and idealized cloud-resolving simulations, and what remains to be learned? *Environmental Research Letters*, 15 (3). doi:10.1088/1748-9326/ab7130.

Muller, C. J., O'Gorman, P. A. and Back, L. E. (2011). Intensification of precipitation extremes with warming in a cloud-resolving model. *Journal of Climate*, 24 (11), 2784–2800. doi:10.1175/2011JCLI3876.1.

Nieuwolt, S. (1982). Tropical rainfall variability — The agroclimatic impact. *Agriculture and Environment*, 7 (2), 135–148. doi:10.1016/0304-1131(82)90003-0.
URL https://linkinghub.elsevier.com/retrieve/pii/0304113182900030

Page, W. A. (1982). Nasa experiment on tropospheric-stratospheric water vapor transport in the intertropical convergence zone, Guest Editorial. *Geophysical Research Letters*, 9 (6), 599–599. doi:10.1029/GL009i006p00599.
URL http://doi.wiley.com/10.1029/GL009i006p00599

Randall, D., Hu, Q., Xu, K.-M. and Krueger, S. (1994). Radiative-convective disequilibrium. *Atmospheric Research*, 31 (4), 315–327. doi:10.1016/0169-8095(94)90006-X.
URL https://linkinghub.elsevier.com/retrieve/pii/016980959490006X

Randall, D., Khairoutdinov, M., Arakawa, A. and Grabowski, W. (2003). Breaking the Cloud Parameterization Deadlock. *Bulletin of the American Meteorological Society*, 84 (11), 1547–1564. doi:10.1175/BAMS-84-11-1547.
URL https://journals.ametsoc.org/doi/10.1175/BAMS-84-11-1547

Reed, K. A., Silvers, L. G., Wing, A. A., Hu, I. K. and Medeiros, B. (2021). Using Radiative Convective Equilibrium to Explore Clouds and Climate in the Community Atmosphere Model. *Journal of Advances in Modeling Earth Systems*, 13 (12). doi:10.1029/2021MS002539.

Rieck, M., Hohenegger, C. and van Heerwaarden, C. C. (2014). The Influence of Land Surface Heterogeneities on Cloud Size Development. *Monthly Weather Review*, 142 (10), 3830–3846. doi:10.1175/mwr-d-13-00354.1.

Riemann-Campe, K., Fraedrich, K. and Lunkeit, F. (2009). Global climatology of Convective Available Potential Energy (CAPE) and Convective Inhibition (CIN) in ERA-40 reanalysis. *Atmospheric Research*, 93 (1-3), 534–545. doi:10.1016/j.atmosres.2008.09.037.
URL https://linkinghub.elsevier.com/retrieve/pii/S0169809508002706http://dx.doi.org/10.1016/j.atmosres.2008.09.037

Rochetin, N., Couvreux, F. and Guichard, F. (2017). Morphology of breeze circulations induced by surface flux heterogeneities and their impact on convection initiation. *Quarterly Journal of the Royal Meteorological Society*, 143 (702). doi:10.1002/qj.2935.

Rochetin, N., Lintner, B. R., Findell, K. L., Sobel, A. H. and Gentine, P. (2014). Radiative-convective equilibrium over a land surface. *Journal of Climate*, 27 (23), 8611–8629. doi:10.1175/JCLI-D-13-00654.1.

Romps, D. M. (2011). Response of Tropical Precipitation to Global Warming. *Journal of the Atmospheric Sciences*, 68 (1), 123–138. doi:10.1175/2010JAS3542.1.
URL https://journals.ametsoc.org/doi/10.1175/2010JAS3542.1

Romps, D. M. (2019). Evaluating the Future of Lightning in Cloud-Resolving Models. *Geophysical Research Letters*, 46 (24), 14863–14871. doi:10.1029/2019GL085748.

Romps, D. M. (2019). Evaluating the Future of Lightning in Cloud-Resolving Models. *Geophysical Research Letters*, 46 (24), 14863–14871. doi:10.1029/2019GL085748.

Romps, D. M., Charn, A. B., Holzworth, R. H., Lawrence, W. E., Molinari, J. and Vollaro, D. (2018). CAPE Times P Explains Lightning Over Land But Not the Land-Ocean Contrast. *Geophysical Research Letters*, 45 (22), 12,623–12,630. doi:10.1029/2018GL080267.

Romps, D. M., Seeley, J. T., Vollaro, D. and Molinari, J. (2014). Projected increase in lightning strikes in the united states due to global warming. *Science*, 346 (6211), 851–854. doi:10.1126/science.1259100.

Rosenfeld, D., Lohmann, G., Raga, G. B., O'Dowd, C. D., Kulmala, M., Fuzzi, S., Riessel, A. and Andreae, M. O. (2008). Flood or drought: How do aerosols affect precipitation? *Science*, 321 (5894), 1309–1313.

Sato, Y., Miyamoto, Y. and Tomita, H. (2019). Large dependency of charge distribution in a tropical cyclone inner core upon aerosol number concentration. *Progress in Earth and Planetary Science*, 6 (1). doi:10.1186/s40645-019-0309-7.

Satoh, M., Stevens, B., Judt, F., Khairoutdinov, M., Lin, S. J., Putman, W. M. and Düben, P. (2019). *Global Cloud-Resolving Models*.

Seeley, J. T. and Romps, D. M. (2015). Why does tropical convective available potential energy (CAPE) increase with warming? *Geophysical Research Letters*, 42 (23), 10429–10437. doi:10.1002/2015GL066199.
URL https://onlinelibrary.wiley.com/doi/abs/10.1002/2015GL066199

Seeley, J. T. and Romps, D. M. (2016). Tropical cloud buoyancy is the same in a world with or without ice. *Geophysical Research Letters*, 43 (7), 3572–3579. doi:10.1002/2016GL068583.

Sharifnezhadazizi, Z., Norouzi, H., Prakash, S., Beale, C. and Vardi, R. (2019). A global analysis of land surface temperature diurnal cycle using modis observations. *Journal of Applied Meteorology and Climatology*, 58 (6), 1279–1291. doi:10.1175/JAMC-D-18-0256.1.

Silvers, L. G., Stevens, B., Mauritsen, T. and Giorgetta, M. (2016). Radiative convective equilibrium as a framework for studying the interaction between convection and its large-scale environment. *Journal of Advances in Modeling Earth Systems*, 8 (3), 1330–1344. doi:10.1002/2016MS000629.
URL http://doi.wiley.com/10.1002/2016MS000629

Singh, M. S., Kuang, Z., Maloney, E. D., Hannah, W. M. and Wolding, B. O. (2017). Increasing potential for intense tropical and subtropical thunderstorms under global warming. *Proceedings of the National Academy of Sciences*,, 201707603.doi:10.1073/pnas.1707603114.
URL http://www.pnas.org/lookup/doi/10.1073/pnas.1707603114

Singh, M. S. and O'Gorman, P. A. (2013). Influence of entrainment on the thermal stratification in simulations of radiative-convective equilibrium. *Geophysical Research Letters*, 40 (16), 4398–4403. doi:10.1002/grl.50796.

Singh, M. S. and O'Gorman, P. A. (2015). Increases in moist-convective updraught velocities with warming in radiative-convective equilibrium. *Quarterly Journal of the Royal Meteorological Society*, 141 (692), 2828–2838. doi:10.1002/qj.2567.

Sobel, A. H. and Camargo, S. J. (2011). Projected future seasonal changes in tropical summer climate. *Journal of Climate*, 24 (2), 473–487. doi:10.1175/2010JCLI3748.1.

Sobel, A. H., Nilsson, J. and Polvani, L. M. (2001). The weak temperature gradient approximation and balanced tropical moisture waves. *Journal of Atmospheric Sciences*, 58 (23), 3650–3665.

Taylor, C. M., Harding, R. J., Thorpe, A. J. and Bessemoulin, P. (1997). A mesoscale simulation of land surface heterogeneity from HAPEX-Sahel. *Journal of Hydrology*, 188-189 (1-4), 1040–1066. doi:10.1016/S0022-1694(96)03182-4.

Tompkins, B. A. M. and Craig, G. C. (1998). Radiative-convective equilibrium in a three-dimensional cloud-ensemble model,, 2073–2097.

Toracinta, E. R. and Zipser, E. J. (2001). Lightning and SSM/I-ice-scattering mesoscale convective systems in the global tropics. *Journal of Applied Meteorology*, 40 (6), 983–1002. doi:10.1175/1520-0450(2001)040¡0983:LASIIS¿2.0.CO;2.

Trapp, R. J., Diffenbaugh, N. S., Brooks, H. E., Baldwin, M. E., Robinson, E. D. and Pal, J. S. (2007). Changes in severe thunderstorm environment frequency during the 21st century caused by anthropogenically enhanced global radiative forcing. *Proceedings of the National Academy of Sciences*, 104 (50), 19719–19723. doi:10.1073/pnas.0705494104.

Trapp, R. J. and Hoogewind, K. A. (2016). The realization of extreme tornadic storm events under future anthropogenic climate change. *Journal of Climate*, 29 (14), 5251–5265. doi:10.1175/JCLI-D-15-0623.1.

Van de Walle, J., Thiery, W., Brogli, R., Martius, O., Zscheischler, J. and van Lipzig, N. P. (2021). Future intensification of precipitation and wind gust associated thunderstorms over Lake Victoria. *Weather and Climate Extremes*, 34 (April), 0–13. doi:10.1016/j.wace.2021.100391.

Wei, Y. and Pu, Z. (2022). Diurnal cycle of precipitation and near-surface atmospheric conditions over the maritime continent: land–sea contrast and impacts of ambient winds in cloud-permitting simulations. *Climate Dynamics*, 58 (9-10), 2421–2449. doi:10.1007/s00382-021-06012-3.
URL https://doi.org/10.1007/s00382-021-06012-3

Williams, E., Chan, T. and Boccippio, D. (2004). Islands as miniature continents: Another look at the Land-ocean lightning contrast. *Journal of Geophysical Research D: Atmospheres*, 109 (16), 2–6. doi:10.1029/2003JD003833.

Williams, E., Mushtak, V., Rosenfeld, D., Goodman, S. and Boccippio, D. (2005). *Thermodynamic conditions favorable to superlative thunderstorm updraft, mixed phase microphysics and lightning flash rate.*

Williams, E., Mushtak, V., Rosenfeld, D., Goodman, S. and Boccippio, D. (2005). Thermodynamic conditions favorable to superlative thunderstorm updraft, mixed phase microphysics and lightning flash rate. *Atmospheric Research*, 76 (1-4), 288–306. doi:10.1016/j.atmosres.2004.11.009.

Williams, E. and Renno, N. (1993). An Analysis of the Conditional Instability of the Tropical Atmosphere. *Monthly Weather Review*, 121 (1), 21–36. doi:10.1175/1520-0493(1993)121¡0021:AAOTCI¿2.0.CO;2.
URL https://journals.ametsoc.org/view/journals/mwre/121/1/1520-0493_1993_121_0021_aaotci_2_0_co_2.xmlhttp://journals.ametsoc.org/doi/10.1175/1520-0493(1993)121%3C0021:AAOTCI%3E2.0.CO;2

Williams, E. and Stanfill, S. (2002). *Williams, Stanfill - 2002 - The physical origin of the land–ocean contrast in lightning activity.pdf*.

Williams and Renno (1993). An Analysis of the Conditional Instability of the Tropical Atmosphere. *Monthly Weather Review*,.

Wing, A. A., Emanuel, K., Holloway, C. E. and Muller, C. (2017). *Convective Self-Aggregation in Numerical Simulations: A Review*.

Wing, A. A., Reed, K. A., Satoh, M., Stevens, B., Bony, S. and Ohno, T. (2018). Radiative–convective equilibrium model intercomparison project. *Geoscientific Model Development*, 11 (2), 793–813. doi:10.5194/gmd-11-793-2018.
URL https://gmd.copernicus.org/articles/11/793/2018/

Wing, A. A., Stauffer, C. L., Becker, T., Reed, K. A., Ahn, M. S., Arnold, N. P., Bony, S., Branson, M., Bryan, G. H., Chaboureau, J. P., De Roode, S. R., Gayatri, K., Hohenegger, C., Hu, I. K., Jansson, F., Jones, T. R., Khairoutdinov, M., Kim, D., Martin, Z. K., Matsugishi, S., Medeiros, B., Miura, H., Moon, Y., Müller, S. K., Ohno, T., Popp, M., Prabhakaran, T., Randall, D., Rios-Berrios, R., Rochetin, N., Roehrig, R., Romps, D. M., Ruppert, J. H., Satoh, M., Silvers, L. G., Singh, M. S., Stevens, B., Tomassini, L., van Heerwaarden, C. C., Wang, S. and Zhao, M. (2020). Clouds and Convective Self-Aggregation in a Multimodel Ensemble of Radiative-Convective Equilibrium Simulations. *Journal of Advances in Modeling Earth Systems*, 12 (9), 1–38. doi:10.1029/2020MS002138.

Wu, C. M., Lo, M. H., Chen, W. T. and Lu, C. T. (2015). The impacts of heterogeneous land surface fluxes on the diurnal cycle precipitation: A framework for improving the GCM representation of land-atmosphere interactions. *Journal of Geophysical Research*, 120 (9), 3714–3727. doi:10.1002/2014JD023030.

Wu, Z., Xiao, H., Lu, G. and Chen, J. (2015). Assessment of climate change effects on water resources in the yellow river basin, China. *Advances in Meteorology*, 2015, 8–12. doi:10.1155/2015/816532.

Yang, G.-Y. and Slingo, J. (2001). The Diurnal Cycle in the Tropics. *Monthly Weather Review*, 129 (4), 784–801. doi:10.1175/1520-0493(2001)129¡0784:TDCITT¿2.0.CO;2.
URL http://journals.ametsoc.org/doi/10.1175/1520-0493(2001)129%3C0784:TDCITT%3E2.0.CO;2

Zhang, G. J. (2009). Effects of entrainment on convective available potential energy and closure assumptions in convection parameterization. *Journal of Geophysical Research Atmospheres*, 114 (7), 1–12. doi:10.1029/2008JD010976.

Zhang, W. and Zhou, T. (2019). Significant increases in extreme precipitation and the associations with global warming over the global land monsoon regions. *Journal of Climate*, 32 (24), 8465–8488.

Zhao, Y., Norouzi, H., Azarderakhsh, M. and AghaKouchak, A. (2021). Global patterns of hottest, coldest, and extreme diurnal variability on earth. *Bulletin of the American Meteorological Society*, 102 (9), E1672–E1681. doi:10.1175/BAMS-D-20-0325.1.

Zhou, W. and Xie, S. P. (2019). A conceptual spectral plume model for understanding tropical temperature profile and convective updraft velocities. *Journal of the Atmospheric Sciences*, 76 (9), 2801–2814. doi:10.1175/JAS-D-18-0330.1.

Zipser, E. J., Cecil, D. J., Liu, C., Nesbitt, S. W. and Yorty, D. P. (2006). Where are the most: Intense thunderstorms on Earth? *Bulletin of the American Meteorological Society*, 87 (8), 1057–1071. doi:10.1175/BAMS-87-8-1057.

Zipser, E. J. and Lutz, K. R. (1994). The Vertical Profile of Radar Reflectivity of Convective Cells: A Strong Indicator of Storm Intensity and Lightning Probability? *Monthly Weather Review*, 122 (8), 1751–1759. doi:10.1175/1520-0493(1994)122¡1751:TVPORR¿2.0.CO;2.
URL https://journals.ametsoc.org/view/journals/mwre/122/8/1520-0493_1994_122_1751_tvporr_2_0_co_2.xmlhttp://journals.ametsoc.org/doi/10.1175/1520-0493(1994)122%3C1751:TVPORR%3E2.0.CO;2